C.P. No. 1232

MINISTRY OF DEFENCE (PROCUREMENT EXECUTIVE)

AERONAUTICAL RESEARCH COUNCIL

CURRENT PAPERS

A Review of Wind Tunnel Tests on Circulation-Control Devices for Aircraft Control

By

F. G. Maccabee, B. R. Hilton

and

J. I. Marsh

Dept. of Transport Technology, Loughborough University of Technology

LONDON HER MAJESTY'S STATIONERY OFFICE

1972

PRICE £1.35 NET

CP No. 1232*
July, 1971

A REVIEW OF WIND TUNNEL TESTS ON CIRCULATION-CONTROL DEVICES FOR AIRCRAFT CONTROL

by

F. G. Maccabee, B. R. Hilton
and
J. I. Marsh

Originally published as Loughborough University Report TT 71 R 04 dated July 1971; further details of other reports and notes in the series may be obtained from:

Professor and Head of
Department of Transport Technology,
The University of Technology,
Loughborough, Leicestershire,
England.

---

*Replaces A.R.C.33 456

CONTENTS

SUMMARY

This Report reviews the results of wind tunnel tests made during 1968 - 1971 in an experimental study of the application of blowing on sections of circular cylinders aimed at exploring the possibility of producing aircraft controlling and braking forces at low speeds. Various aspect ratios and blowing arrangements have been examined, including the use of two cylinders producing mutual interference effects.

ACKNOWLEDGEMENTS

The authors wish to acknowledge the generous assistance during the period of Messrs. N. Gregory and S.F.J. Butler of the Ministry of Technology/Ministry of Defence, Mr. J.J. Spillman of the Cranfield Institute of Technology, and Mr. W.J.G. Trebble of the R.A.E., Farnborough, whose detailed comments and advice have led to improvements in the method of test and in the value of the Report.

Acknowledgement is also due to Mr. S.R. Tyler, Technical Director, Dowty-Boulton Paul Ltd., in whose name some of the devices tested are patented.

1.0 INTRODUCTION

Since the introduction of the jet flap in the early 1950's, the application of blowing has been extended to include such devices as the circulation-controlled circular or elliptical cylinder. In most cases the major interest has been in achieving an enhanced lift, although the associated drag (or thrust) change has frequently been regarded as advantageous.

This report describes briefly the results of a programme of research designed to explore the potential of blown sections for control and braking of aircraft at relatively low speeds. A particular object has been the achievement of high values of the total aerodynamic force coefficient (preferably with an easy means of controlling the division of the force into lift and drag) and also, or alternatively, of providing high initial rates of force production as blow is applied. The latter implies high values of the initial force amplification (or magnification) factors $\frac{dC_L}{dC_\mu}$ and $\frac{dC_D}{dC_\mu}$, for values of C_μ appreciably less than 1.0.

One potential application of such devices is as low-speed control surfaces on STOL aircraft (used, for example, at the tail or nose and perhaps at least partly retractable). Dr. Küchemann has coined the term "motivators" for devices of this type.

Since the inception of the work in the autumn of 1968, research has proceeded in an ad hoc manner by means of a series of wind-tunnel tests, using sections of circular cylinders fitted with two blowing slots. The circular cylinder shape was chosen principally for its simplicity in providing various possibilities for assembly; in practice, these have included such features as change of aspect ratio in the range 2 -8, opposed blowing (opposite sign of applied circulation) on adjacent sections of one cylinder assembly , and mutual interference between two blown cylinders. In application to aircraft insensitivity to gusts may in any case be important, and the circular cylinder is a good choice for this reason also.

The results of these wind-tunnel tests have been reported in Refs. 1 - 4. Flow visualization studies and tests aimed at investigating the uniformity of flow through the slots have also been conducted (Refs. 5 and 6). The present report seeks to condense this material by selecting some of the main features,

and is largely based on a lengthy review of Refs. 1 - 3 (Ref. 7).

2.0 BACKGROUND

The use of circular cylinders for circulation control applications has been reviewed by Dunham (Ref. 8), where most of the cases dealt with are of high aspect ratio or approach two-dimensionality so that a theoretical determination of the performance can be made with some confidence (Refs. 9 and 10).

Here, on the other hand, a major object is the exploitation of low aspect ratio so that the effective drag coefficient

$$C_D = C_{D_0} - rC_\mu + k \frac{C_L^2}{\pi A + 2C_\mu}$$

(as defined in Ref. 11) may be made as high as possible. More importantly, the ratio $\frac{C_D}{C_\mu}$ (especially the initial rate of change $\frac{dC_D}{dC_\mu}\Big|_{C_\mu \to 0}$) is desirably large in this case. The eventual value of C_D achieved at a given C_μ clearly depends critically on the values of the factors r (the sectional-thrust factor) and k (the finite aspect-ratio drag factor), where these may be expected to be functions of several variables (aspect-ratio, C_μ, Reynolds No., etc.) in the case covered here. Korbacher (Ref. 12) suggests that good agreement with theoretical approaches can be obtained for very low aspect-ratio orthodox jet-flap wings. Now that a large amount of experimental data is available, it is hoped that the analysis now in progress will reveal the extent of agreement with theoretical methods (e.g. based on computer studies like those in Refs. 9 and 10) available for circular cylinders and/or other shapes.

3.0 TEST EQUIPMENT AND PROGRAMME

3.1 Basic Design of Blown Cylinders

In order to make a wide-ranging test programme possible in a relatively short series of tests, the test equipment was designed to be comparatively simple and of considerable flexibility in application.

The basic piece of equipment was the circular cylinder itself, of which five sections were made. Each was made of steel, and of dimensions: length - 0.30m (11.8in), outside diameter - 0.159m (6.25in), wall thickness - 9.51mm (0.375in). Two slots, of nominal thickness 0.127mm (0.005in), but actually shimmed to 0.152mm (0.006in) to achieve uniformity, extended along the entire length of each section. The slots were spaced so that the position of their outer lips subtended an angle of 60° at the cylinder centre, and the slot axes made an angle of 15° with the local tangent at the exit from the slot. The air supply to the slots from the common plenum chamber(represented by the interior of the cylinder)was achieved by means of a series of holes drilled through the inner part of the cylinder shell, while the outer part was cut away locally to accommodate a steel strip "slot former". This strip and the cylinder were shaped to form a convergent approach to the slot. Fig. 1 shows details of the construction and the slot geometry. The slot design is identical with that used at Hawker-Siddeley Aviation, Woodford (Ref. 13) and closely related to that used by Lockwood (Ref. 14).

The aspect ratio of the blown cylinder/s was defined as

$$AR_B = \frac{\text{slot length}}{\text{cylinder diameter}}$$

The value of AR_B for each section of cylinder was 11.8/6.25 = 1.89. Most references to AR_B in this report and in *Refs.* 1 - 7 use the nominal values, related to the actual values as follows:

Number of cylinder sections	1	2	4
Nominal value of AR_B	2	4	8
Actual value of AR_B	1.89	3.78	7.56

In cases where the principal interest lies in a detailed consideration of aspect ratio effects the actual value has been employed.

The air supply for the blown cylinders was measured by an orifice (or orifices) in the supply pipeline, which then divided to pass through the six-component balance structure and via a blowing box to a steel tube forming the model support strut. The air supply passed down this strut (referred to here as the balance/air supply strut) to a position at mid-height of the tunnel at the virtual centre of the balance. The small amount of balance constraint produced in the air supply system was allowed for in the subsequent reduction of balance measurements to give lift and drag. Lift and drag, as referred to here and elsewhere, are respectively the normal-to-stream and parallel-to-stream forces. No downwash corrections were made.

The blown cylinders were constructed on a disc screwed on to the balance/air supply strut, tie rods being used to connect this disc to other discs at the ends of the sections of the cylinder, or to intermediate positions as appropriate. Figures 2 and 3 show views of an arrangement (having a nominal value of $AR_B = 4$) built up from two sections. Most of these discs had twelve holes drilled through, of which four were used to accommodate the tie rods, the remaining eight passing the air supply to the adjacent blown sections. The central disc had holes of 9.51mm (0.375in.) in diameter, while the remaining discs used 7.92mm (0.312in.) diameter holes. The end discs were treated differently, having only four 7.92mm (0.312in.) diameter holes for the tie rods.

A different treatment was also necessary for the blown sections mounted on the balance above its virtual centre, where an internal cylinder surrounding, but clear of, the balance/air supply strut demanded an annular plenum chamber in this region. Figures 2 and 3 show further details.

Fig. 4(a) - (d) includes diagrams illustrating the various single-cylinder assemblies used during the tests, with the various end-extensions, end-plates and flaps also illustrated.

The twin cylinder tests were made using a two-section ($AR_B = 4$) blown cylinder mounted on the balance as described above, together with another two-section assembly mounted on an air supply strut passing through the floor of the balance turntable. The air

supply pressure was nominally the same in each case, but differences in the approach lines led to values of C_μ differing by up to about 20% for the two cylinders. Throughout the report, the values of C_μ are regarded as identical except where stated otherwise. Figure 5 illustrates the twin cylinder arrangement. The centre-to-centre distance of the cylinders was usually 0.738m (29in.), giving a spacing/diameter ratio of 4.64, but for comparison a short series of tests with a spacing of 0.458m (18in.) was also made. The turntable movement allowed the second ("passive") cylinder to be traversed through a full 360° arc around the balance-mounted ("active") cylinder.

Although the basic design was intended to be as flexible as possible in application, it should be noted that the slot geometry and spacing has not been changed. The plenum was also always common to both slots and therefore the C_μ contribution from each slot was nearly equal.

3.2 Test Programme

The test series has produced results in four basic categories:

(i) single cylinder lift and drag (by balance measurements) for symmetrical (or uni-directional) blowing from the two slots, for Reynolds Numbers Re_D ranging from 1.34×10^5 to 6.7×10^5 with values of the momentum coefficient C_μ ranging up to 8.5 and slot incidence β varying between -10 and 60 degrees.
Within this broad framework, some tests have been devoted to an examination of various end conditions of types generally relevant to possible aircraft applications, including gaps, end-plates, end-extensions and simulated fuselage (or other structure) junctions, while others have used flaps (basically of Thwaites-type in effect) downstream of the second blowing slot.

(ii) single cylinder lift and drag by balance measurement for arrangements in which adjacent cylinder sections have opposed blowing. Apart from an examination of the effect of use of flaps and of small fences at the junctions between sections, these tests have been generally less exhaustive than those in (i) above.

(iii) twin cylinder, mutual interference, cases involving lift and drag by balance measurements for various combinations of slot incidence and relative orientation of two parallel cylinders about five diameters apart (centre-to-centre).

(iv) single cylinder pressure distribution measurements, for both symmetrical and opposed blowing. Four spanwise positions have been used, sometimes with three positions being recorded for one test condition to determine spanwise changes. Balance measurements were also made simultaneously in most cases.

Details are included in Refs. 1 - 4 and Ref. 7; the Cranfield 8' x 6' low-speed (max. speed = 250ft./sec. = 76m/s approx.) was used for these tests. Supporting tests which were made in the Loughborough open-jet tunnel (3' x 3½'; max. speed = 100ft./sec. = 30m/s approx.) included an investigation of slot flow non-uniformity, conducted under static conditions (Ref. 6), and an investigation of the nature of the flow using various flow visualization techniques (Ref. 5).

3.3 Reduction of Results

As indicated, most of the tests involved balance measurements of lift and drag. (Note (as above) that the lift was strictly the force normal to the tunnel centre-line and the drag the parallel component). These were recorded on position meters and corrected for tare and constraint effects before reduction to the equivalent forces. The tunnel speed was set on an orthodox static calibration and cross-checked using a pitot-static tube mounted roughly 0.61m(2ft.) upstream and 0.91m (3ft.) to one side of the model. When the ground-plane was used, a further measurement below the plane was also made.

From this data, lift and drag coefficients were determined, usually by means of a computer.

Twin cylinder tests were handled in a similar manner; measurements of lift and drag were only possible for the cylinder mounted on the balance itself (called the "active" cylinder).

Values of the momentum coefficient C_μ were calculated using orifice measurements of mass flow rate and assuming free isentropic expansion through the slot for the determination of the jet (slot) velocity V_j (as in Ref. 15).

Wind-tunnel corrections were applied in the manner described by Maskell (Refs. 16 and 17). Graphs (included in the earlier reports, Refs. 1 and 2) show that the division of drag coefficient into three components (a basic no-lift component (C_{D_o}), a part proportional to C_L^2 in a pre-stall flow regime, and a further part (C_{D_s}) increasing rapidly, usually with a fall in the lift coefficient, at and beyond the stall) is sound. Corrections then amount to up to about 4% in the pre-stall regime and about 25% in the post-stall condition. The word "stall" as used here describes the point at which the lift coefficient reaches a maximum. At values of C_μ in the range 0.1 - 0.3 (approx.) there is frequently a relatively abrupt change in slope of the lift coefficient vs. C_μ curve, which is also of basic significance for the performance of the cylinder as a lifting section.

The correction method also appears to apply with reasonable validity to the twin cylinder case (even in the case where the two cylinders are disposed across the tunnel section) and was accordingly used here. However, it is probably desirable to confirm that this approach is really justifiable.

In the pressure distribution tests the pressures were recorded on simple multi-tube manometer banks.

3.4 Restrictions on Testing : Cranfield

There were two basic restrictions on the test programme:

(i) the tunnel's available speed range. Nominally about 12.2 - 76.1m/s (40 - 250ft./sec.), this in practice proved to be limited at its upper end to about 61 or 48.8m/s (200 or 160ft./sec.), for most of the one or two section single cylinder tests (AR_B = 2 or 4) especially with moderate or high C_μ, and to 36.6m/s (120ft./sec.) in the remainder of the tests. The corresponding Reynolds and Mach Nos. are:

Velocity, m/s (ft/sec.)	12.2 (40)	18.3 (60)	24.4 (80)	36.6 (120)	48.8 (160)	61 (200)
Re_D	1.34 x 10^5	2.00 x 10^5	2.67 x 10^5	4.01 x 10^5	5.34 x 10^5	6.68 x 10^5
M	0.036	0.055	0.073	0.11	0.145	0.18

(ii) the air supply available.

The supply was capable of delivering up to approximately 0.45kg/s (1lb./sec. or 0.031 slug/sec.), at a delivery pressure of $3.8 \times 10^5 N/m^2$ ($55 lb./in.^2$) gauge, so that the pressure ratio across the slot varied up to nominal values of about 5. In fact, internal losses produced an actual pressure ratio lower than the nominal by up to about 15%. Values of C_μ of up to about 8 were used (for aspect ratio $AR_B = 2$, $Re_D = 1.34 \times 10^5$) with most tests concentrated in the range $C_\mu < 1$.

A further reason for restriction of model testing was the occasional occurrence of a vibration which was regarded as excessive, at least from the standpoint of obtaining reliable balance and other readings. This was clearly in part due to the type of test being conducted, implying the presence of intermittent, powerful, vortex-shedding at some conditions, and also due to the construction, where the cantilevered strut mounted on the balance blowing box supports a model acting as a type of dumb-bell about the central disc (see Figs. 2 and 3). At no time was there any mechanical trouble or threat of disintegration; at its worst, the amplitude of the vibration was about 0.15in. at the end of the model with a frequency in the range 0 - 10 cycles/sec.

The results recorded were found to be repeatable to within approx. 5%.

4.0 RESULTS AND DISCUSSION: SINGLE CYLINDER TESTS

This section deals with the basic force measurements on single cylinder assemblies, whether with use of symmetrical (uni-directional) blow or opposed blowing.

4.1 Unblown Cases

Unblown drag coefficients are included in Refs. 4 and 7. These show that for the case where the cylinder alone is mounted on the balance/air supply strut (with the perspex shroud in place; a small amount of interference drag is then unavoidably present, important especially for the low aspect ratio case) there is a general trend to reduce variation in C_D by comparison with the standard results of Wieselsberger and Gottingen (for nominally infinite aspect ratio). This is presumably directly attributable to the finite aspect ratio. In other tests, the results were rather scattered, especially in cases where there were rather rough-surfaced end-extensions such as wooden dummy ends. No transition-fixing devices were used, but the influence of the slots in tripping a boundary layer separation can be identified in some cases.

4.2 Basic Single Cylinder Tests with Symmetrical Blowing

4.2.1 Tests with No Dummy Ends

The results of a series of tests using the configurations shown in Fig. 4(b) (J) - (L) are presented in Figs. 6 - 12. These include details of the effect of slot incidence on lift and drag coefficient at given aspect ratio. Figure 6 summarises the data for AR_B = 2, indicating clearly the effect of Reynolds No. Figures 7 - 9 present a summary for AR_B = 4 together with the complete data for a Reynolds No. of 5.34×10^5. The influence of incidence change is shown on the latter curves. Figures 10 -12 give similar information for AR_B = 8.

In general terms, the full results show that:

(i) the effect of incidence change within the limits (0 - 45°) employed is relatively weak. The incidence at which highest lift coefficient is achieved appears to shift from 15° (approx.) for aspect ratio 2 to 25° for aspect ratio 8; however, the change in C_L involved in a choice of incidence anywhere within this range is slight.

The effect of Reynolds No. and incidence change is occasionally difficult to distinguish; most attention has been given (where possible) to the results obtained at higher Reynolds Nos. in these remarks (but see also below (ii)).

High incidences (greater than 25^{o}) lead to low lift coefficients at low values of C_{μ}, particularly for low aspect ratio. This is almost certainly due to an initial failure to produce attached Coanda-type flow. The pressure distributions, to be discussed later, also show marked differences in behaviour of the pressure variation downstream of the second slot, which probably has a similar effect on the lift and drag behaviour for more widely-varying values of C_{μ} at some incidences.

(ii) the effect of increase of Reynolds No. in the range 1.34×10^{5} to 5.34×10^{5} is not consistent, and in any case is not marked. There is a tendency to higher lift and drag coefficients for the higher Reynolds Nos., most noticeable for $AR_B = 2$ in Fig. 6, although it is also seen to some extent on Figs. 7 ($AR_B = 4$) and 10 ($AR_B = 8$).

(iii) the effect of increase in aspect ratio is to produce the expected increase in lift coefficient. There are two aspects of this:

(a) the initial rate of increase of lift coefficient with momentum coefficient dC_L/dC_{μ}: This value increases from about 8 - 10 at $AR_B = 2$ to about 24 at $AR_B = 8$. The increase is effective from a very low value of C_{μ}, (probably not zero, but for all practical purposes to be regarded as such) and applies always up to a C_{μ} value of approx. 0.35.

(b) the eventual value of C_L achieved at the stall: Early results, in Refs. 1 and 2, show some examples of the achievement of stalls at values of C_{μ} as low as 0.5 when the incidence is 60^{o}. However, it is by no means clear how behaviour in this regard is linked to aspect ratio (or, indeed, to other factors, like incidence) with any certainty at the present stage.

Accepting that the pre-stall, low C_μ, behaviour is most important for the systems being studied, Figures 13 and 14 give curves of lift and drag coefficient for various aspect ratio and for selected low values of C_μ. The latter curves show that at C_μ = 0.2 to 0.3 the following rough rules apply:

$$\underline{Re_D = 4 \times 10^5}$$

$$AR_B = 2 : C_L = 8\, C_\mu \qquad (\beta = 25^\circ)$$
$$AR_B = 4 : C_L = 15\, C_\mu \qquad (\beta = 15^\circ)$$
$$AR_B = 8 + C_L = 23\, C_\mu \qquad (\beta = 15^\circ)$$

i.e. at fixed C_μ at values near those quoted

$$\frac{dC_L}{d(AR_B)} = 0.9 \text{ (approx.)}$$

While it must be emphasised that these are approximate figures, they do suggest that the increase in lift coefficient due to increase in aspect ratio is more marked than finite wing (lifting-line) theory would normally suggest. The flow visualization tests reported later suggest that this is due to the fact that the flow sheds powerful vortices well inboard especially at low aspect ratio.

The corresponding drag curves are rather flat, showing a weak maximum at about AR_B = 4 for each C_μ value.

Discussion of the initial value of dC_D/dC_μ, the rate of increase of drag coefficient with momentum coefficient, must be based on an assumed range for C_μ, because the value of dC_D/dC_μ at C_μ = 0 is virtually zero and remains small for an interval of C_μ. Accepting that the main interest lies in values of C_μ less than about 0.5, the values of dC_D/dC_μ are:

$Re_D = 4 \times 10^5$

Range of C_μ	AR_B	Mean dC_D/dC_μ in range
$0 < C_\mu < 0.2$	2	5
	4	9
	8	5
$0 < C_\mu < 0.5$	2	3.6
	4	5.2
	8	4

Here (and elsewhere) there is the suggestion that an aspect ratio of approx. 4 is the optimum for high drag production.

Figures 13 and 14, summarising the behaviour of the lift and drag coefficient at various aspect ratios, illustrate these points.

4.2.2 Effect of Varying End Conditions

Of the different configurations adopted for modifying the cylinder configurations, illustrated on Fig. 4(a) - (d), the most significant changes were produced by the end-plates and the ground-board (the former at both ends, the latter at one only). Use of dummy ends (unblown) had relatively less effect.

The tests included several showing the effect of:

(i) dummy ends at both ends;

(ii) dummy ends at one end only;

(iii) no dummy ends (but note that in this case the perspex shroud round the balance/air supply strut is not very far removed from a full cylinder, at least in its effect on spreading or suppressing the effect of the circulation on the blown cylinder. The major axis of the elliptical shroud was always aligned with the undisturbed tunnel airstream direction in these tests).

(iv) no dummy ends, but with end-plates screwed on to the blown cylinder itself. (The drag of the end-plates is thus included in the cylinder drag.)

The end plates produced an increase in lift coefficient of up to about 30% with the increase beginning to take effect from about C_μ = 0.2, and increasingly thereafter. The increase in C_D due to the use of end-plates was roughly half this (15%). See Figs. 15 - 19.

Figures 17 - 19 examine the effect of end-plates in conjunction with aspect ratio change. It is seen that, in round figures, the same value of lift coefficient is achieved with AR_B = 4 plus end-plates as with AR_B = 8 without end-plates, although not at the same C_μ. Drag coefficient behaviour is more erratic, and it is difficult to make any generalisation.

Fig. 19 summarises the induced-drag behaviour relating to use of end-plates. There appears to be no direct link between the induced drag coefficient and the momentum coefficient, C_μ. The slopes of the curves of C_D vs. C_L^2 compare with the values of $\frac{1}{\pi A}$ (c.f. $C_D = \frac{k\, C_L^2}{\pi A}$) as follows:

AR_B (=A)	$\frac{1}{\pi A}$	Measured value at Re_D = 2.67×10^5 (Fig.41 of Ref. 7)	Measured value at Re_D = 4.01×10^5 (Figure 19)
3.78 with end-plates	0.097	0.058	0.084
3.78 without end-plates	0.097	0.115	0.1225
7.56 without end-plates	0.0498	0.04	0.0358

The last two cases imply values of k of more and less than one respectively.

However, although C_μ does not appear to be a significant factor in deciding the value of C_D here, later results show a more definite link; results of this type are shown in Fig. 24.

The effect of a ground board at one end is shown in Figs. 20 - 23 (see Fig. 4(a) - top for geometrical details). The ground board generally reduced the lift, and, more strikingly, the drag. In this respect, its effect contrasted sharply with that of the end-plates.

The earlier reports (Refs. 1 - 5) include more details of the effect of dummy ends, in particular.

4.2.3 Effect of Use of Flaps

In considering the use of flaps, the choice between a mechanical type or a pneumatic type is one which might merit a programme of research in itself. In a completely flexible system, there could be four or more slots - two above and two below to provide for different directions of applied circulation - of which one could act as a separation-fixing "flap". In the present case, a mechanical flap was chosen, as shown in Figure 4(d).

Results of adding a flap are shown in Figs. 24 - 26. The flap angle is specified by the angle measured downstream of the second slot: e.g., $\beta = 20^{\circ}$, $\delta_f = 60^{\circ}$ implies first slot at $\theta = 110^{\circ}$, second slot at $\theta = 170^{\circ}$ and flap at 230°. The results show that the general effect of a flap is to increase the lift, particularly at higher values of C_μ (see Fig. 26), where the C_L value continues to rise steadily(the flap was always positioned so that the flow was still attached at the flap, providing a contribution to lift from the high local near-stagnation pressure in the slot flow, realised as it turned away from the flap face to form a powerful jet sheet in a direction also producing high lift). The drag is generally reduced, partly due to the high pressure region in the flow before the flap, which is on the rear of the cylinder.

Figs. 26 and 27 show the spanwise distribution of lift and drag for cases with and without flap.

4.3 Basic Single Cylinder Tests with Opposed Blowing

4.3.1 Tests With and Without Dummy Ends

The results of tests using the configurations shown in Fig. 4(a) - (b) are included in Figs. 27 - 29. Of these the first two cover cases where two cylinder sections only were blown, with and without a flap, but without dummy ends. As in all opposed-blow cases the lift was very small, usually with values of C_L considerably less than 1.0. Use of a flap again reduces the drag

coefficient, which is in most cases near the corresponding value obtained with symmetrical blowing.

Use of small fences to split two opposed-blow cylinder sections (fitted with dummy ends) gives the result shown in Fig. 29. No change of great significance is noted; however, the fences were admittedly very small.

5.0 RESULTS AND DISCUSSION: TWIN CYLINDER MUTUAL INTERFERENCE TESTS

In the investigations carried out to establish the effect of the mutual interference of one blown cylinder on another, both cylinders employed an $AR_B = 4$ assembly and blowing in the same direction on any given cylinder. Two basic types of test were then possible: those where the blowing was in the same direction on each cylinder, and those where it was opposite. Both types of test were made, together with a few where one cylinder only was blown.

5.1 Both Cylinders with Dummy Ends; No Ground Board

The first test series used an incidence of 15° with dummy ends always fitted (basically to provide adequate support for the model) as in Fig. 5. The test results are summarised in Figs. 30 and 31, and Figure 32 shows a comparison of the lift/drag ratio achieved using the twin cylinder arrangement with those for the corresponding isolated single cylinder. These figures make it clear that the changes in performance available through mutual interference are substantial. In particular, on Fig. 30, the drag coefficient in a single cylinder in a favourable opposed-blowing interference case is reduced to about 0.7 ($\pm$0.1) over the range of C_μ up to 0.6 compared with a single cylinder value rising to 3.6. The lift coefficient is not greatly affected - in most cases it is reduced - so that the overall lift/drag ratio of a two-cylinder combination with interference, by comparison with two isolated single cylinders, is increased by a factor of 2 at $C_\mu = 0.6$.

Here it should again be noted that the value of C_μ on each of the cylinders has normally been assumed to be the same through most of this paper and in the references. This is in fact not the case: the values differ by as much as 20%. Allowance for this difference has been made in the production of Figure 32.

Figs. 33 and 34 continue with the presentation of twin cylinder results and comparisons, mainly dealing with the earlier tests for which the incidence on an individual cylinder was as high as 45^{o}.

In many respects the results follow the pattern established with the single cylinder. For example, it appears to be generally true that a Reynolds No. of $4x10^{5}$ gives a higher lift coefficient than is the case at lower Reynolds No., and the same conclusion is substantially correct for the drag coefficient. However, there are strong indications that the incidence producing maximum interference effect may be higher than that producing best results on a single cylinder. Thus, a comparison of the results for three incidences (15^{o}, 30^{o} and 45^{o}) shown on the Figures makes it clear that in some respects an incidence of 30^{o} is most attractive from the standpoint of drag production.

5.2 Cylinders Without Dummy Ends; With Ground Board

Further tests were concentrated on higher Reynolds No. cases and involved finite aspect ratio cylinders mounted on a ground board. Figures 35 - 39 include results of this type, including also the effect (in one case) of varying the lateral separation of the cylinders. The results are not markedly different in form from those discussed previously including, for example, an increase in lift with some flap positions. However, the reductions in both lift and drag due to use of flap are more striking.

Fig. 37 shows that direction of blow (or reduction of C_{μ} to zero on one cylinder) has relatively little effect on the forces produced when the configuration is such that $\gamma = -120^{o}$, while Figs. 38 and 39 show that reducing the separation of the cylinders from 0.738m (29in.) to 0.458m (18in.) reduces lift and increases drag, in each case by up to 15 - 20%.

6.0 RESULTS AND DISCUSSION: PRESSURE DISTRIBUTION TESTS AND SPANWISE VARIATIONS

In this section, additional data which help to interpret the previous results are presented. A general discussion of the pressure distributions recorded is given, with further attention to the spanwise variations following later, the latter including remarks on slot flow variations and vortex structure.

Figures 40 - 42 present examples of the pressure distributions which have been integrated to obtain the data for the following discussion. In the pressure distribution records as a whole, the following points are noted:

(i) Failure of the flow to attach behind the first slot is occasionally observed, at low C_μ and high incidence especially.

(ii) The second slot frequently has a weak effect on the production or maintenance of high negative pressure coefficient. This suggests that it may be desirably re-located (at, say, 45° behind the first slot) or blown at a different value of C_μ.

(iii) When a flap is used, the values of C_p achieved in front of the flap (i.e., upstream) are frequently very high, reaching peak values of +17. This appears to be mainly a consequence of the high energy in the slot flow (in relation to the mainstream flow), which reaches a near-stagnation condition as the flow is turned by the flap.

6.1 Spanwise Variation of the Flow Through the Slots

Reference 6 describes the results of an investigation (made at Loughborough) of the effect of variation of internal pressure, cylinder arrangement and slot cleanliness on the dynamic pressures produced downstream of the slot. The latter was presumed to give a direct indication of the velocity (and thus mass flow and C_μ) produced at the slot. The tests were made under static conditions (no free-stream flow other than that induced by the slot flow itself).

Miniature pitot and static tubes were used to augment the internal pressure readings in obtaining pressure traverses at a distance of 6.35mm (0.25in.) downstream of the first slot.

Vertical (normal to cylinder) traverses showed that the dynamic pressure variations ranged up to approx. 20%, although a typical deviation was within $\pm$ 5%. Fig. 43 shows one set of curves. Spanwise traverses at a fixed height of 0.05mm (0.002in.) also revealed a variation of a similar order of magnitude, not apparently directly linked to any feature of the geometry such as the slot design; Fig. 44 shows one such result.

Careful cleaning of the slots after a period of testing resulted in a general improvement in performance (by up to approx. 20% of dynamic pressure); Fig. 45 illustrates this feature. This decay in performance is almost certainly exacerbated at Loughborough by the oil vitiating the compressor air supply, and is probably not representative of the Cranfield tests.

6.2 Spanwise Variation of Force Production

The spanwise changes of pressure distribution were used to give "integrated" values of the local lift and drag coefficient (as in (i) above) at some positions along the cylinder span for comparison with the average levels of the coefficients given by the corrected balance results for the appropriate value of C_μ.

The average integrated results agree closely with the balance readings, an error of up to about 10% being fairly common, with extreme discrepancies (especially for drag) of up to 30%. In this connection, it may be remarked that the complete recovery of slot thrust (along the slot axis) is assumed, an assumption which is not usually regarded as entirely valid. However, the effect of an error in this assumption can easily be assessed, and is for most of these tests not great.

Figures 46 and 47 give comparisons of lift and drag distributions along the length of cylinders with aspect ratios ranging from 2 to 8 for two values of C_μ(0.27 and 0.90). By moving the pressure-tapped cylinder section to different positions in the assembly, data has been collected for various spanwise positions, as indicated earlier.

The effect of the flap is most marked near the centre of the cylinder, with the augmentation of lift and reduction of drag most prominent there. These effects appear to be closely linked with the flow behaviour revealed by the flow visualization tests reported below.

Also of interest are comparisons between the results for corresponding cases of tests at Cranfield and Loughborough, with the associated behaviour of the total force vectors.

Examples are given on Figs. 48 and 49, and indicate close agreement. The direction of the force vectors does not appear to change much along the span of the cylinder.

6.3 Flow Visualization Tests

The general similarity (noted above) between the pressure distributions around the cylinder obtained at Cranfield and Loughborough implies that flow visualization tests in the (open-jet) tunnel at Loughborough have a general validity as a means of determining the flow behaviour. Accordingly, tests on $AR_B = 2$ and $AR_B = 4$ arrangements (the latter including opposed blowing) for the range $0.25 < C_\mu < 1.0$ have been made, and are to be fully reported in Ref. 5.

Figures 50 and 51 are based on sketches obtained during these tests (using surface-flow methods, wool-tufts and spin meters as sources of basic information). Important features include:

(i) at $AR_B = 2$: Vortices stream off at the tip of the cylinder, leaving the surface between slots 1 and 2 in a similar manner for cases without and with a flap fitted. These vortices leave the cylinder with a relatively small inclination downwards (about 20° for $C_\mu \approx 1.0$) and noticeably "toe-in" towards each other, having a spacing of about 70% of the cylinder span at six cylinder diameters downstream.

When no flap is fitted, subsidiary vortices (which may be more powerful than those shed at the tip) occur near the centre of the span, with a spacing of less than the cylinder diameter. These leave the cylinder in a direction nearly normal to the free-stream direction ($\theta = 260 - 290^\circ$ approx.) for $C_\mu \approx 1.0$ and turn slowly into the free-stream direction downstream, so that the angle between the vortex cores and the free-stream direction is about 60° at a distance of four cylinder diameters below the cylinder. These vortices presumably reflect an augmented circulation near mid-span (similar to a deflected flap on a wing) and may explain the shape of the lift distribution curves (Figs. 46 and 47).

The surface flow upstream of the first slot had a strong (spanwise) inflow tendency which had almost disappeared at a height of 12.7mm (0.5in.) above the surface. Thus, the entrainment may embody a strong vorticity (not apparently traceable in the vorticity shed from the cylinder, although it may account for the division of the shed vorticity into two powerful vortices on each side).
So far as vorticity production is concerned, the flow is apparently more normal when a flap is fitted, with only the tip vortices detectable; however, the lift and drag obtained from the integrated pressure distribution are very similar in shape to the unflapped case.

(ii) at $AR_B = 4$: the cases for high incidence ($\beta = 45^\circ$), and generally when a flap is fitted, are like those for $AR_B = 2$.
When $\beta = 0^\circ$, with no flap, the flow divides at the junction between the two cylinder sections, where the slot flows are interrupted over a length of 9.51mm (0.375in.), forming two distinct $AR_B = 2$ flow cells, with the associated vortex structure.

(iii) with opposed blowing, the results include no surprising features.

7.0 GENERAL DISCUSSION

This review presents some of the more important results of the experimental study of the potential of blown devices to act as versatile controlling and braking "motivators". It is likely that the full potential has not yet been revealed, for example particularly in the mutual interference cases where the geometrical and blowing variations are virtually endless. Thus, while it has been our purpose here to examine the performance shown to be available in these tests, it should be remembered that performance may in fact be considerably improved in various respects.

It is also desirable to consider briefly the potential applications. Ref. 18 shows that STOL aircraft with wing loadings near their current values require an augmentation of normal aerodynamic methods of force production when they are required to operate into 2000ft. fields with approach speeds of less than 90 knots. Motivators or similar devices are then possible means of achieving the blend of thrust, control force and drag necessary for adequately-controlled flight on a flight path chosen to fit noise limits. "Puffer jets" on VTOL aircraft may also be modified or replaced by motivators to suit the particular application. It is possible that the full use of motivators or other blown devices may involve large changes in the basic design on intermediate types of V/STOL aircraft. Figure 52 illustrates some possible designs for motivators, of which the cruciform has not been investigated here.

Finally, before proceeding to the detailed discussion of the performance achieved, it is worth remarking that some aspects have not been covered, including for example gust sensitivity and dynamic performance in general.

7.1 Performance Available

As indicated earlier, the performance required may be regarded as having two important facets:

(i) the ability to achieve absolute values of force coefficient, with considerable flexibility in choice of direction.

(ii) alternatively, but preferably in addition, the ability to maintain a high multiplication of the nominal slot momentum force (i.e., equivalent jet thrust) again with flexibility in choice of direction.

In either or both cases, the performance should preferably be available with a clear possibility of reasonable ease of control, either by regulation of the blowing air supply or adjustment of geometry (flaps, etc.).

The discussion in Sections 4 and 6, especially on pp. 10-13, above has shown that on both grounds the performance available from a single blown cylinder is sufficiently good to suggest that the main objectives have been achieved. Thus, the measured values of lift coefficient range as high as 21 with the initial

value of $\frac{dC_L}{dC_\mu}$ (near $C_\mu = 0$) having values as high as 23; both of these values apply for an aspect ratio of 7.56 and performance at lower aspect ratio is appreciably reduced. So far as drag is concerned, at an aspect ratio of 3.78, initial values of $\frac{dC_D}{dC_\mu}$ range up to 9, and at $C_\mu = 0.5$ a multiplication of the direct reverse thrust available (represented by C_μ) by 5 is still available.

Some further improvement is possible with various additions to the basic single cylinder shape (such as end-discs, etc.) but these could be offset in practice by compressibility effects (although at low C the high Reynolds No., high Mach No. combinations used in these tests gives the best results) and unfavourable interference with other parts of the aircraft structure (e.g., the fuselage) if the results using a ground-board obtained in these experiments are in this respect representative. It is worth noting that the results at low C have generally shown reasonable linearity of C_L with C_μ and smooth changes of C_D with C_μ with little direct effect of Reynolds No. and incidence. However, some early tests at high incidences ($\beta = 30^\circ$) do show abrupt changes associated with flow separation and attachment.

The exploitation of mutual interference between two blown cylinders gives strikingly different results, especially so far as drag is concerned. In this case, there are so many possible design variables that a systematic study would demand a long test programme; the small investigation so far completed has shown that the lift/drag ratio may be doubled, mainly through an alternation in the drag (see Section 5, especially page 16).

Flow visualization tests suggest that single cylinder performance may be further improved, for example by adjusting the distribution of slot flow along the span to achieve a more uniform lift loading; this may have a beneficial effect in the mutual interference case also.

8.0 CONCLUSIONS

The application of blowing to low aspect-ratio circular cylinders has been shown to give high values of lift and drag coefficient. More importantly, the values of the factors expressing the amplification of the direct thrust effect represented by the

blowing momentum coefficient C_μ are also very high. At representative low-speed flight conditions (on a small aircraft installation) the following figures apply:

Cylinder aspect ratio	For C_μ up to 0.2	For C_μ up to 0.5
$AR_B \approx 2$	$C_L \approx 8C_\mu$; $C_D \approx 5C_\mu$	$C_L \approx 6C_\mu$; $C_D \approx 3.6C_\mu$
$AR_B \approx 4$	$C_L \approx 15C_\mu$; $C_D \approx 9C_\mu$	$C_L \approx 9C_\mu$; $C_D \approx 5.2C_\mu$
$AR_B \approx 8$	$C_L \approx 23C_\mu$; $C_D \approx 5C_\mu$	$C_L \approx 14C_\mu$; $C_D \approx 4C_\mu$

The values are generally highest at high Reynolds No., and for the blowing arrangements studied, the results are generally insensitive to incidence change (at least over a range of $\pm$ 20°). Modifications of the basic cylinder shape (by adding end-discs, or other geometrical changes) change the single-cylinder performance by up to about 30%.

Much more significant are the changes produced when two single cylinders are brought close together and the mutual interference effect exploited. One such arrangement gives a lift/drag ratio twice that of two corresponding single cylinders in isolation.

Further tests and computer studies are in progress.

References

No.	Author(s)	Title, etc.
1	F. G. Maccabee and B. R. Hilton	Preliminary report on wind tunnel tests on high-drag-producing devices. Loughborough University of Technology, TT 6903. February, 1969.
2	B. R. Hilton and F. G. Maccabee	Second preliminary report on wind tunnel tests on high-drag-producing devices. Loughborough University of Technology, TT 6906. May, 1969.
3	B. R. Hilton and F. G. Maccabee	Third preliminary report on wind tunnel tests on high-drag-producing devices. Loughborough University of Technology, TT 70 R 01. January, 1970.
4	J. I. Marsh and F. G. Maccabee	Fourth preliminary report on wind tunnel tests on blown circular cylinders. Loughborough University of Technology, TT 71 R 01. March, 1971.
5	J. I. Marsh and F. G. Maccabee	Flow visualization and pressure studies of spanwise changes on low aspect-ratio blown cylinders. Loughborough University of Technology, TT 71 R 05. November, 1971.
6	J. I. Marsh and F. G. Maccabee	Blown cylinder: An investigation of slot flow non-uniformity by pressure traverses. Loughborough University of Technology, TT 70 R 09. November, 1970.
7	F. G. Maccabee and B. R. Hilton	Review of wind-tunnel tests on high-drag-producing devices. Loughborough University of Technology, TT 70 R 04. October, 1970.
8	J. Dunham	Experiments towards a circulation-controlled lifting rotor. The Aeronautical Journal (R.Ae.S.), Part 1, Jan. 1970; Part 2, Feb. 1970.
9	J. Dunham	A theory of circulation control by slot-blowing applied to a circular cylinder. Journal Fluid Mechanics, Vol.33, Part 3. 1968.

10/

No.	Author(s)	Title, etc.
10	R. J. Kind	A calculation method for circulation control by tangential blowing around a bluff trailing edge. The Aeronautical Quarterly, Vol.19, Pt.3. August, 1968.
11	J. Williams, S. F. J. Butler and M. N. Wood	The aerodynamics of jet flaps. ARC R & M 3304. January, 1961, (pub.1963).
12	G. K. Korbacher	Performance, operation and use of low aspect ratio jet-flapped wings. Journal of Aircraft, Vol.1, No.6. November - December, 1964.
13	-	Lift-dependent-drag for circulation control aerofoils. Hawker Siddeley Aviation Ltd., Manchester, Report No. VS/M/MC/803/11.18.
14	V. E. Lockwood	Lift generation on a circular cylinder by tangential blowing from surface slots. NASA TN D-244.
15	A. Anscombe and J. Williams	Some comments on high-lift testing in wind-tunnels with particular reference to jet-blowing models. J.R.Ae.S. August, 1957.
16	E. C. Maskell	Interference on a three-dimensional jet-flap wing in a closed wind-tunnel. RAE TN Aero 2659. 1959.
17	E. C. Maskell	A theory of the blockage effects on bluff bodies and stalled wings in a closed wind-tunnel. ARC R & M 3400. 1965.
18	D. Howe and R. E. Ward	Some design considerations of STOL transport aircraft. Cranfield Institute of Technology, Cranfield Memo No.44. July, 1971.

NOTATION

AR_B	Blowing aspect ratio = (slot length)/(cylinder dia.)
C_D	Drag coefficient = $D/\frac{1}{2}\rho V^2 S$ (corrected for tunnel interference)
(C_J)	see C_μ
C_L	Lift coefficient = $L/\frac{1}{2}\rho V^2 S$ (corrected for tunnel interference)
C_μ	Momentum coefficient = $(m_j V_j)/\frac{1}{2}\rho V^2 S$
D	Drag (lb.) or cylinder diameter (ft.)
L	Lift (lb.)
m_j	Slot mass flow rate (slug/sec.)
Re_D	Reynolds No. based on cylinder diameter = $\frac{VD}{\nu}$
S	Normally wing area, here cylinder planform area (= frontal area, A) ($ft.^2$)
V	Velocity (ft./sec.)
β	Slot incidence (degrees) - defined with reference to the location of the first slot. When blowing downstream (in the conventional sense) = ($\theta_{\text{first slot exit}}$ - 90)degrees (See Fig. 4(d)).
γ	Position of second cylinder in relation to balance-mounted cylinder in mutual interference tests (See Fig. 5).
ν	Kinematic viscosity
ρ	Density of air ($slug/ft.^3$)
θ	Position on cylinder: angle from front stagnation point (degrees)

FIG. 1

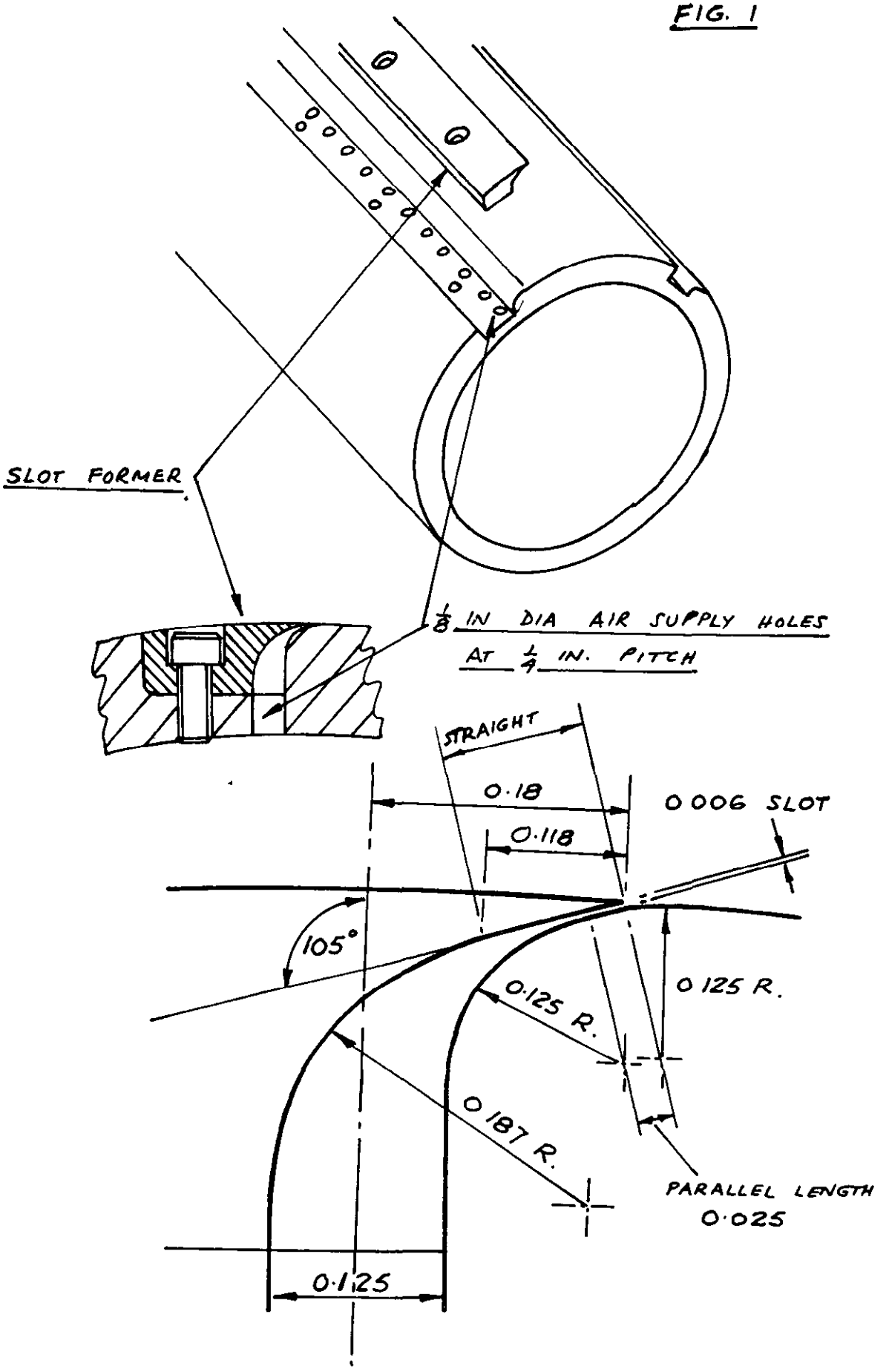

FIG 1. SLOT ARRANGEMENT AND GEOMETRY

(ALL DIMENSIONS IN INCHES)

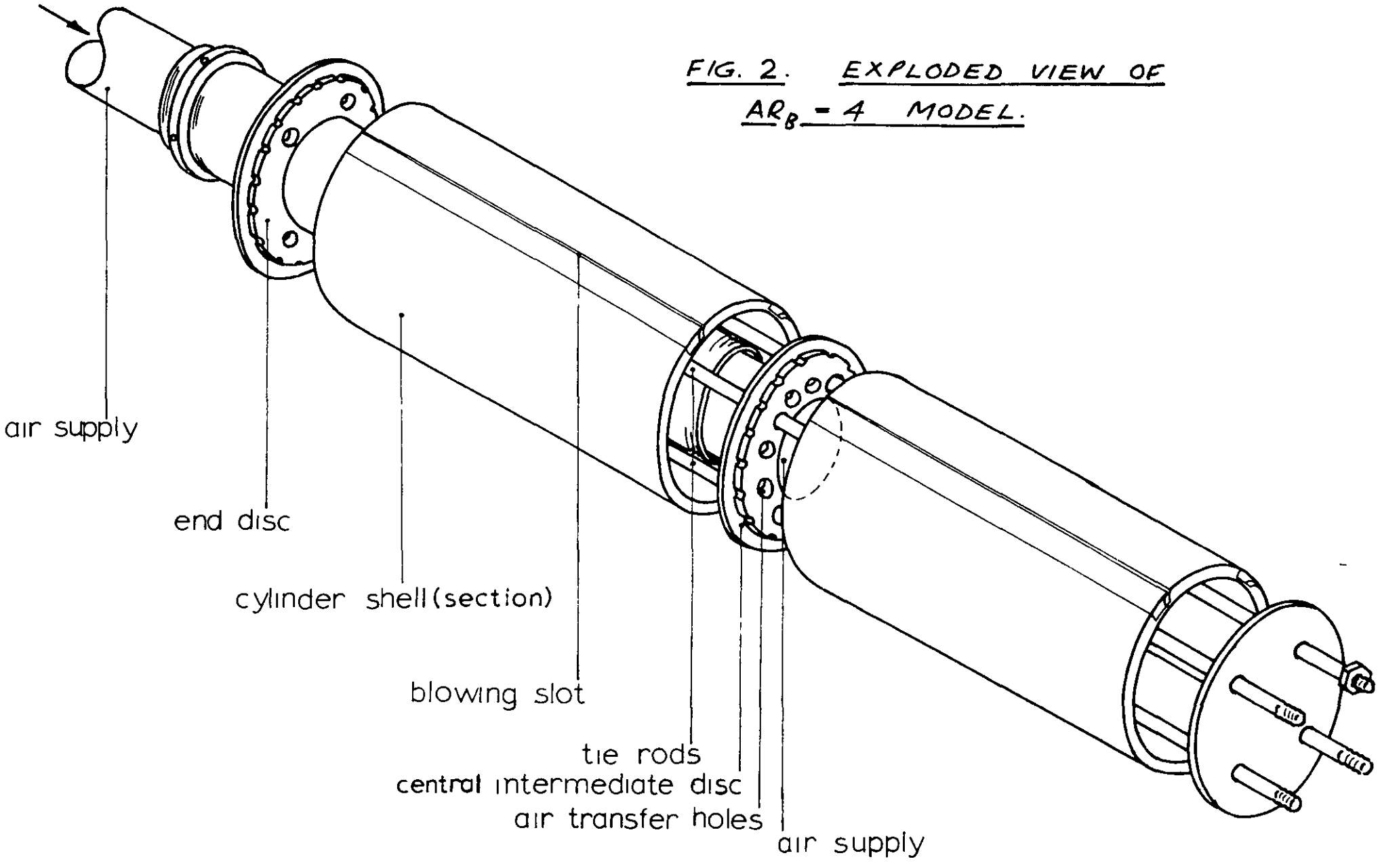

FIG. 2. EXPLODED VIEW OF $AR_B = 4$ MODEL.

FIG. 3.

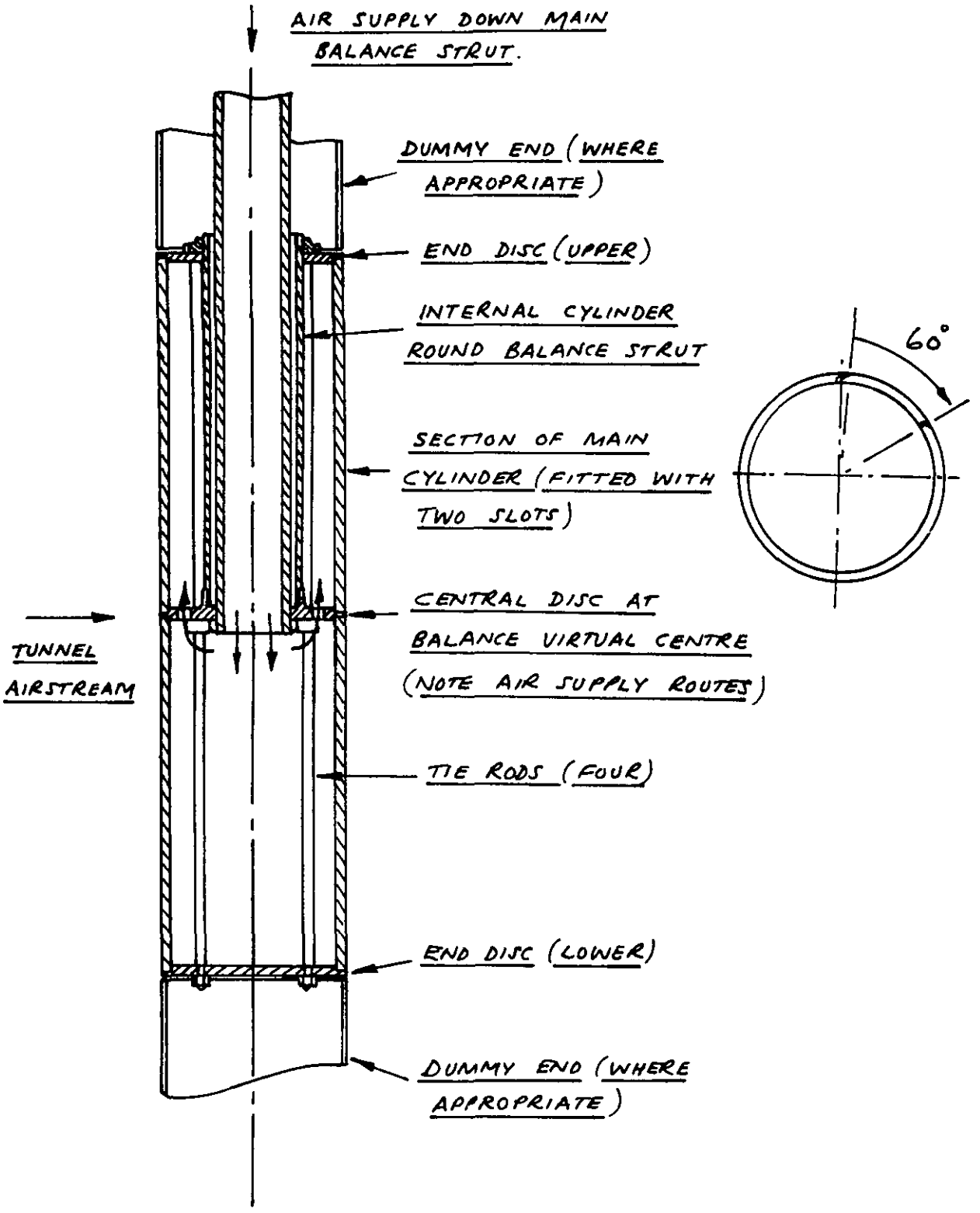

FIG. 3. CONSTRUCTION OF MODEL SINGLE-CYLINDER – ASPECT RATIO $AR_B = 4.0$.

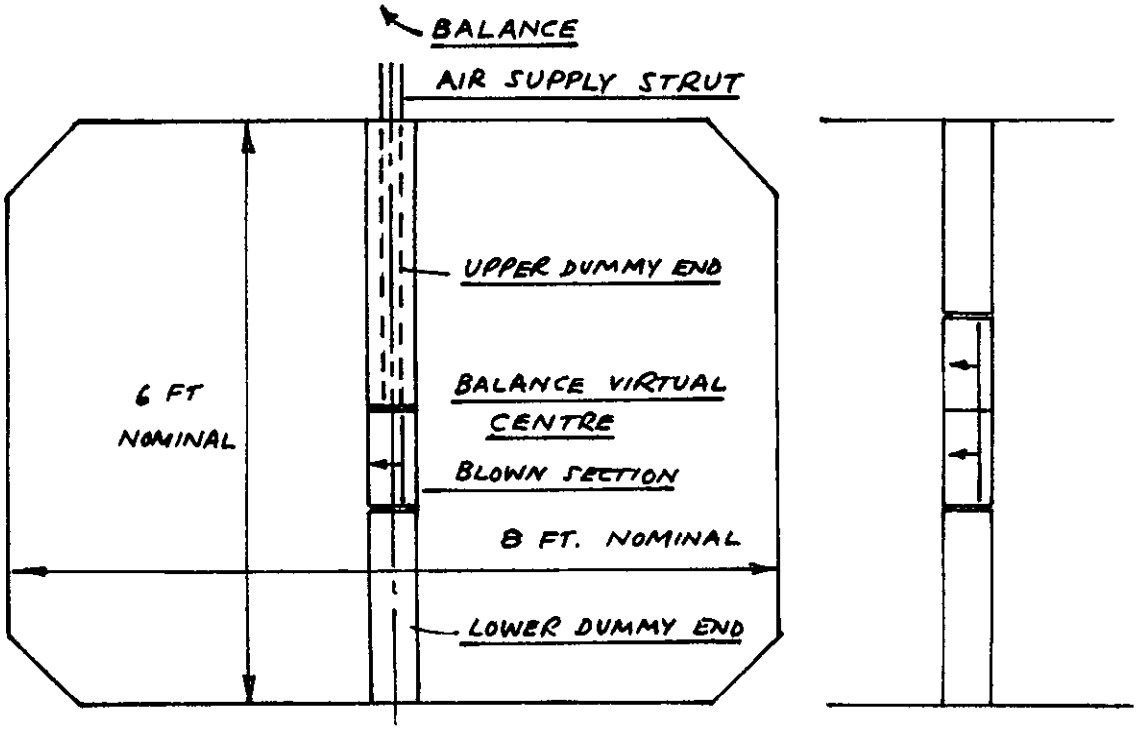

(A) ONE BLOWN SECTION ($AR_B = 2$) WITH DUMMY ENDS

(B) TWO SECTIONS SYMMETRICALLY BLOWN ($AR_B = 4$) WITH DUMMY ENDS.

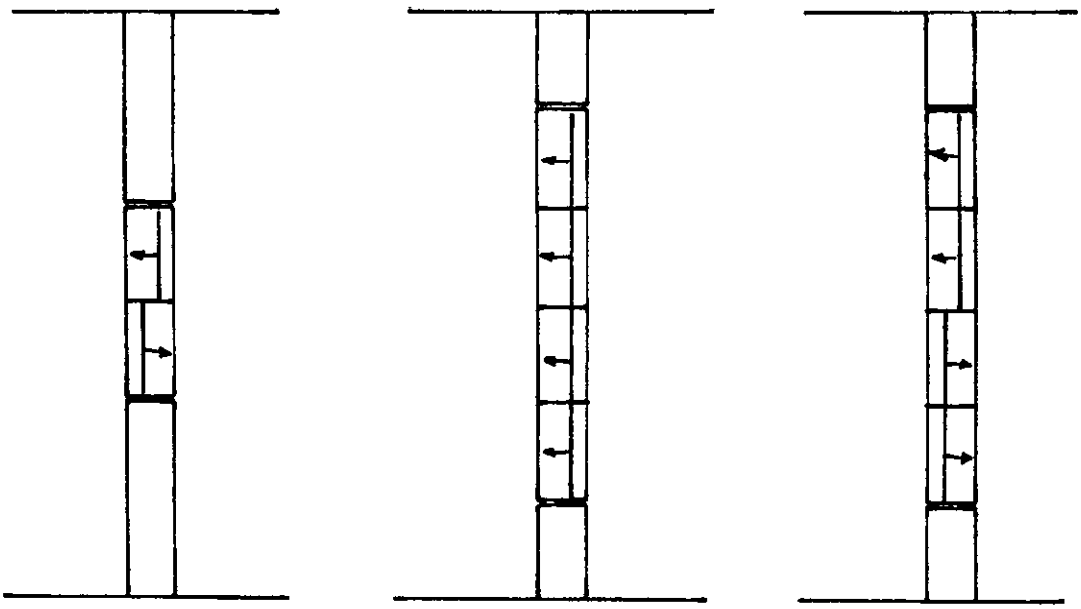

(C) TWO SECTIONS OPPOSITELY BLOWN ($AR_B = 2$) WITH DUMMY ENDS

(D) FOUR SECTIONS SYMMETRICALLY BLOWN ($AR_B = 8$) WITH DUMMY ENDS

(E) FOUR SECTIONS OPPOSITELY BLOWN (+ + − − ; $AR_B = 4$) WITH DUMMY ENDS

FIG. 4(a) TEST CONFIGURATIONS — SINGLE CYLINDERS

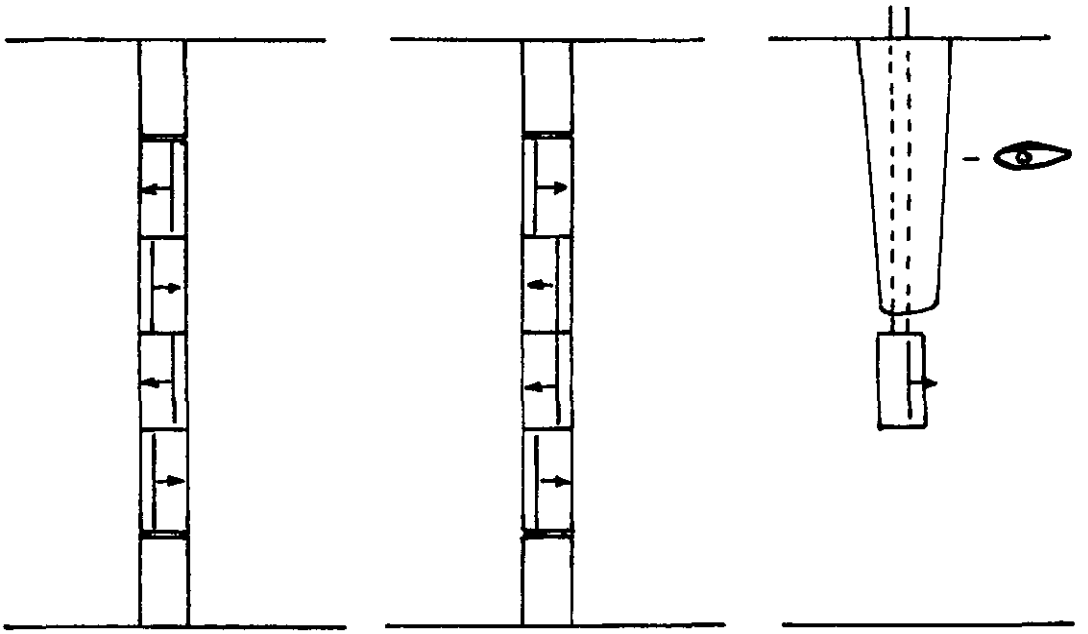

(F) FOUR SECTIONS OPPOSITELY BLOWN (+ − + − ; $AR_B = 2$) WITH DUMMY ENDS

(G) FOUR SECTIONS OPPOSITELY BLOWN (+ − − + ; MIXED ASPECT RATIO) WITH DUMMY ENDS

(H) (SIDE VIEW) ONE SECTION, FAIRING ON BALANCE/AIR SUPPLY STRUT

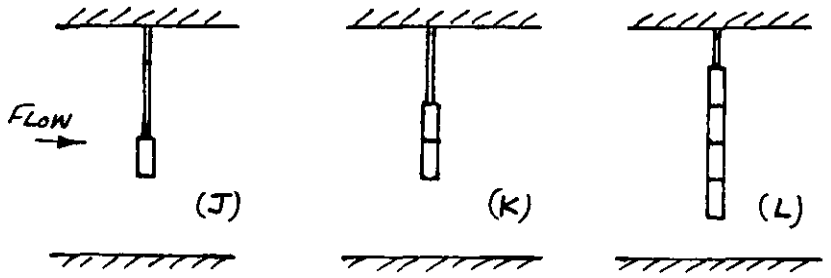

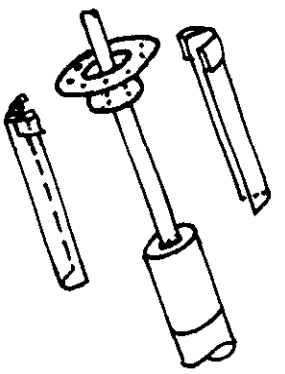

CONFIGURATIONS WITHOUT DUMMY ENDS: IN THE GENERAL SERIES OF TESTS ON THESE ARRANGEMENTS THE BLOWING WAS AS IN (A) — (G) ABOVE IN EVERY CASE THE BALANCE STRUT WAS SHIELDED BY A PERSPEX ELLIPTICAL SHROUD AS AT RIGHT

FIG. 4(b). TEST CONFIGURATIONS — SINGLE CYLINDERS (CONTINUED)

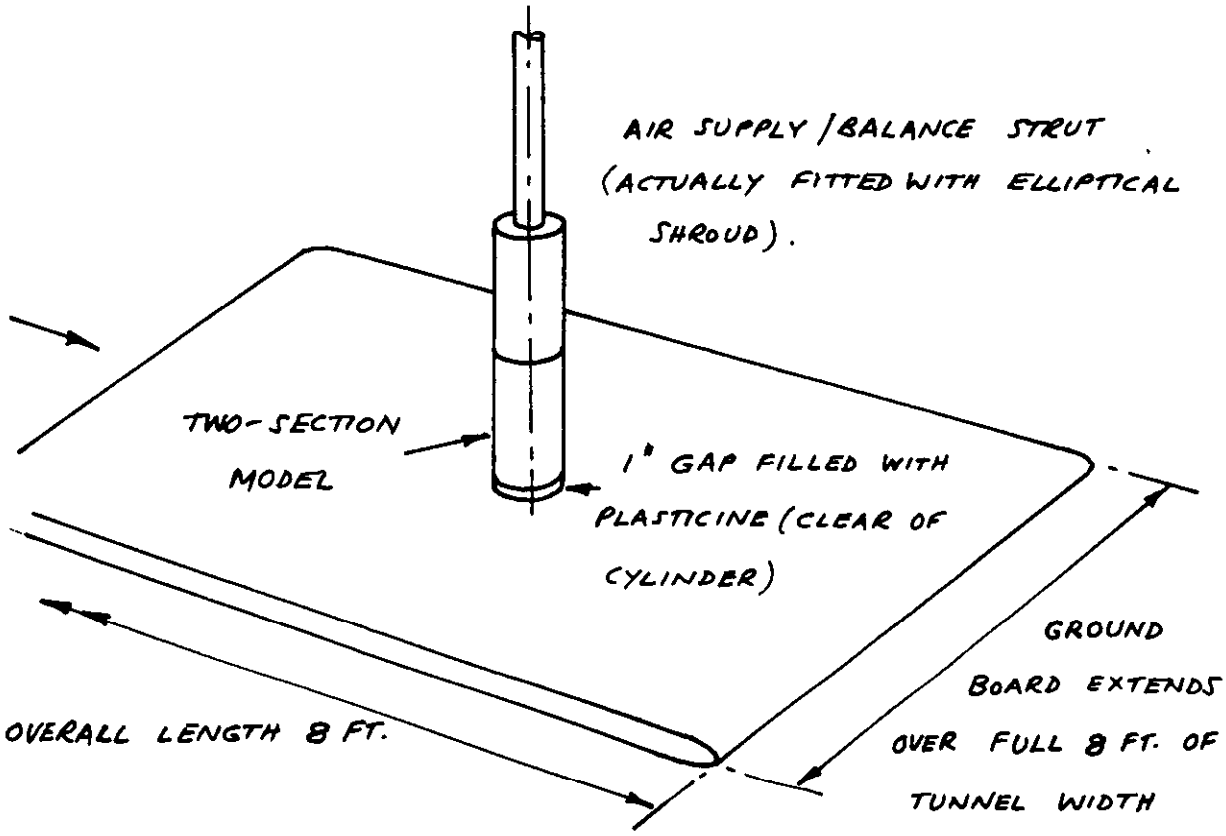

CONFIGURATION USING GROUND BOARD TO SIMULATE PRESENCE OF AIRCRAFT STRUCTURE AT TIP OF CYLINDER. GROUND BOARD IS APPROX. 2 FT. FROM TUNNEL FLOOR

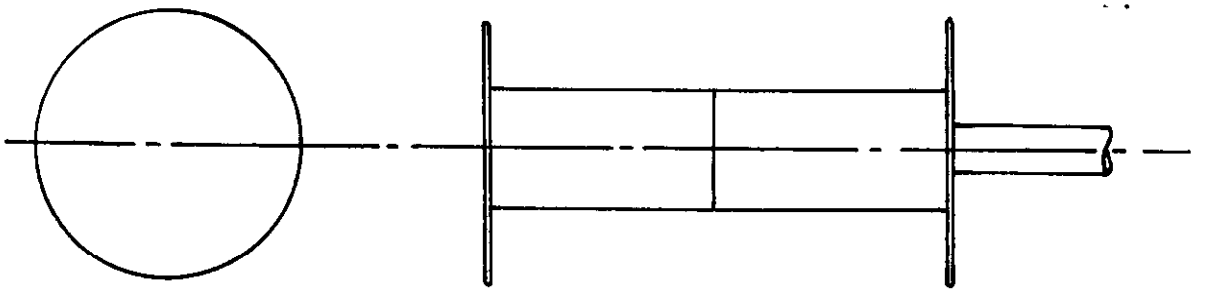

USE OF END-DISCS ($\frac{5}{16}$" THICK PERSPEX WITH BEVELLED EDGES, 13 33" DIA). DISCS ARE BOLTED ON TO ENDS OF CYLINDER, HERE SHOWN AS A TWO-SECTION MODEL

FIG. 4(c) TEST CONFIGURATIONS — SINGLE CYLINDERS (CONCLUDED).

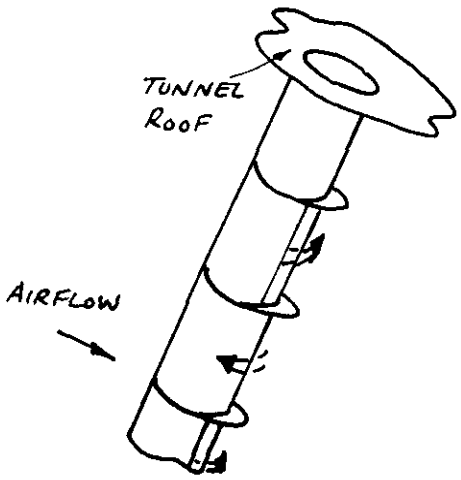

(M) USE OF SMALL INTER-SECTION FENCES (WITH OPPOSED BLOW)

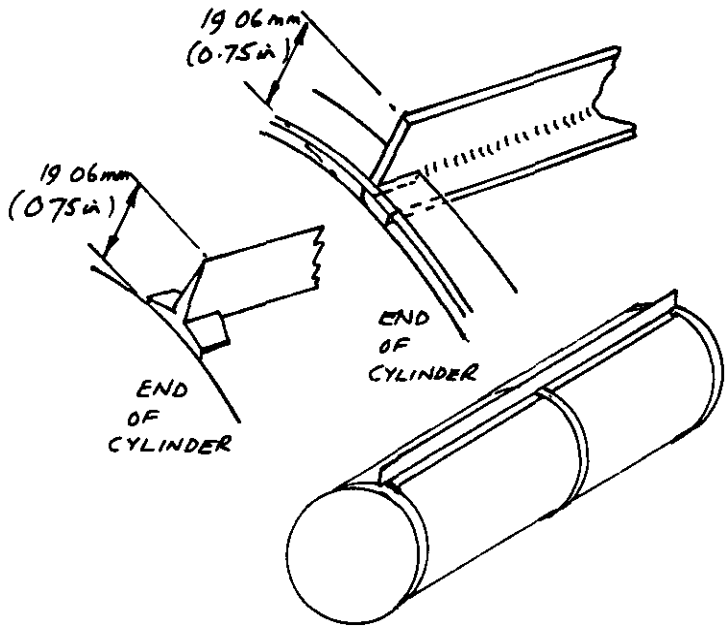

(N) USE OF FLAP (MOST COMMON USE WAS OF TYPE AT RIGHT)

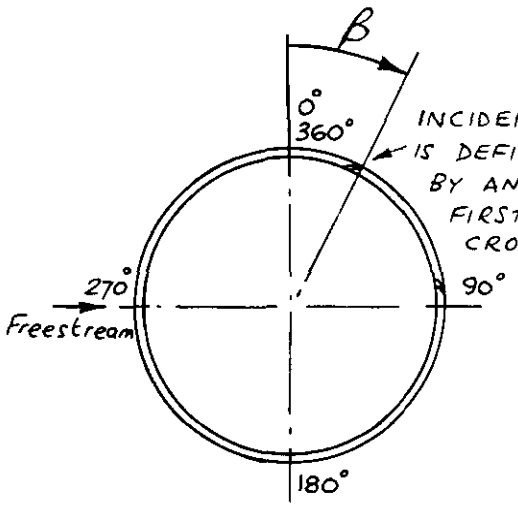

PRESSURE-TAPPING LOCATIONS ARE DEFINED AS AT LEFT

PRESSURE DISTRIBUTION TESTS

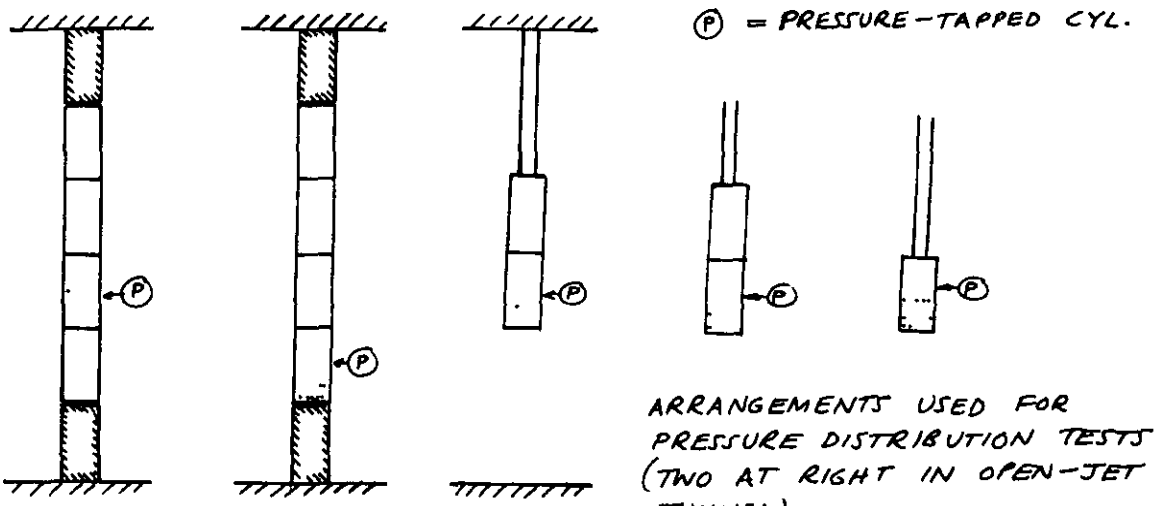

ARRANGEMENTS USED FOR PRESSURE DISTRIBUTION TESTS (TWO AT RIGHT IN OPEN-JET TUNNEL)

FIG 4(d) TEST CONFIGURATIONS—SINGLE CYLINDERS (CONCLUDED)

FIG. 5.

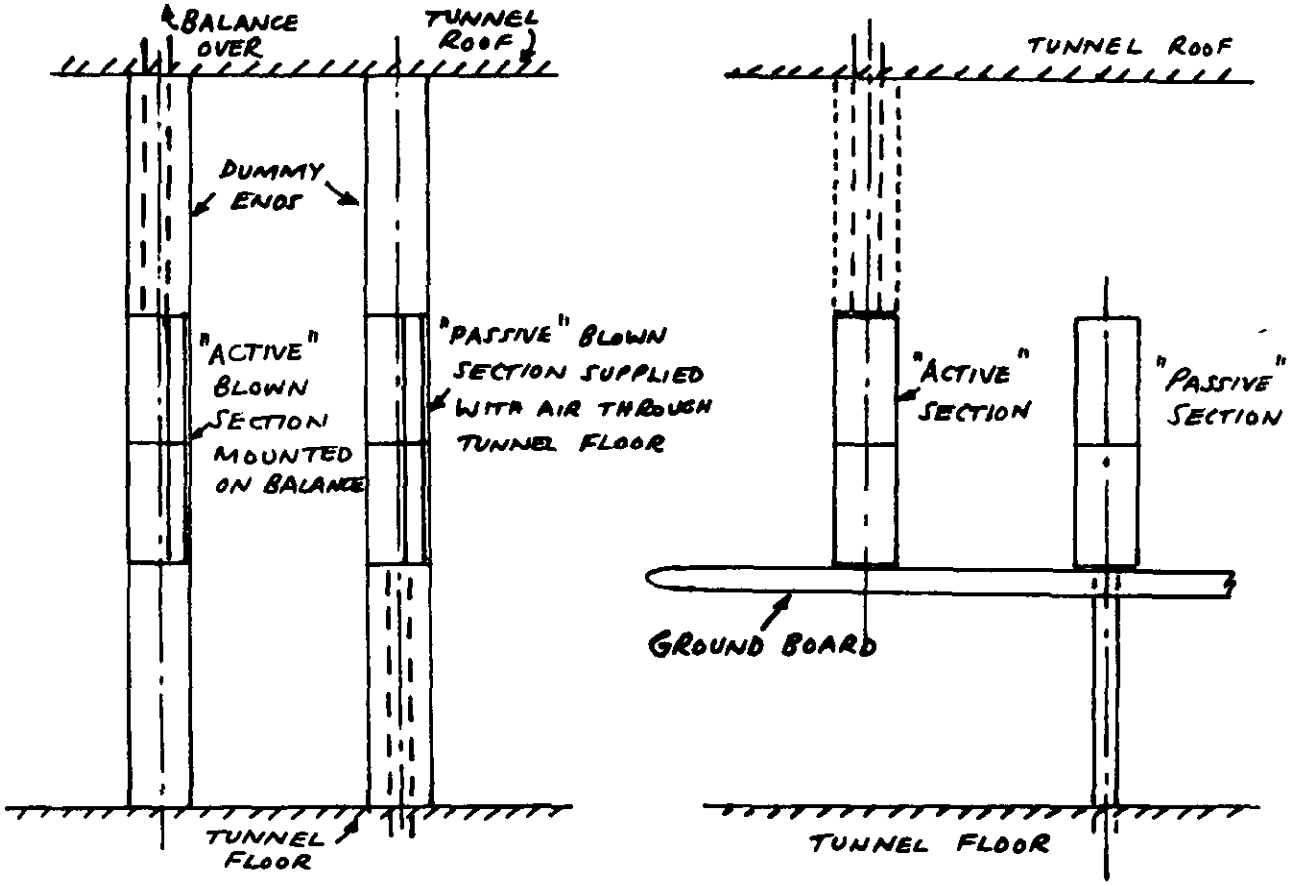

SIDE ELEVATIONS OF ALTERNATIVE INSTALLATIONS IN TUNNEL.

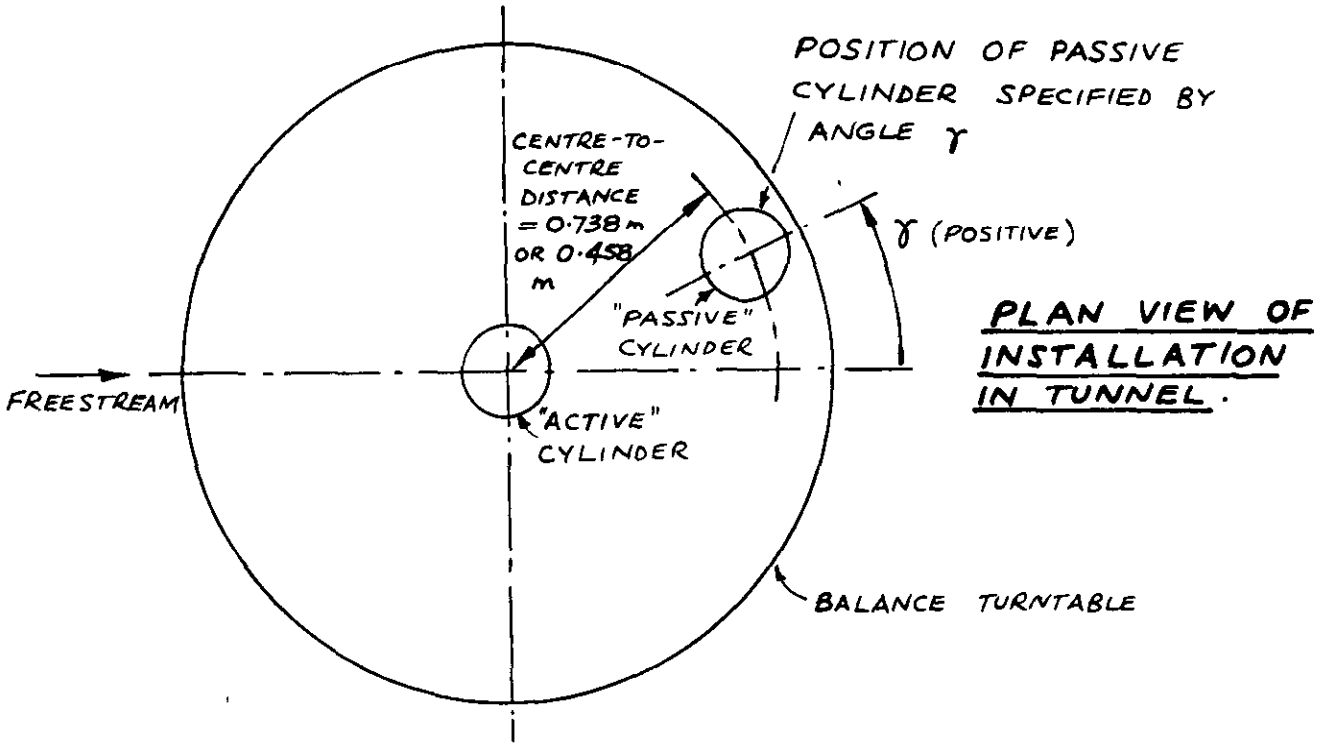

PLAN VIEW OF INSTALLATION IN TUNNEL.

FIG. 5. ARRANGEMENT FOR TWIN CYLINDER TESTS (MUTUAL INTERFERENCE).

FIG. 6

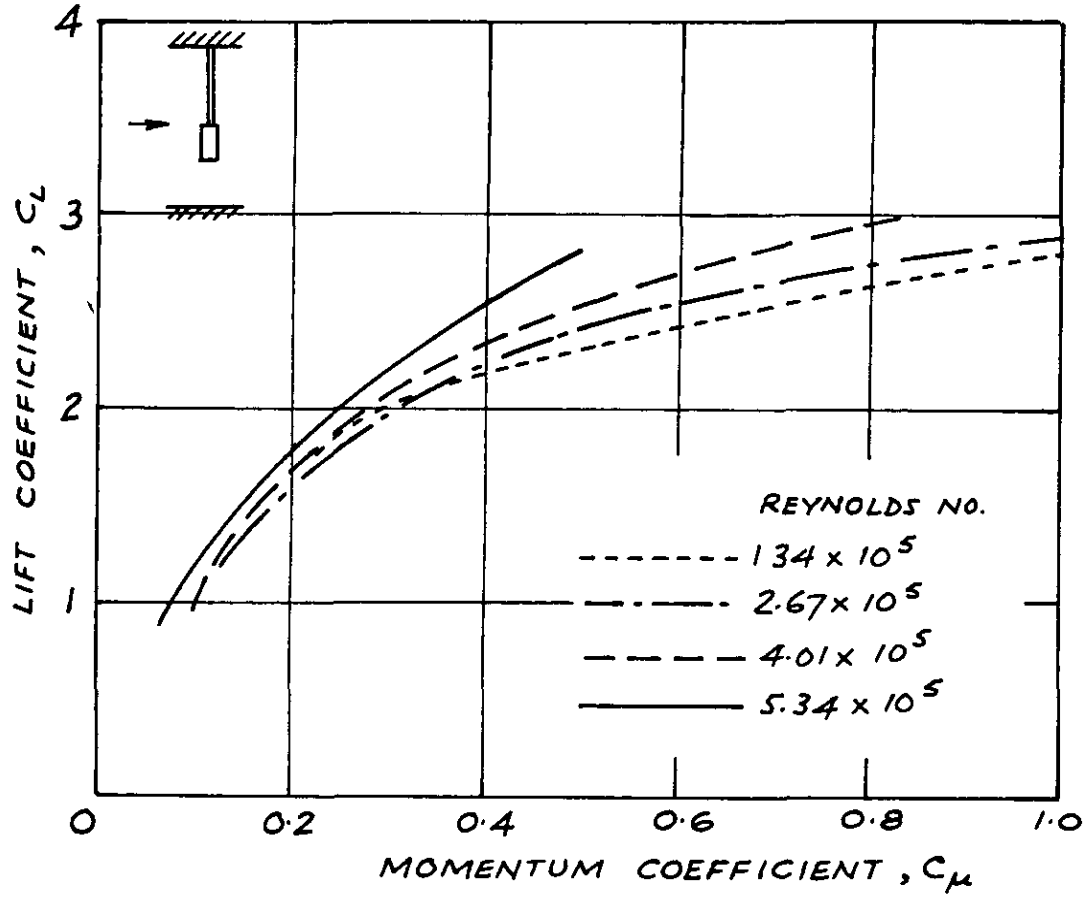

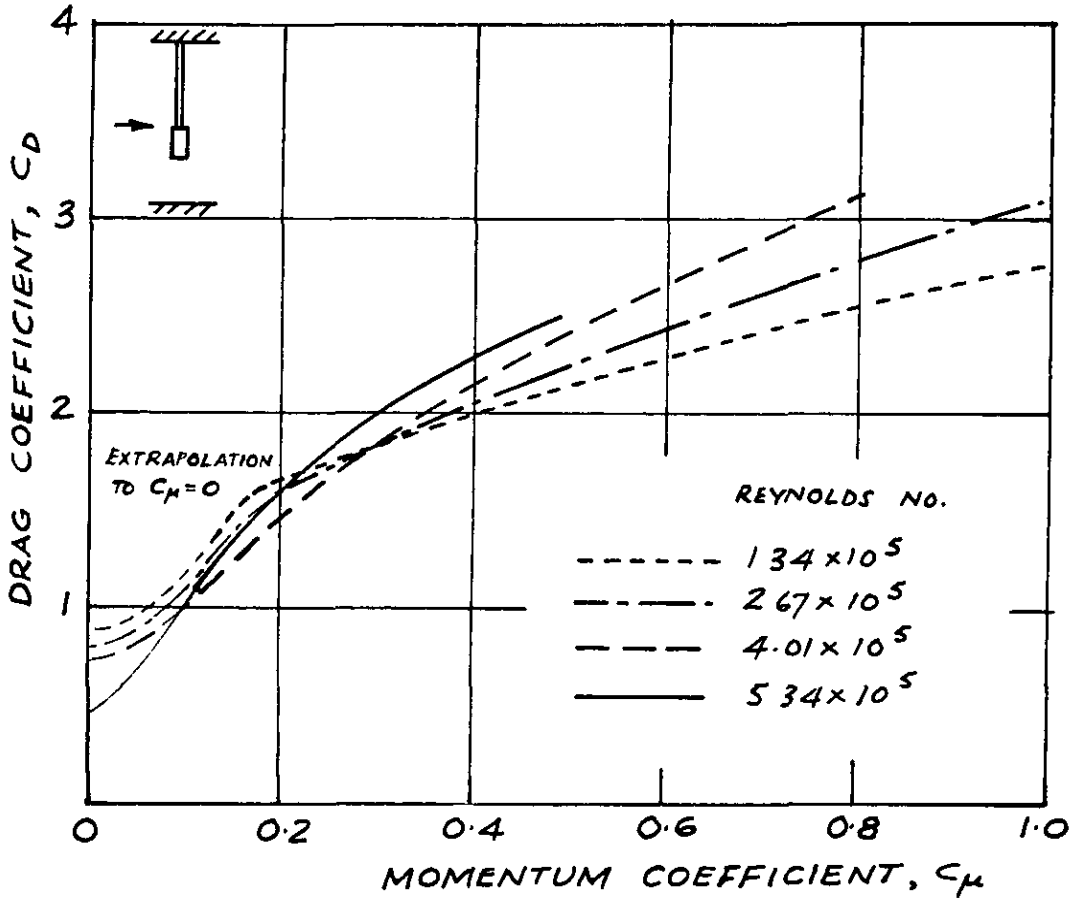

FIG. 6. EFFECT OF REYNOLDS NO. ON LIFT AND DRAG — SINGLE CYLINDER, $AR_B = 2$.
SLOT INCIDENCE "CONSTANT" AT $10° \pm 5°$.

FIG. 7

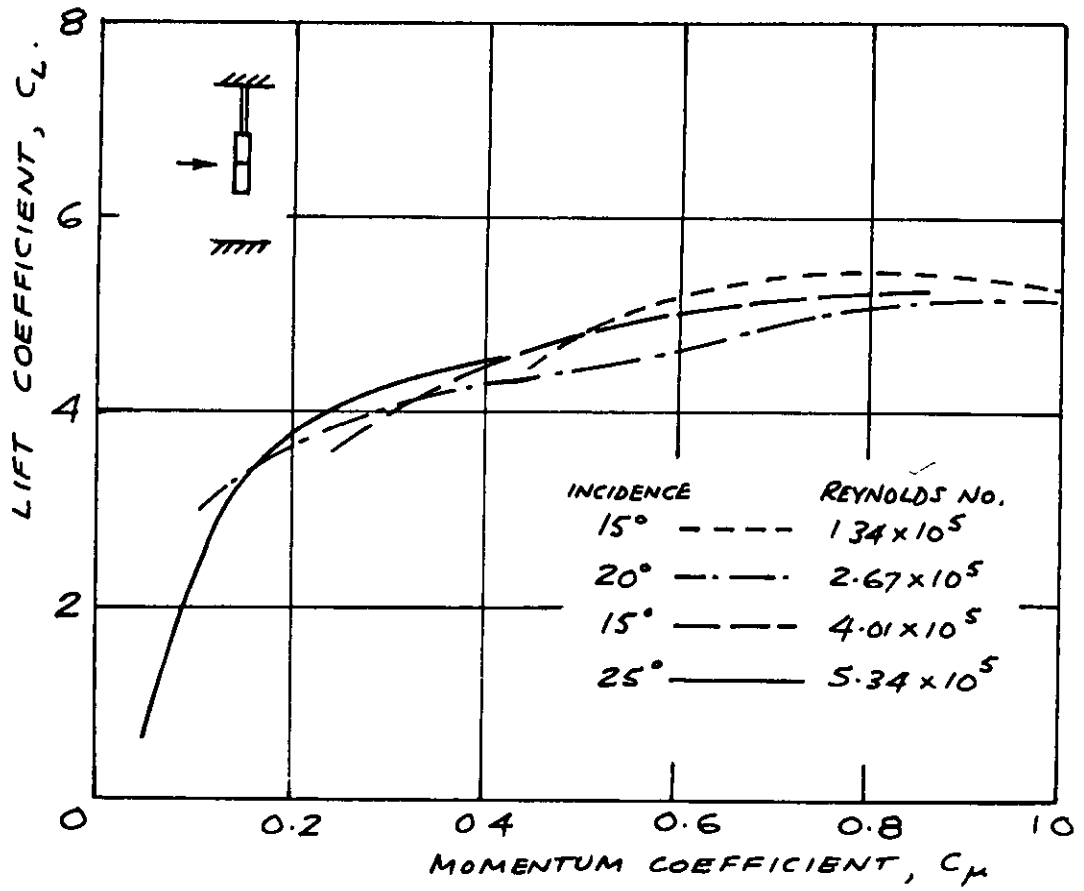

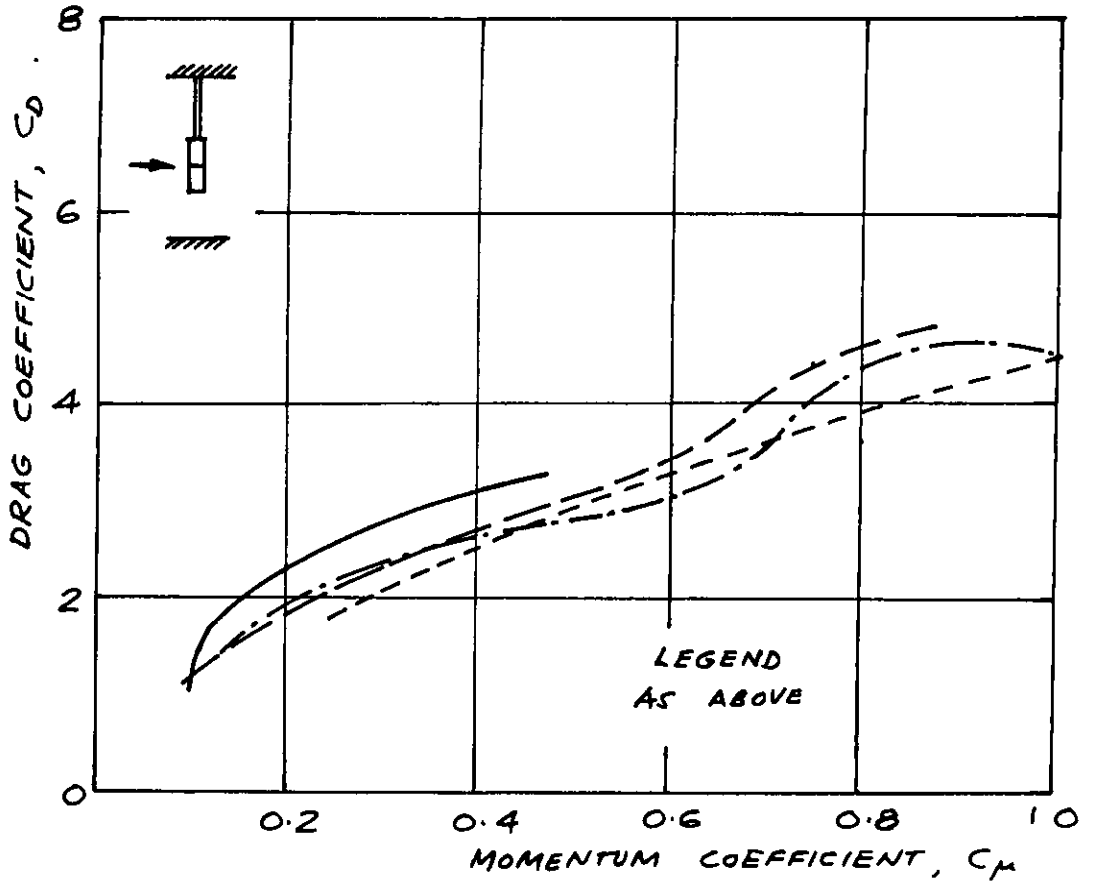

FIG 7. EFFECT OF REYNOLDS NO. ON LIFT AND DRAG — SINGLE CYLINDER $AR_B = 4$

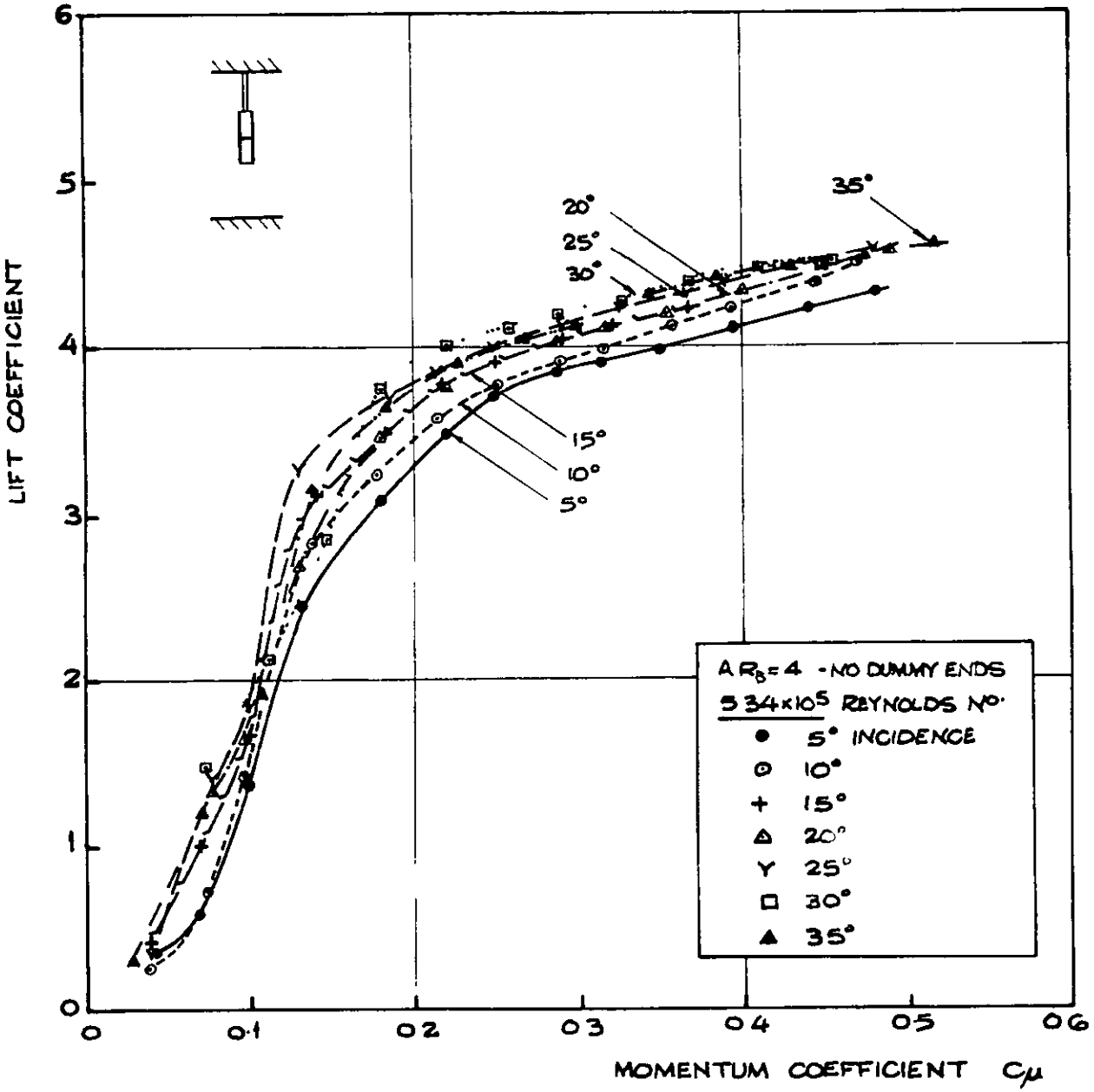

FIG. 8. EFFECT OF INCIDENCE ON LIFT COEFFICIENT (AT LOW MOMENTUM COEFFICIENT) OF AN $AR_B = 4$ MODEL.

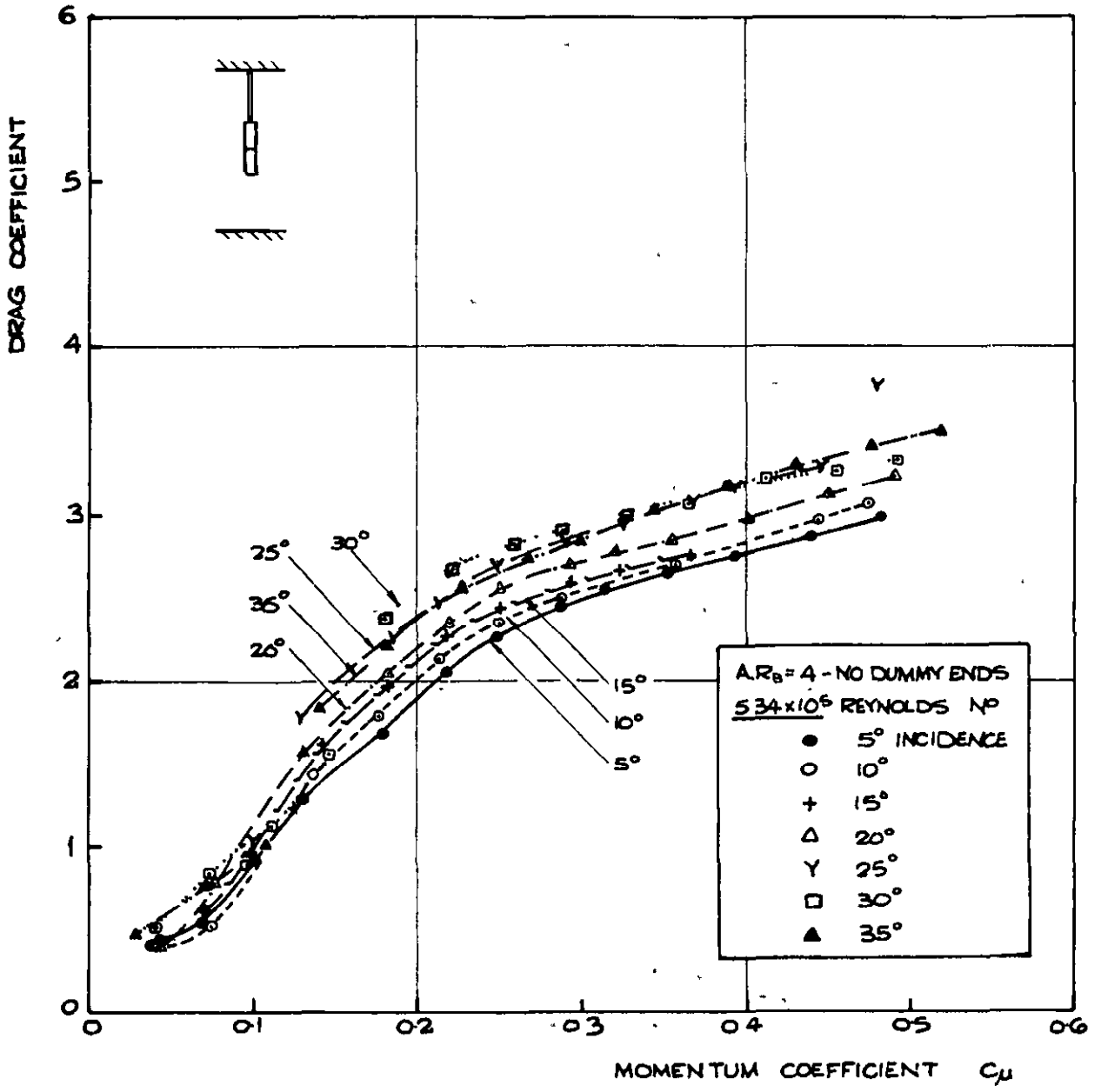

FIG. 9. EFFECT OF INCIDENCE ON DRAG COEFFICIENT (AT LOW MOMENTUM COEFFICIENT) OF AN $AR_B = 4$ MODEL.

FIG. 10.

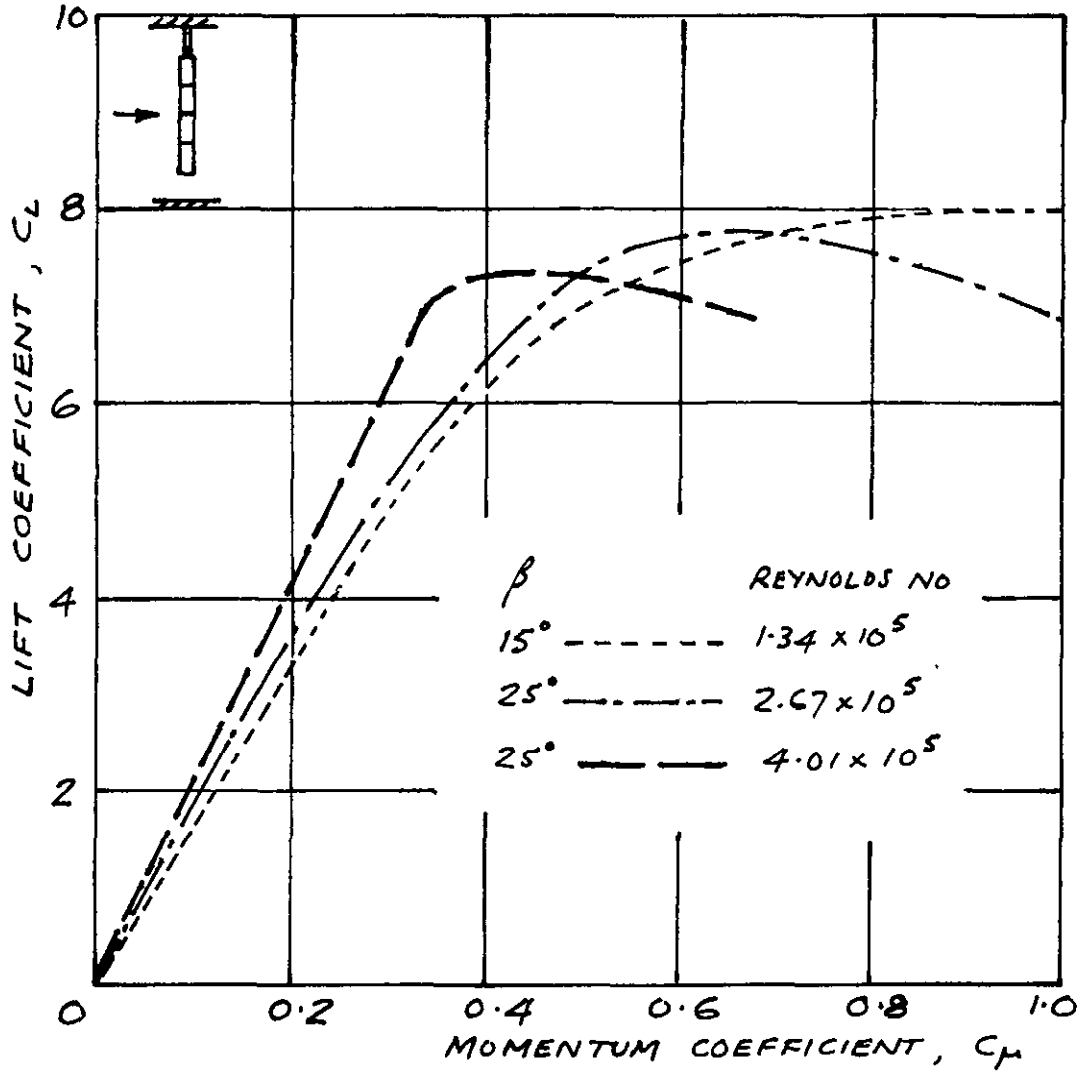

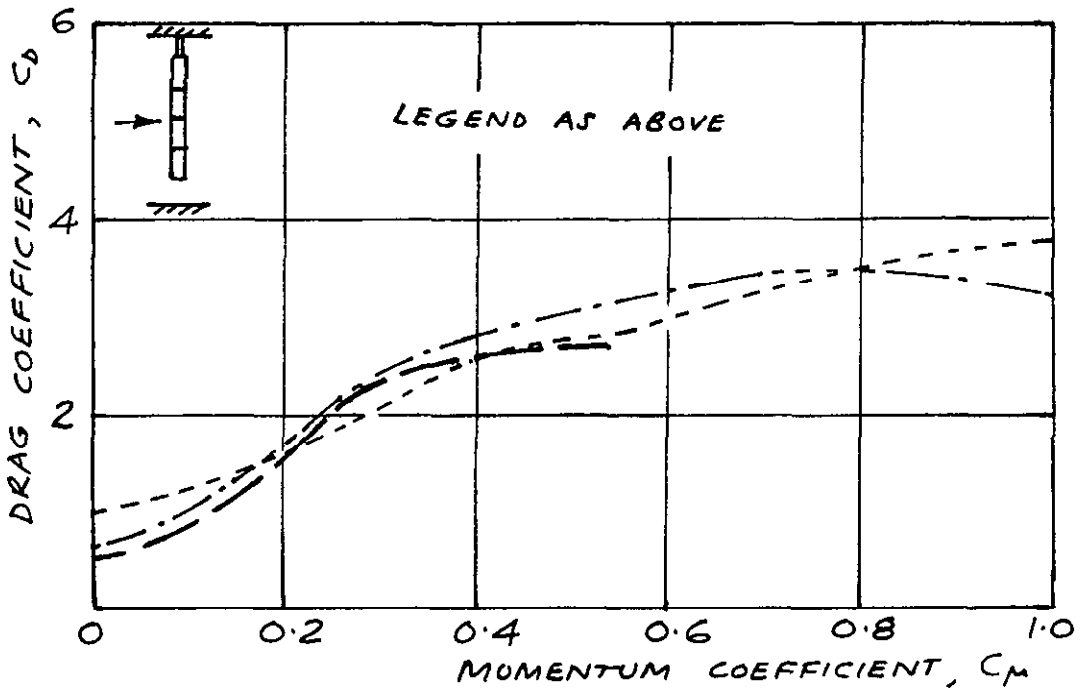

FIG. 10 EFFECT OF REYNOLDS NO. ON LIFT AND DRAG COEFFICIENT – SINGLE CYLINDER $AR_B = 8$.

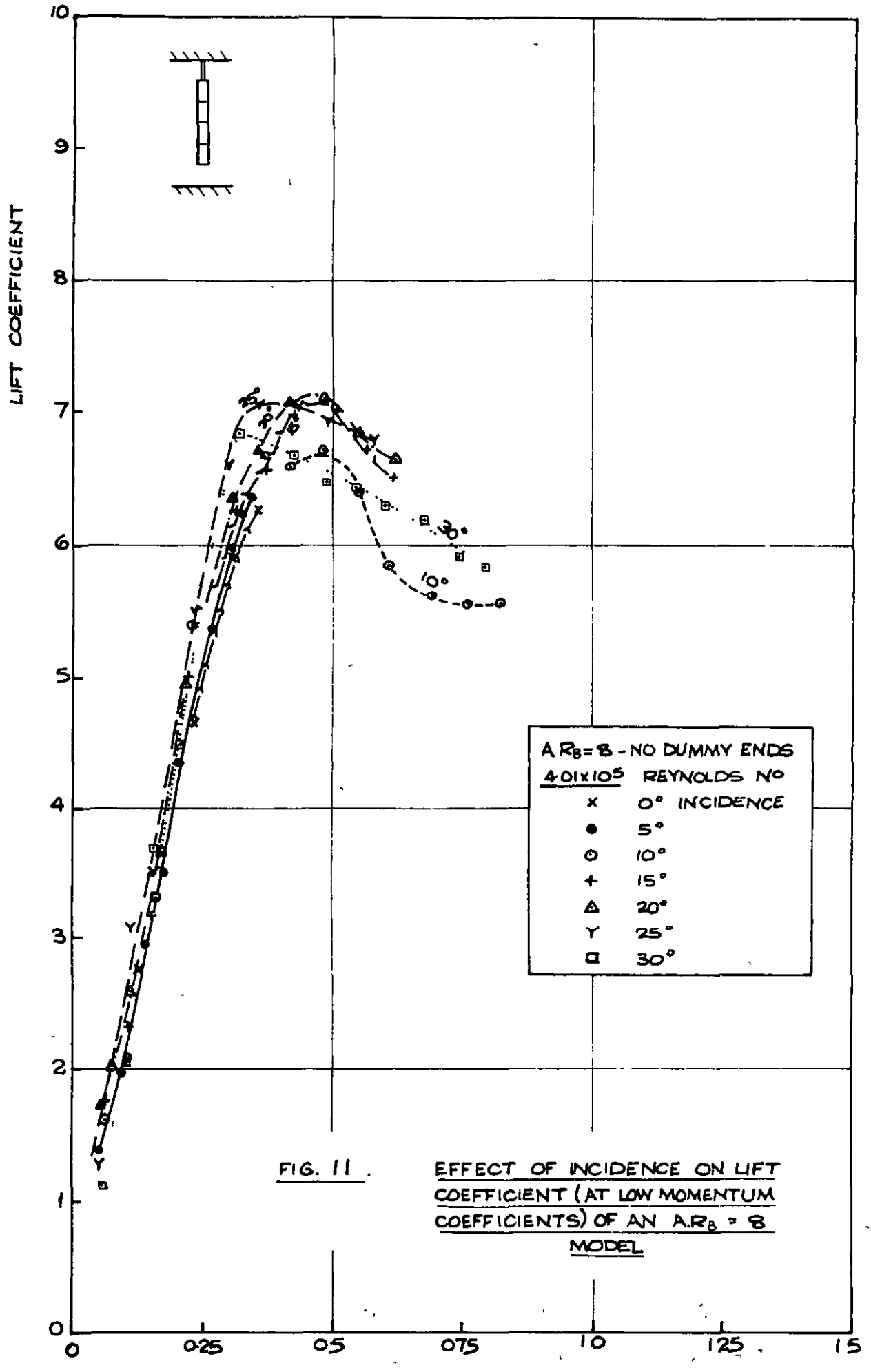

FIG. 11. EFFECT OF INCIDENCE ON LIFT COEFFICIENT (AT LOW MOMENTUM COEFFICIENTS) OF AN A.R_B = 8 MODEL

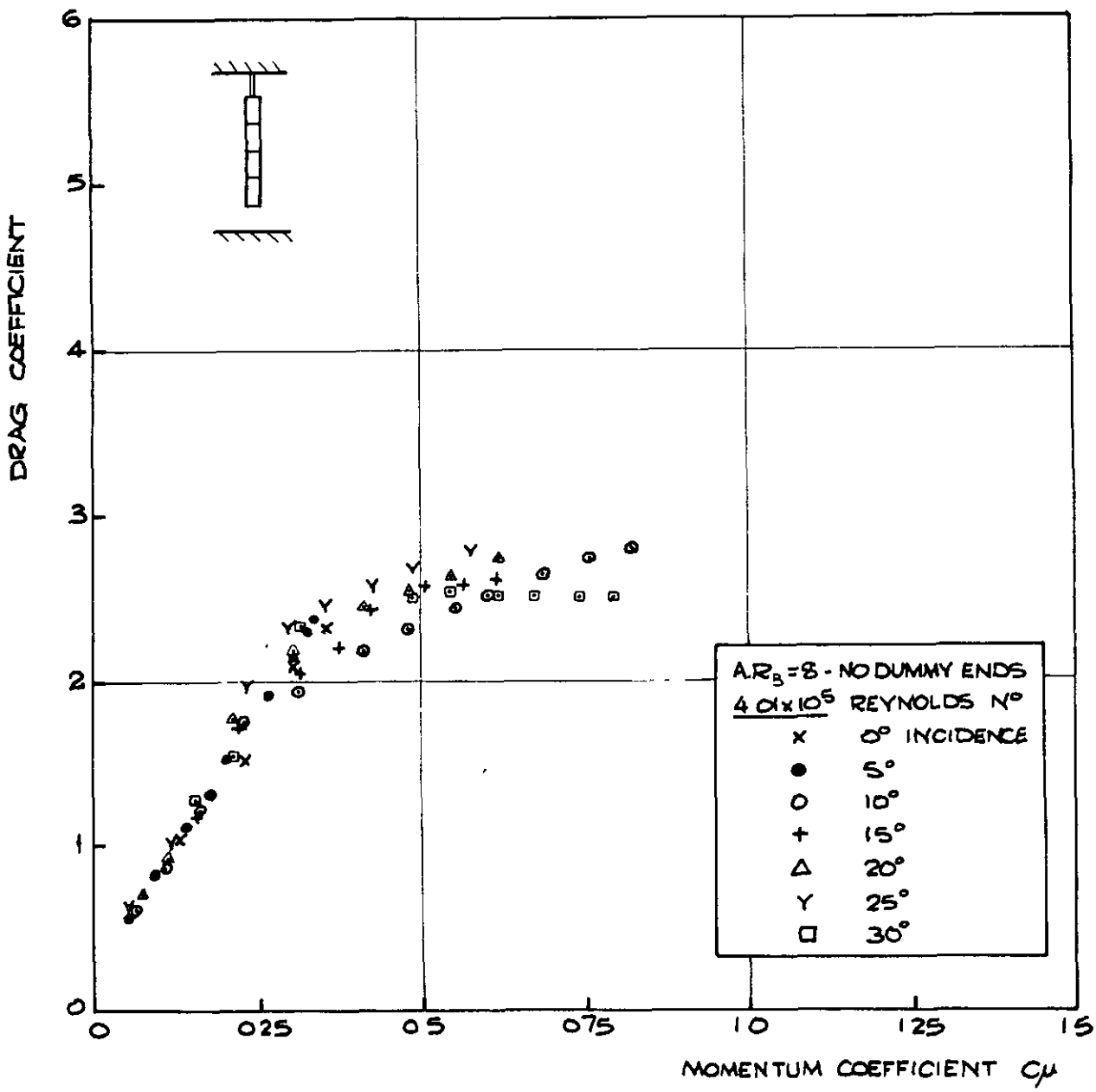

FIG 12 EFFECT OF INCIDENCE ON DRAG COEFFICIENT (AT LOW MOMENTUM COEFFICIENT) OF AN $AR_B = 8$ MODEL

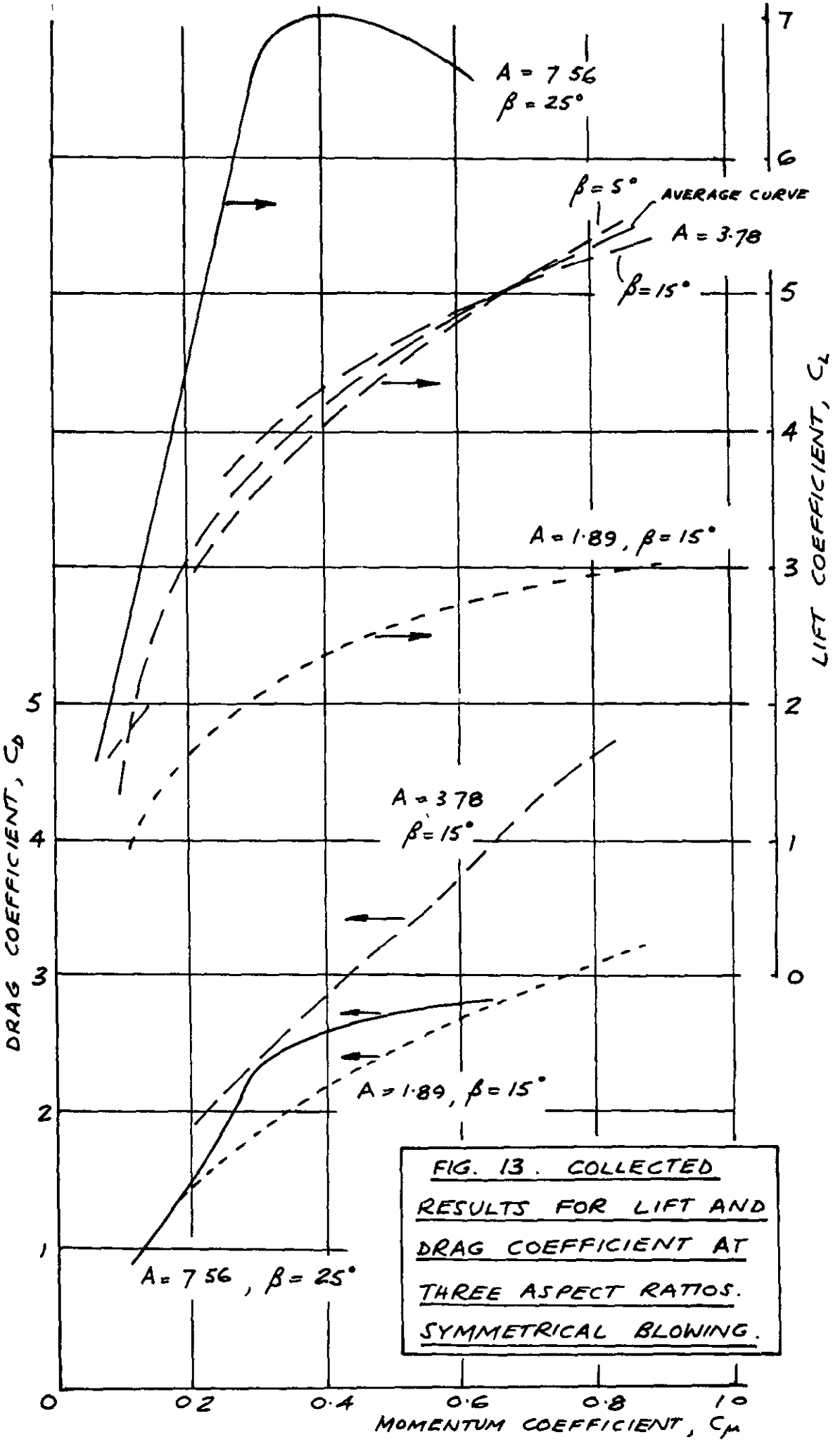

FIG. 13. COLLECTED RESULTS FOR LIFT AND DRAG COEFFICIENT AT THREE ASPECT RATIOS. SYMMETRICAL BLOWING.

FIG. 14.

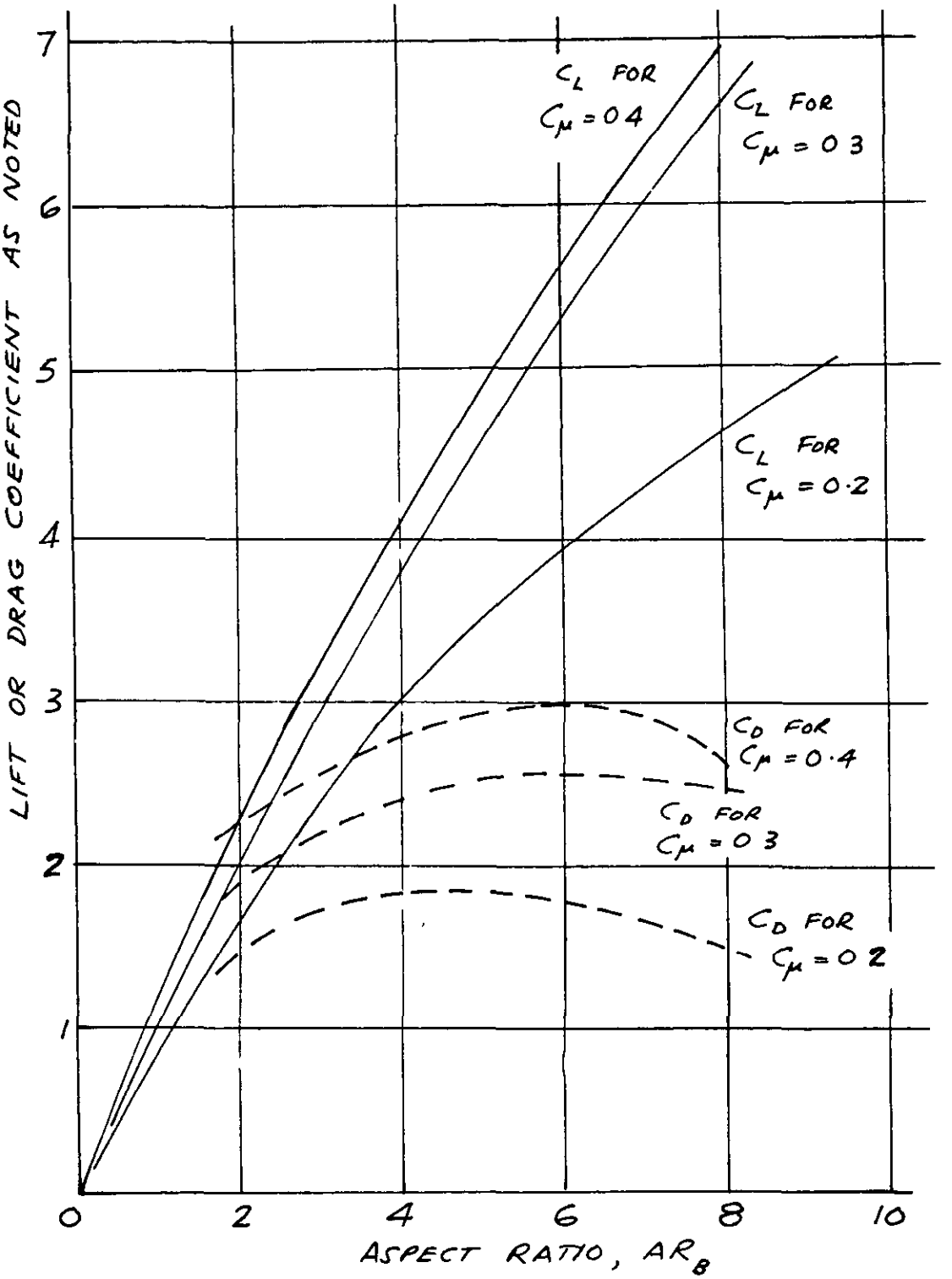

FIG. 14 (CROSS-PLOTTED FROM FIG. 13 OPPOSITE) EFFECT OF ASPECT RATIO AR_B ON LIFT AND DRAG COEFFICIENTS AT FIXED VALUE OF MOMENTUM COEFFICIENT, FOR FAVOURABLE INCIDENCE.

FIG. 15.

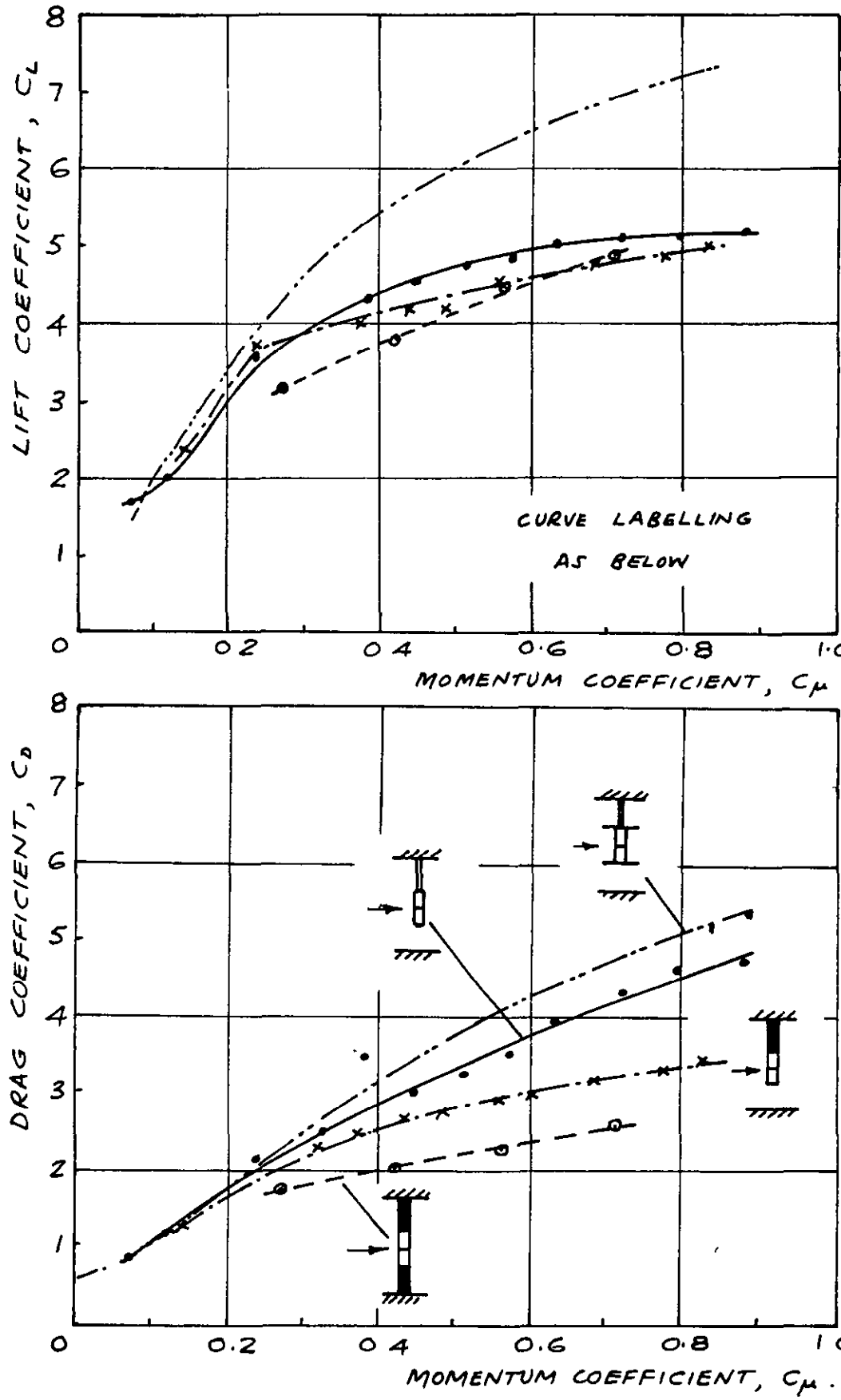

FIG 15. EFFECT OF END CONFIGURATIONS AS ILLUSTRATED ON LIFT AND DRAG COEFFICIENTS SYMMETRICAL BLOWING 15° INCIDENCE $Re_D = 4.01 \times 10^5$ $AR_B = 4$.

FIG. 16

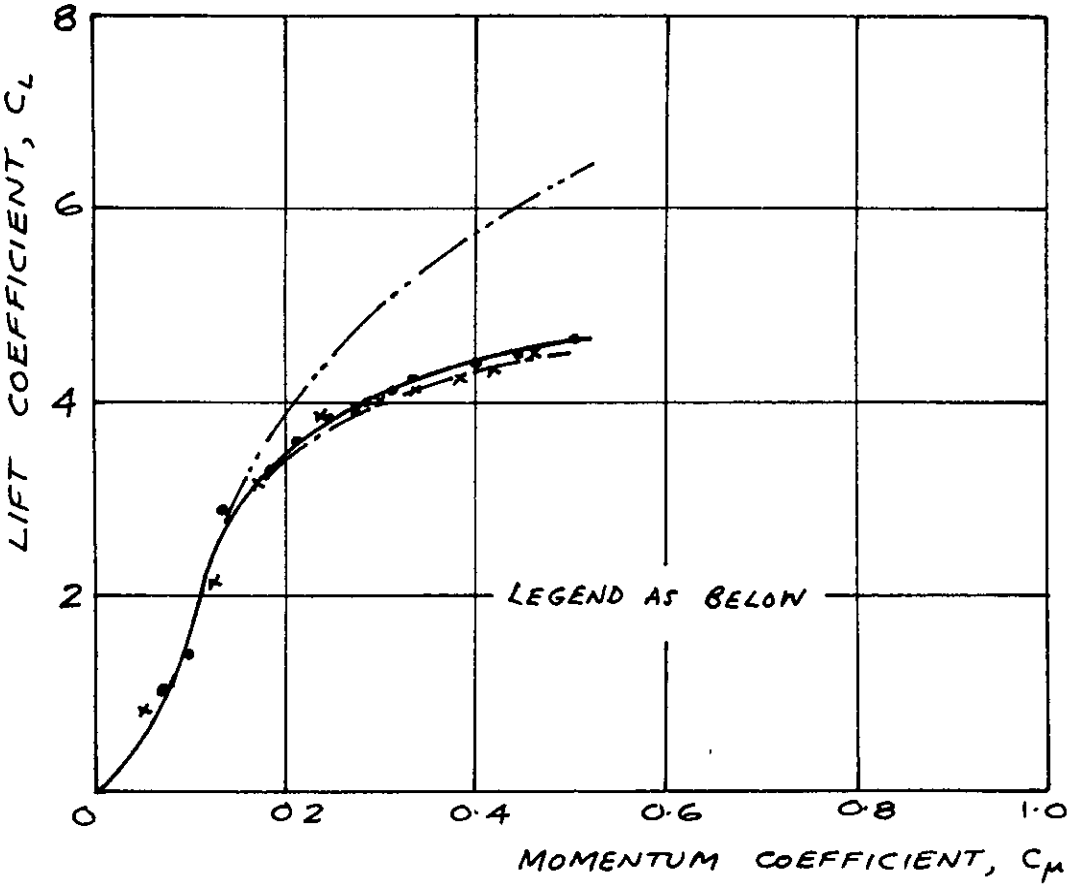

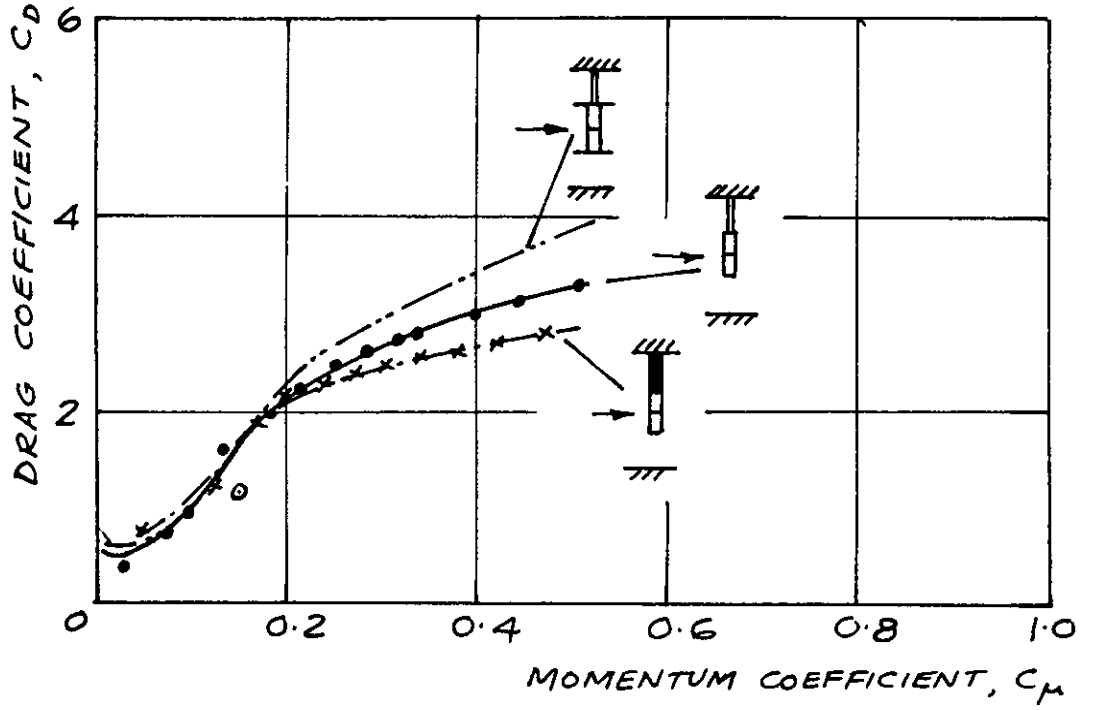

FIG. 16 EFFECT OF END CONFIGURATIONS AS ILLUSTRATED ON LIFT AND DRAG COEFFICIENTS SYMMETRICAL BLOWING 15° INCIDENCE $Re_D = 5.34 \times 10^5$ $AR_B = 4$

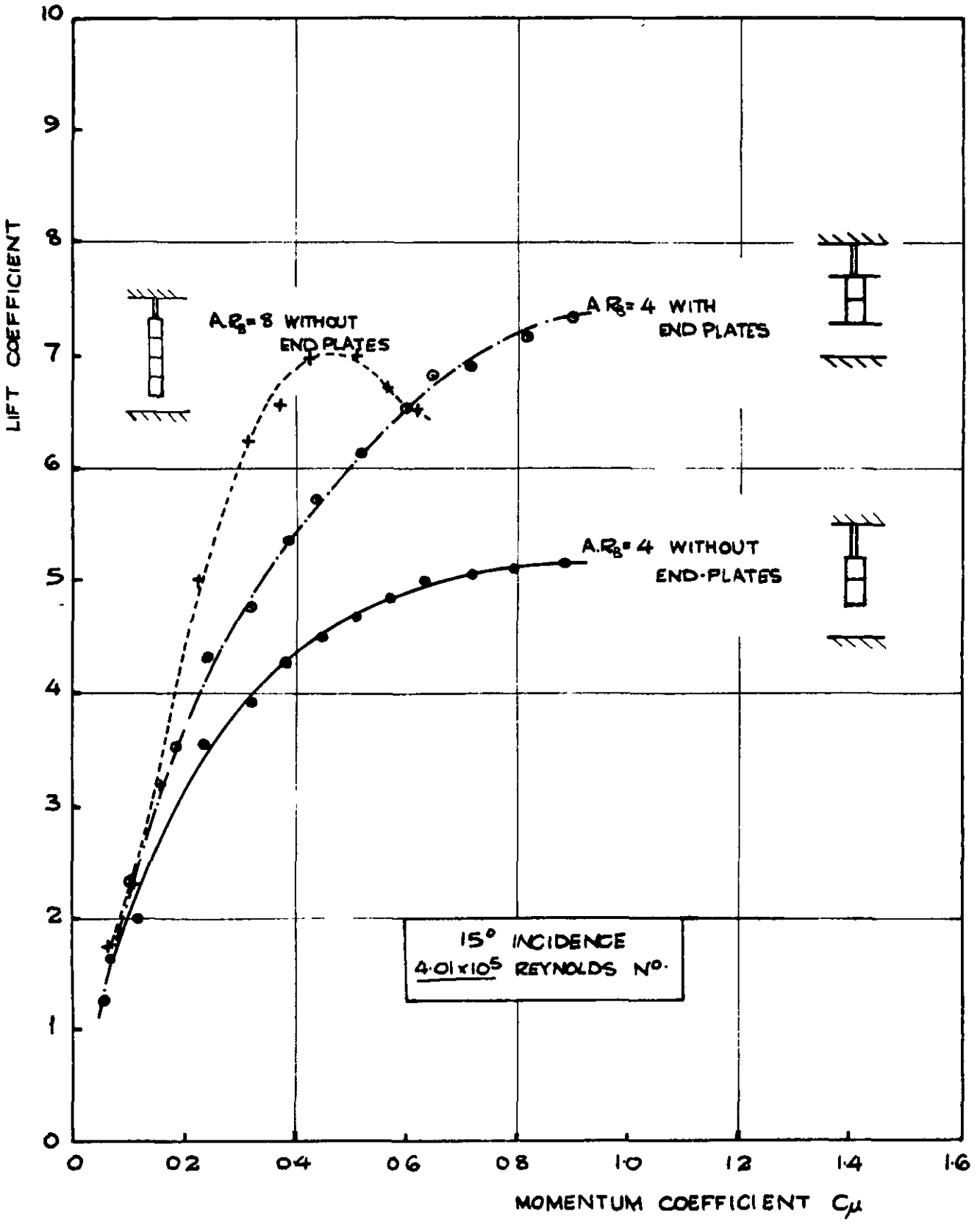

FIG 17 EFFECT OF CIRCULAR END PLATES ON LIFT COEFFICIENT

FIG. 18.

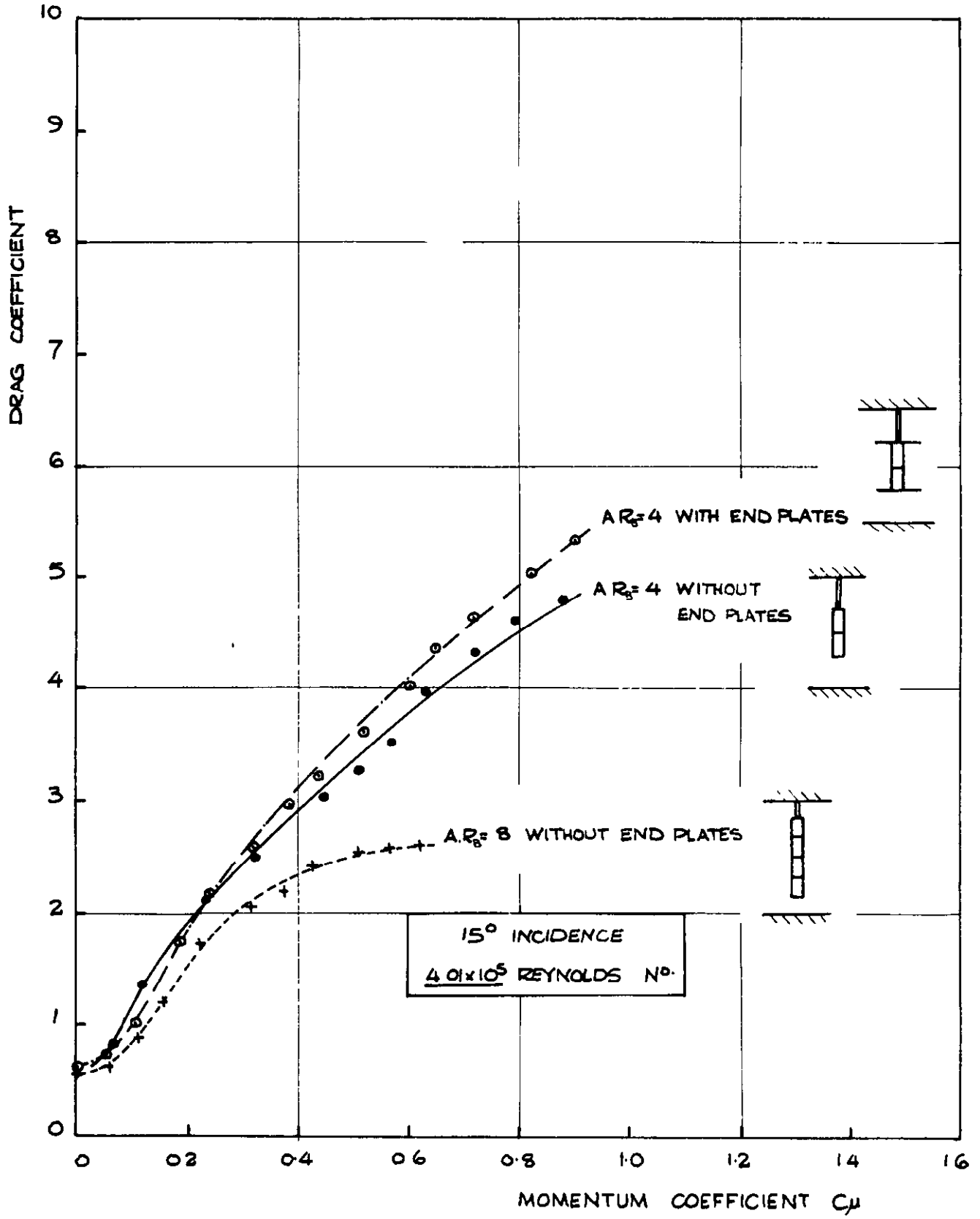

FIG 18. EFFECT OF CIRCULAR END PLATES ON DRAG COEFFICIENT

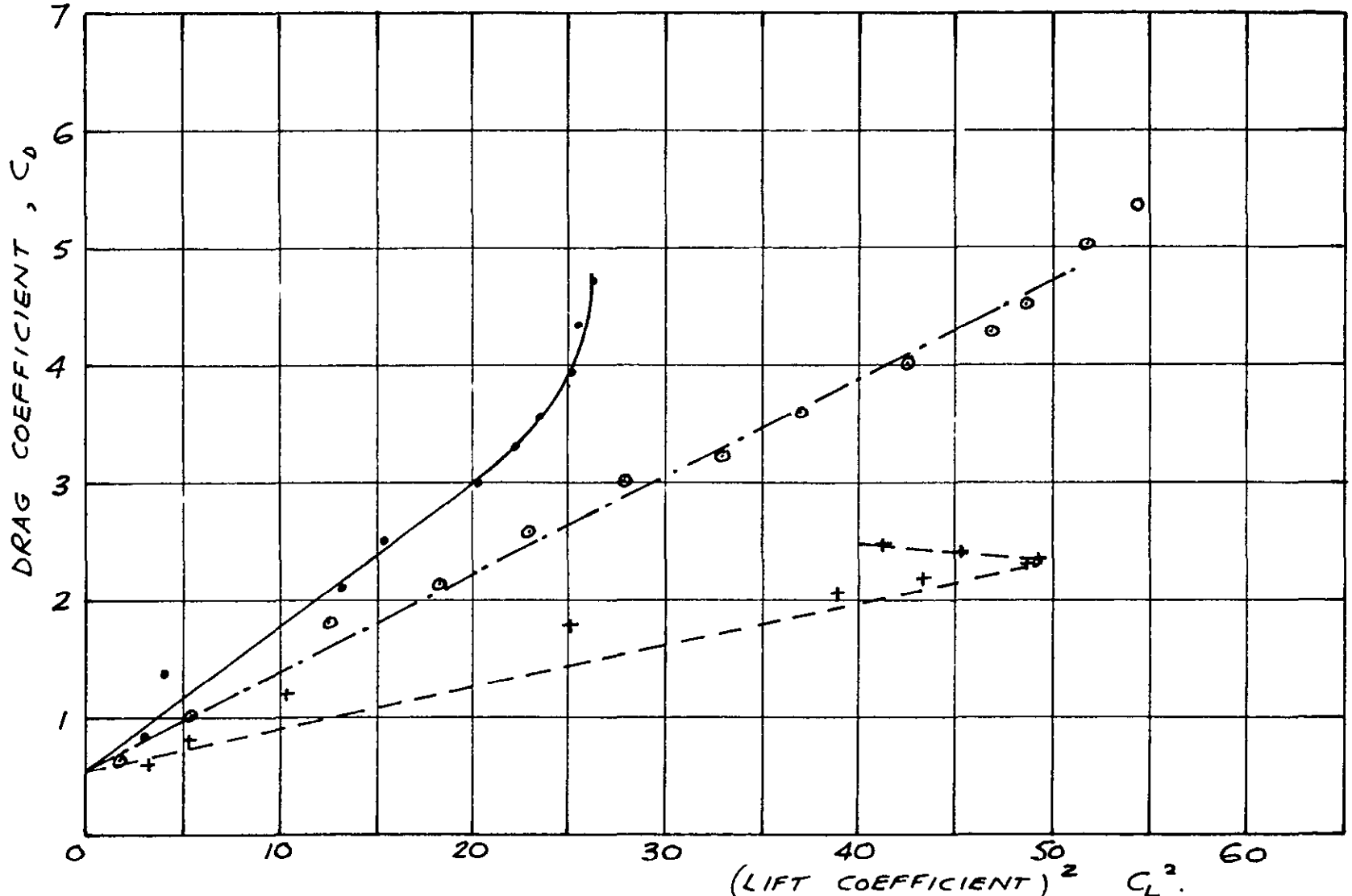

FIG. 19. EFFECT OF END-PLATES; C_D vs C_L^2.

15° INCIDENCE , $Re_D = 4.01 \times 10^5$.

FIG. 19.

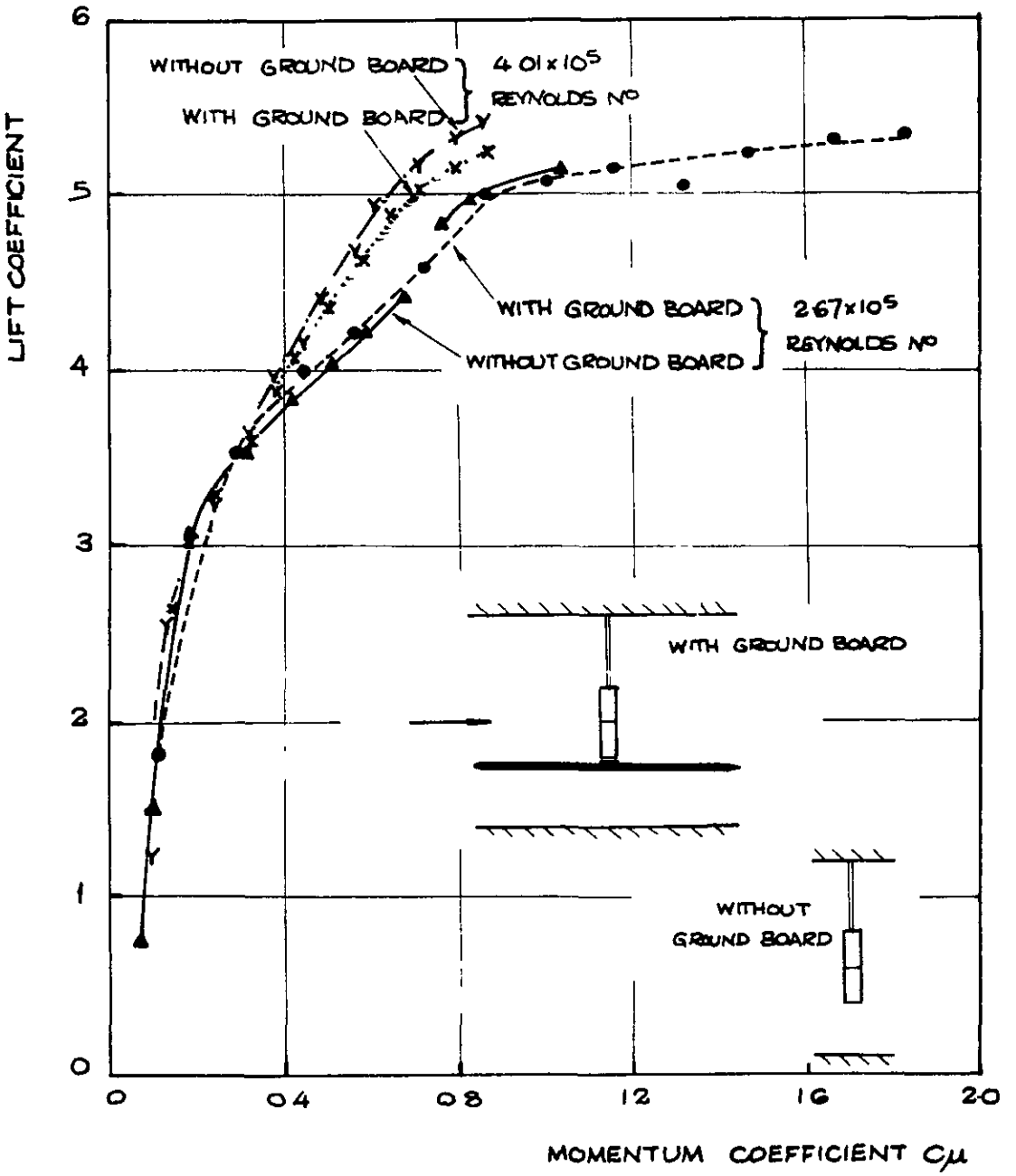

FIG 20 EFFECT OF A GROUND BOARD AT THE TIP OF AN $AR_B = 4$ MODEL (SYMMETRICALLY BLOWN) ON LIFT COEFFICIENT 5° INCIDENCE

FIG 21.

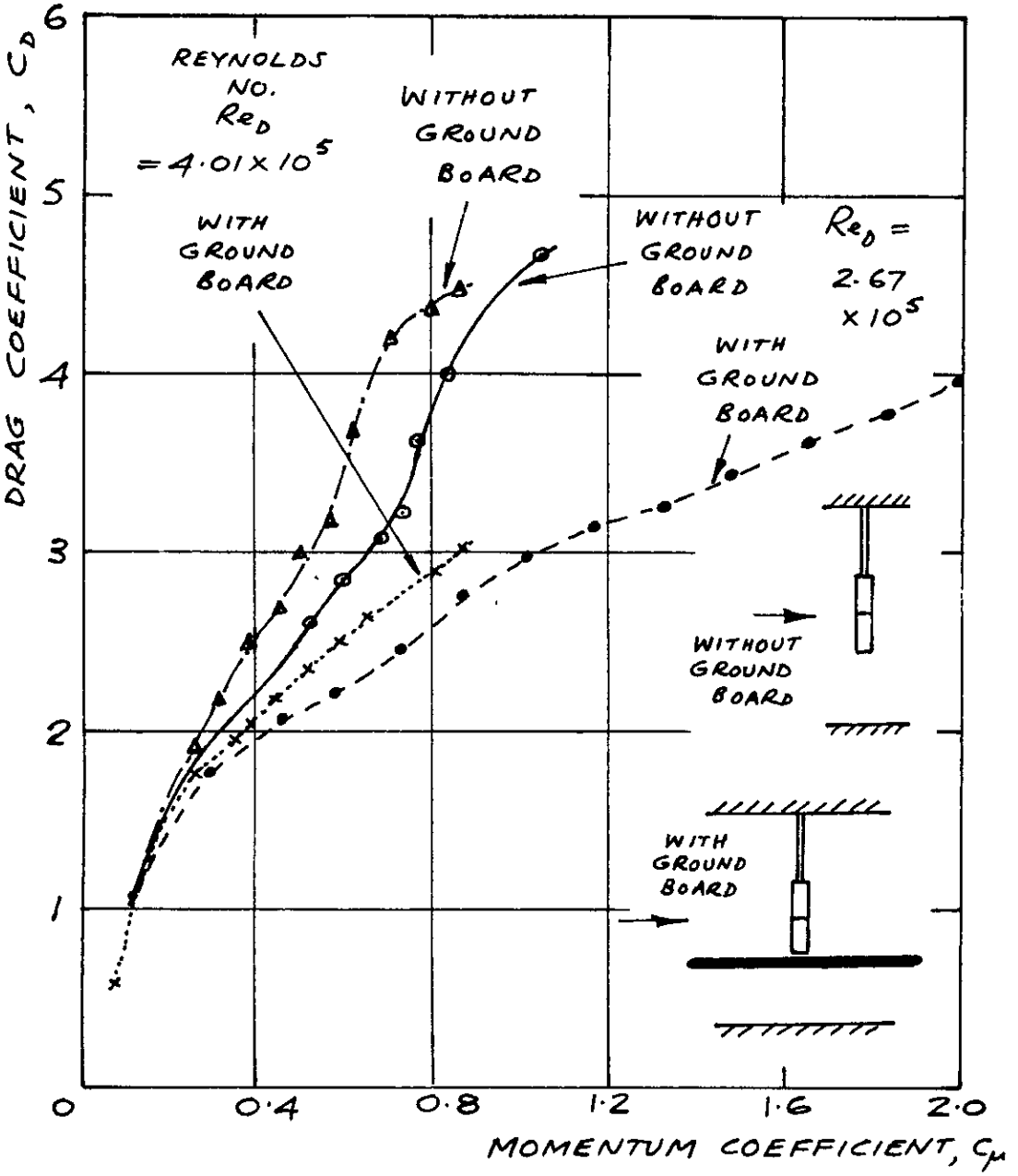

FIG. 21. EFFECT OF A GROUND BOARD AT THE TIP OF AN $AR_B = 4$ MODEL (SYMMETRICALLY BLOWN) ON DRAG COEFFICIENT. 5° INCIDENCE

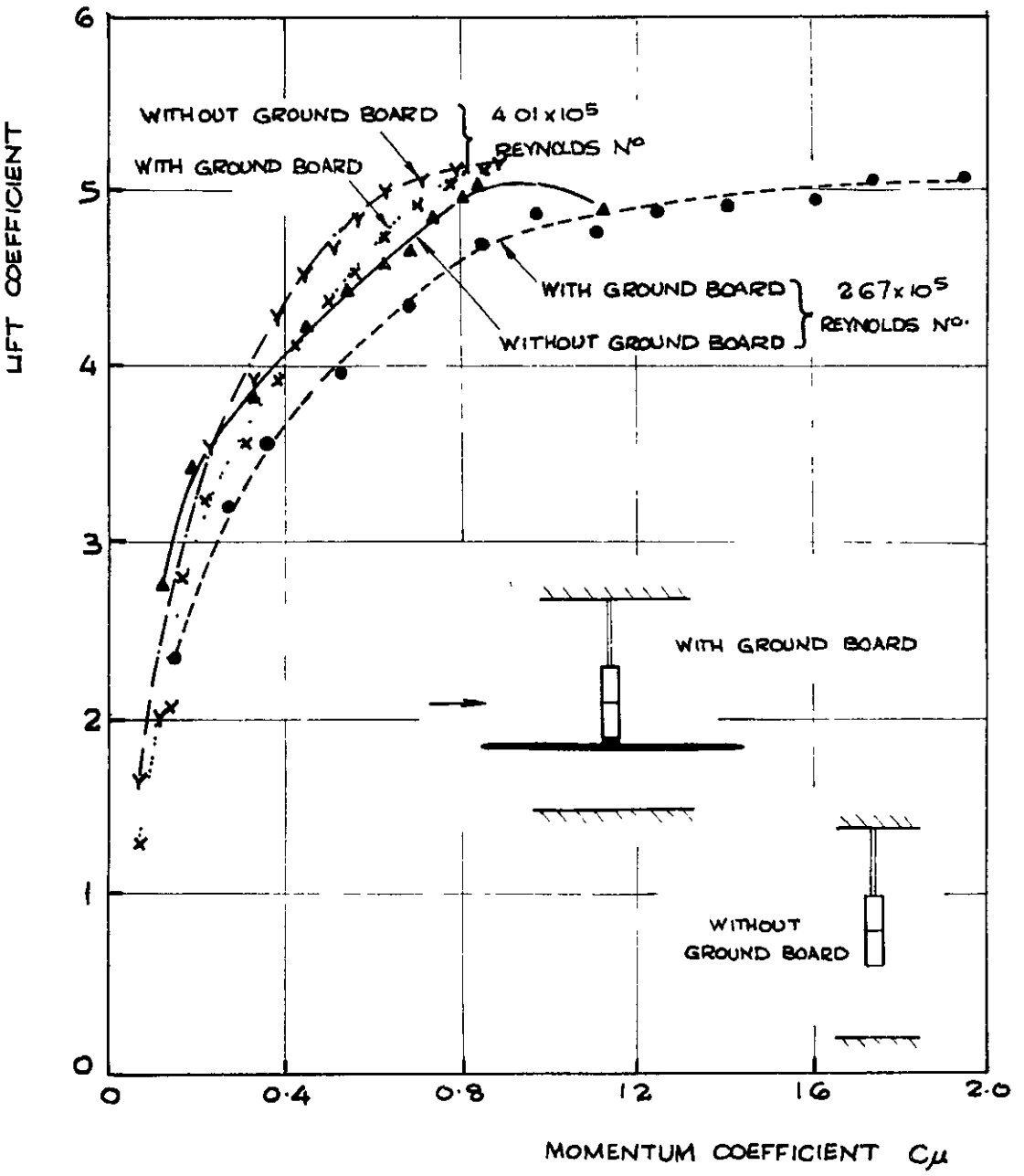

FIG 22 EFFECT OF A GROUND BOARD AT THE TIP OF AN $AR_B = 4$ MODEL (SYMMETRICALLY BLOWN) ON LIFT COEFFICIENT 15° INCIDENCE

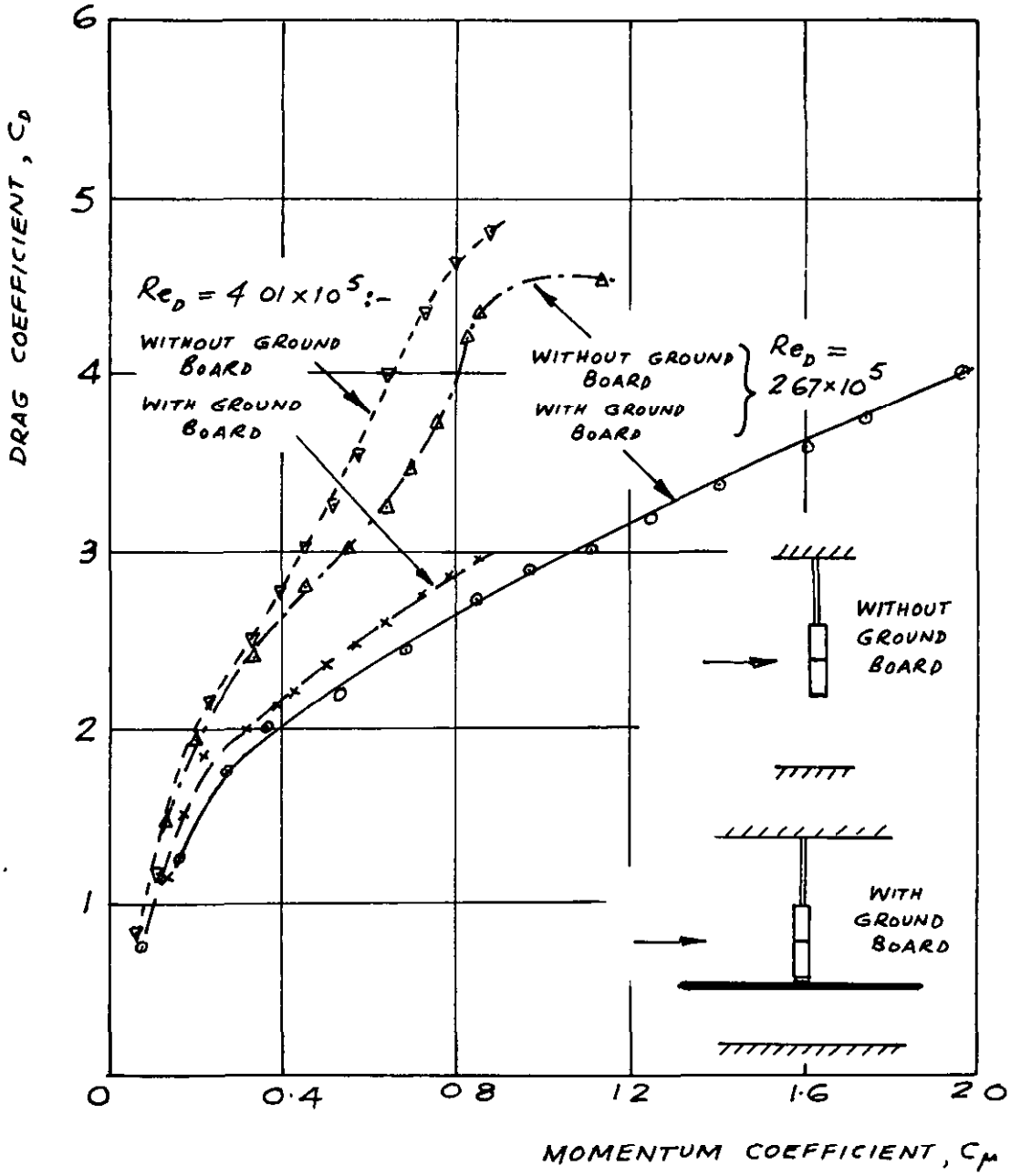

FIG. 23. EFFECT OF A GROUND BOARD ON DRAG COEFFICIENT, $AR_B = 4$, SLOT INCIDENCE = 15°, SYMMETRICALLY BLOWN

FIG. 24.

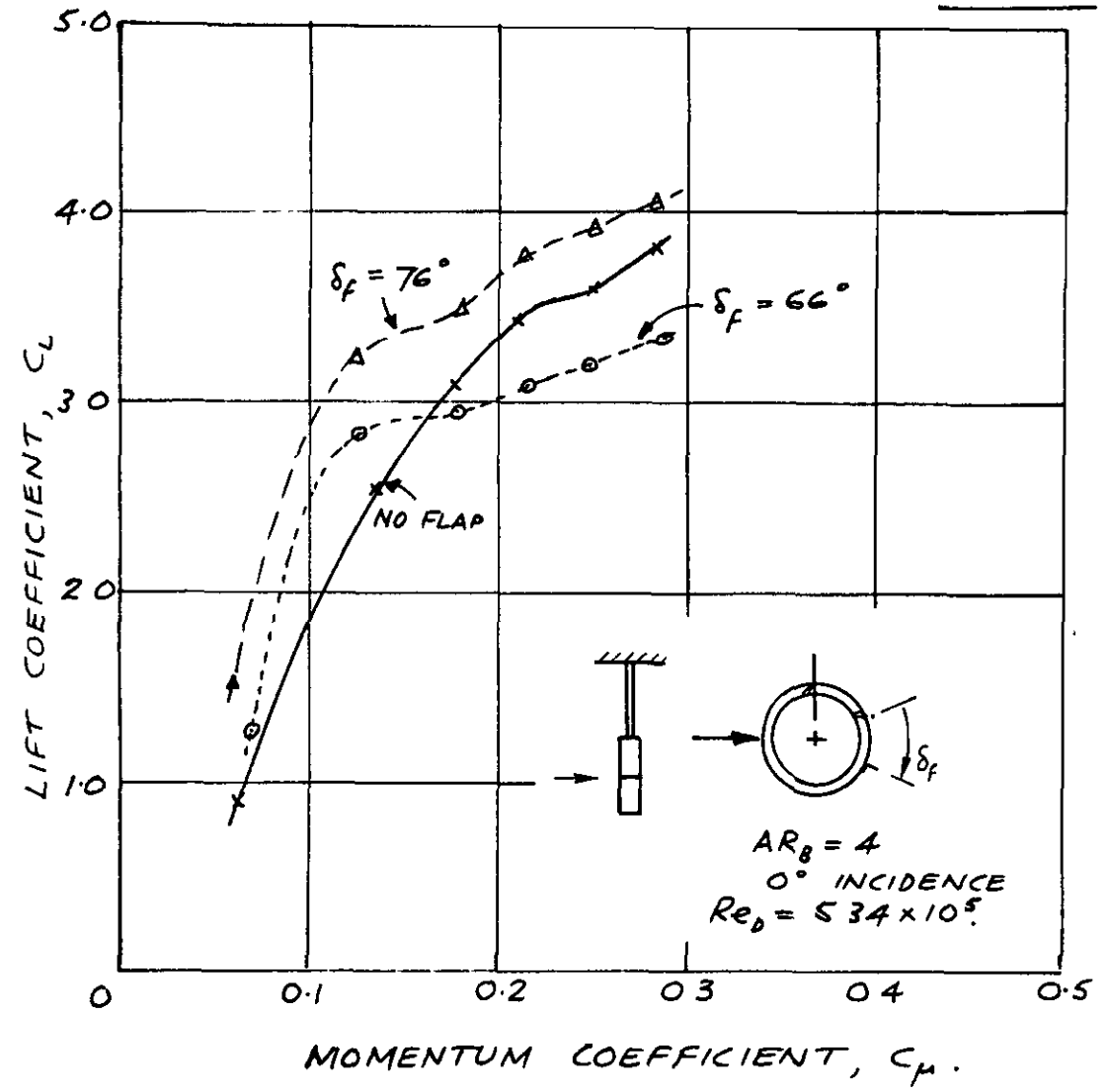

FIG 24. EFFECT OF A FLAP ON LIFT AND DRAG AT HIGH REYNOLDS NO. — SINGLE CYLINDER, $AR_B = 4$; INCLUDING SIMPLE JET FLAP THEORY RESULTS.

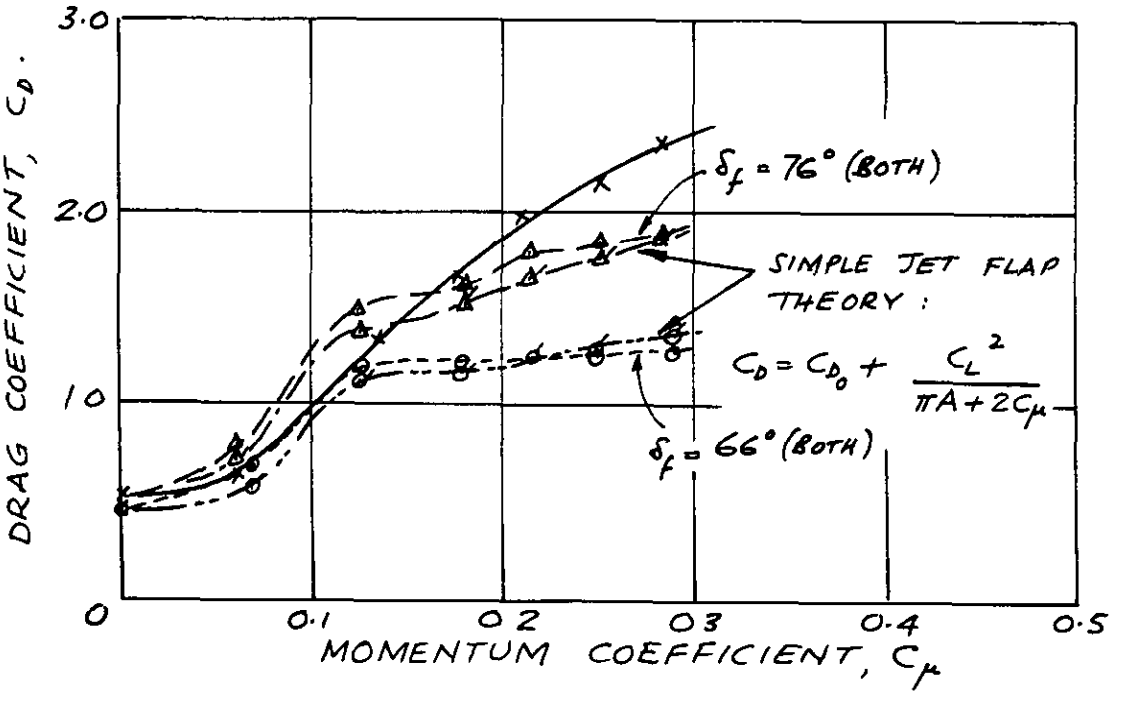

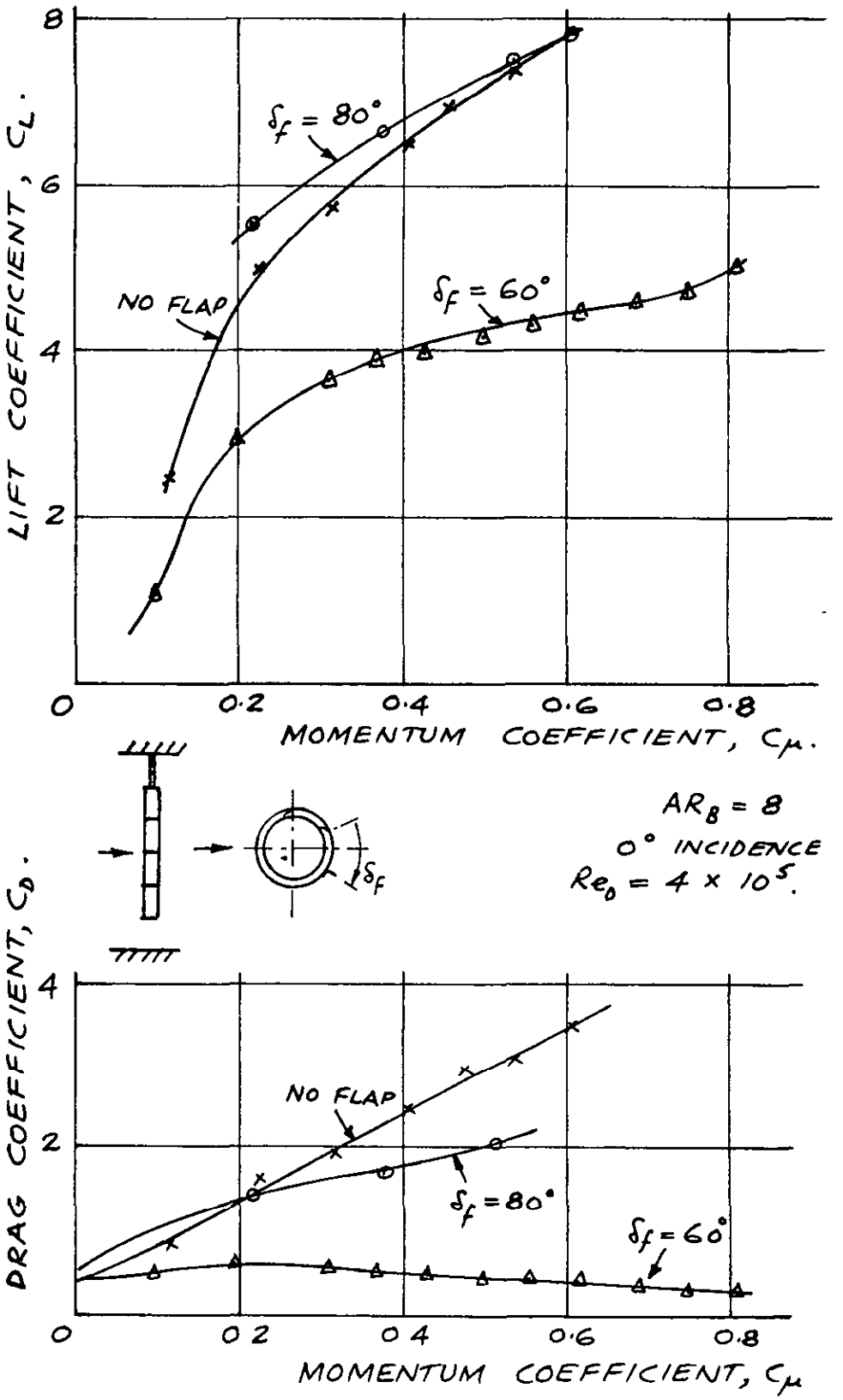

FIG. 25 EFFECT OF A FLAP ON LIFT AND DRAG AT HIGH REYNOLDS NO. SINGLE CYLINDER, $AR_B = 8$, SYMMETRICALLY BLOWN.

FIG. 26.

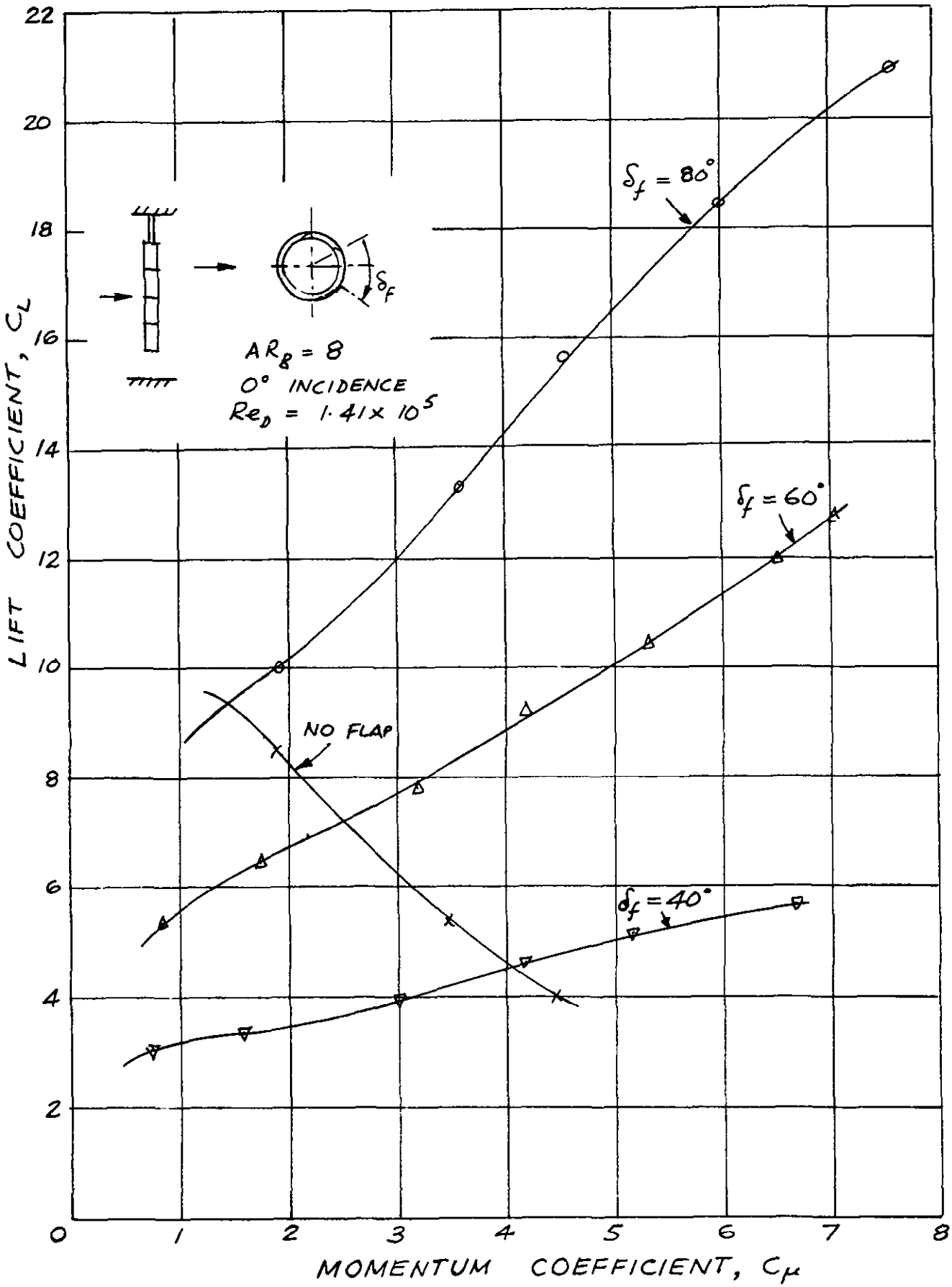

FIG. 26. EFFECT OF USE OF A FLAP ON LIFT AT LOW REYNOLDS NO. SINGLE CYLINDER, SYMMETRICALLY BLOWN, $AR_B = 8$

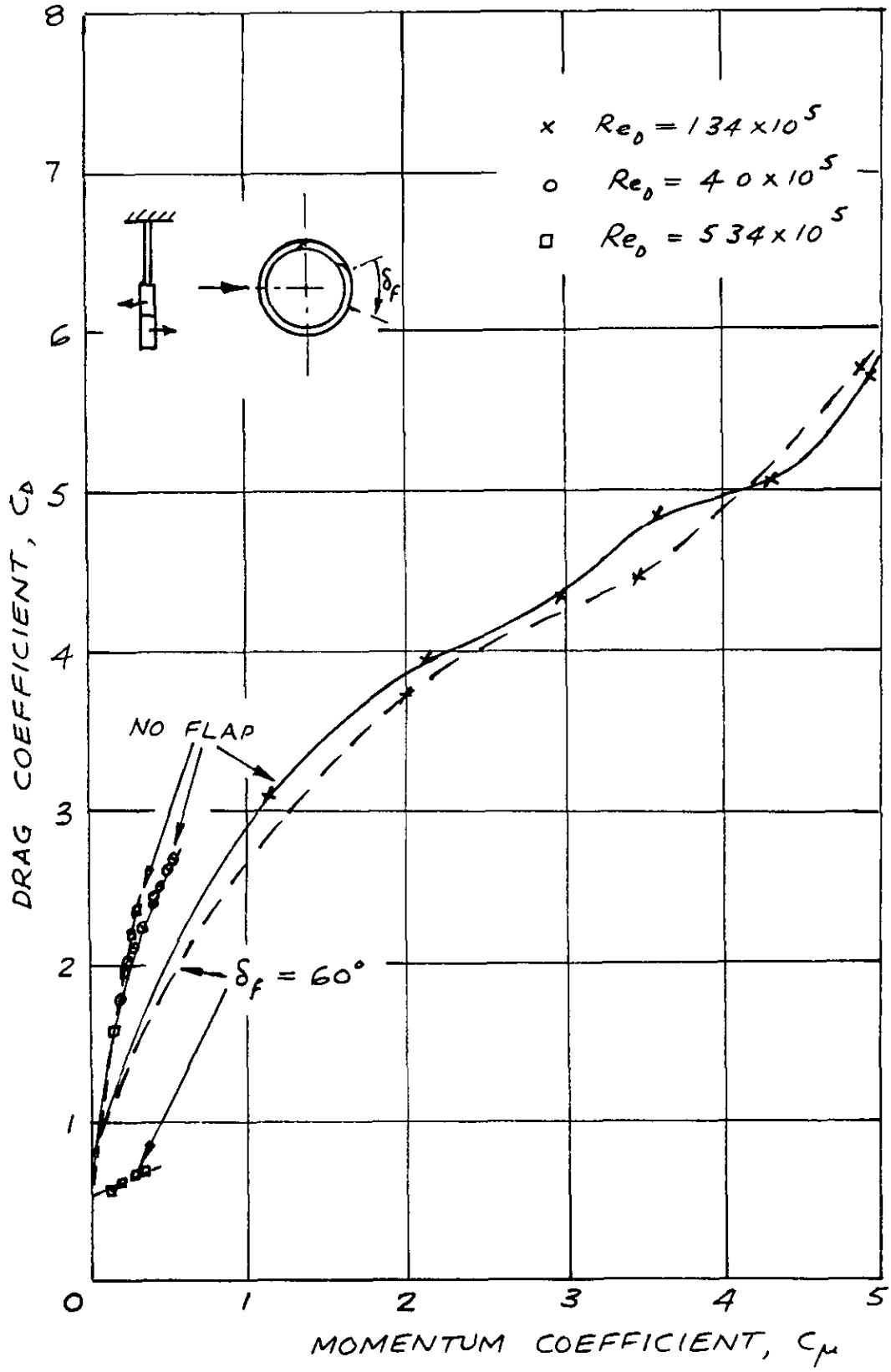

FIG 27 EFFECT OF USE OF A FLAP ON DRAG COEFFICIENT PRODUCED USING OPPOSED BLOWING. TOTAL $AR_B = 4$ $\beta = -10°$

FIG. 28

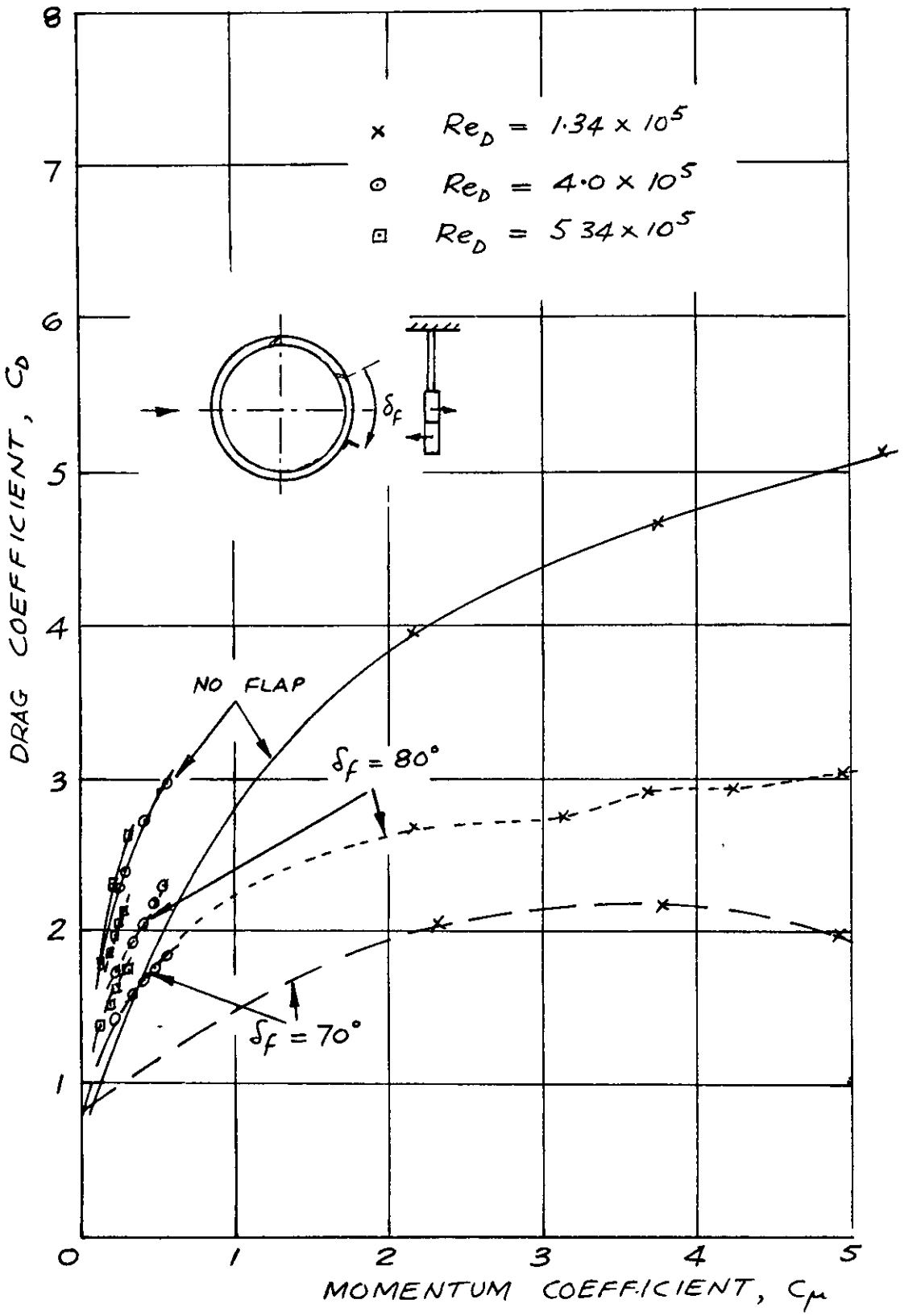

FIG 28. EFFECT OF USE OF A FLAP ON DRAG COEFFICIENT PRODUCED BY OPPOSED BLOWING $\beta = 0°$ TOTAL $AR_B = 4$

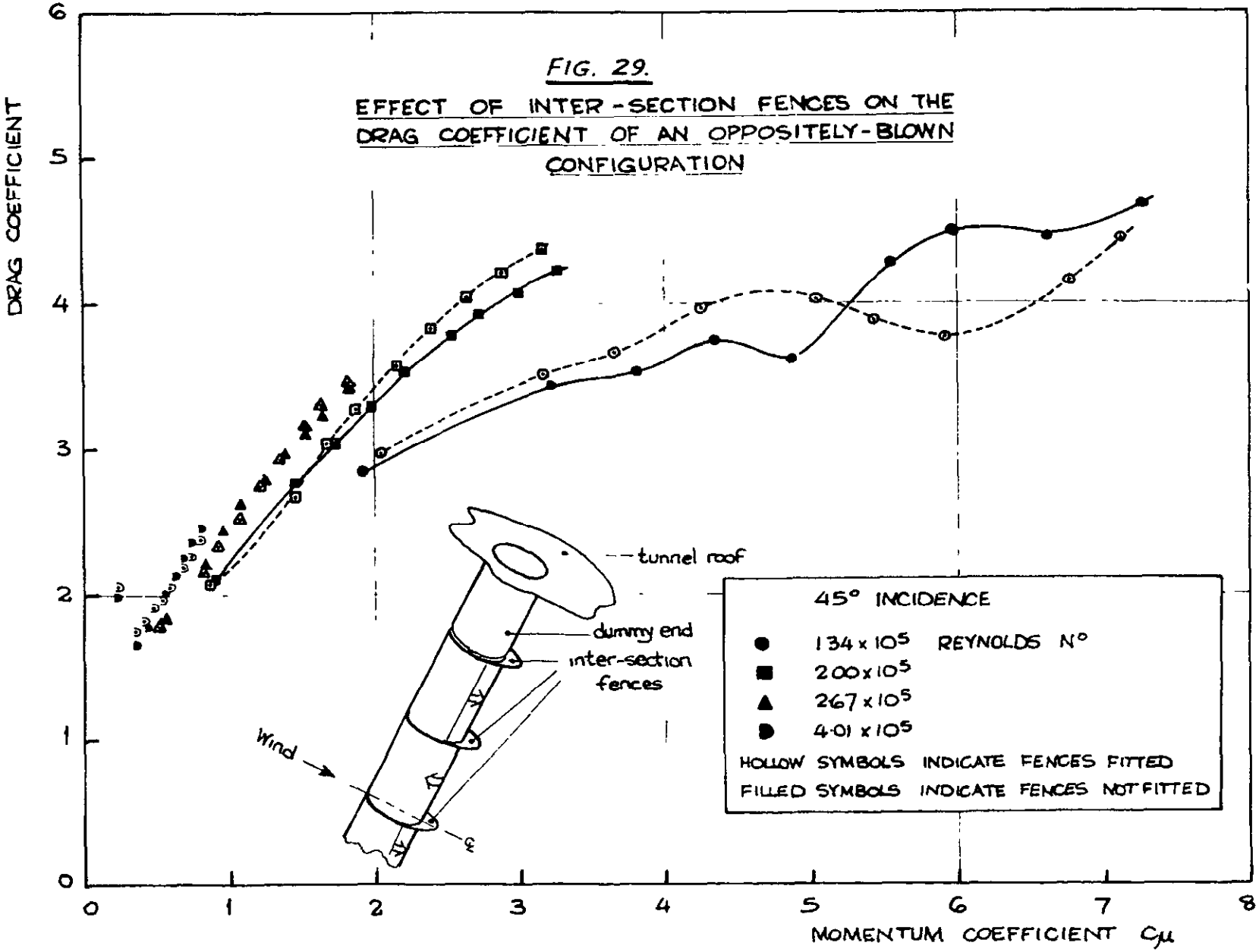
FIG. 29.
EFFECT OF INTER-SECTION FENCES ON THE DRAG COEFFICIENT OF AN OPPOSITELY-BLOWN CONFIGURATION
DRAG COEFFICIENT
MOMENTUM COEFFICIENT Cμ
0
1
2
3
4
5
6
7
8
tunnel roof
dummy end
inter-section fences
Wind
45° INCIDENCE
134 x 10⁵ REYNOLDS N°
200 x 10⁵
267 x 10⁵
4·01 x 10⁵
HOLLOW SYMBOLS INDICATE FENCES FITTED
FILLED SYMBOLS INDICATE FENCES NOT FITTED

FIG. 29.

FIG. 30.

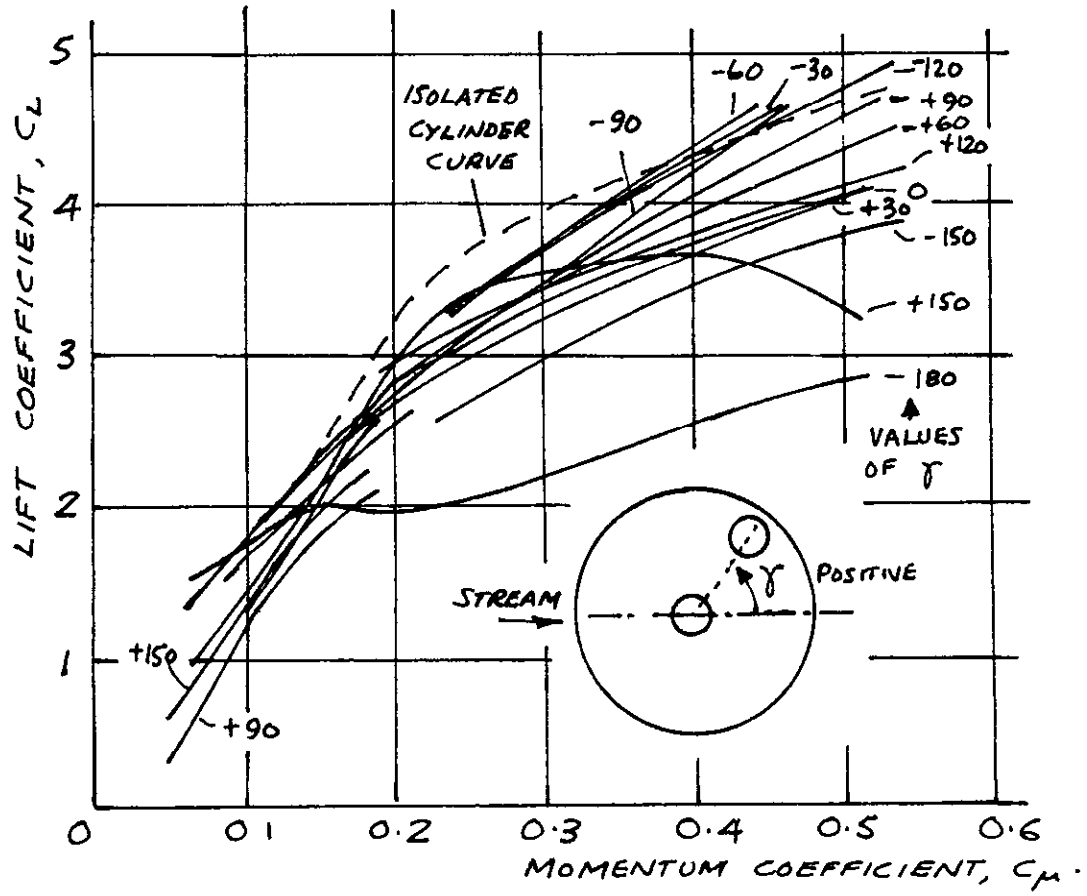

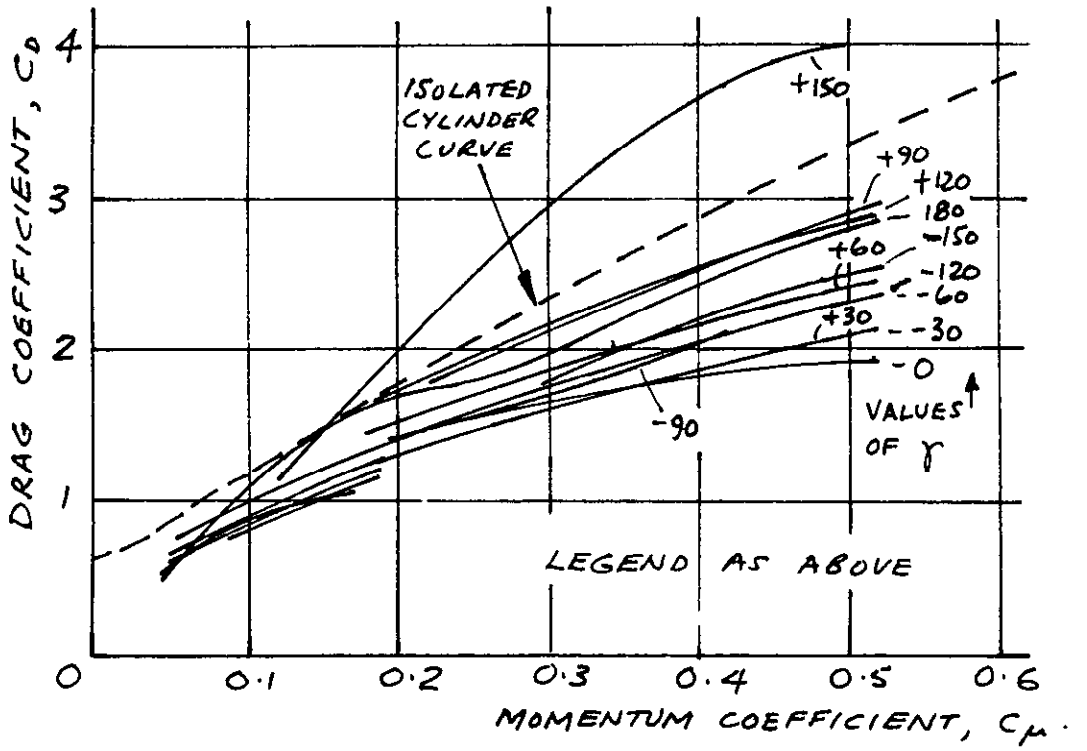

FIG. 30. LIFT AND DRAG COEFFICIENTS OF CYLINDERS WITH MUTUAL INTERFERENCE; SYMMETRICAL BLOWING. $Re_D = 4{\cdot}01 \times 10^5$. $\beta = 15°$.

FIG. 31.

RESTRICTED

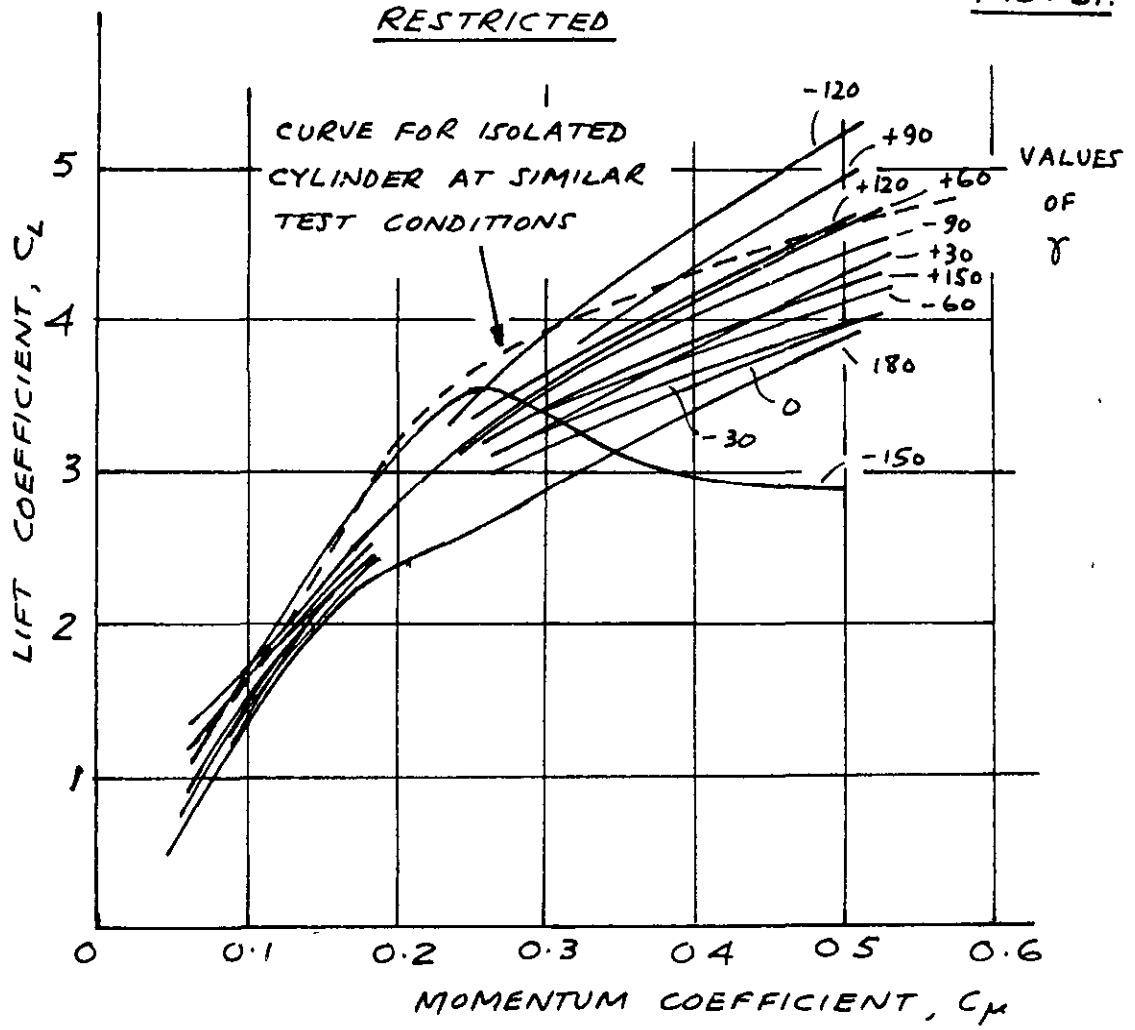

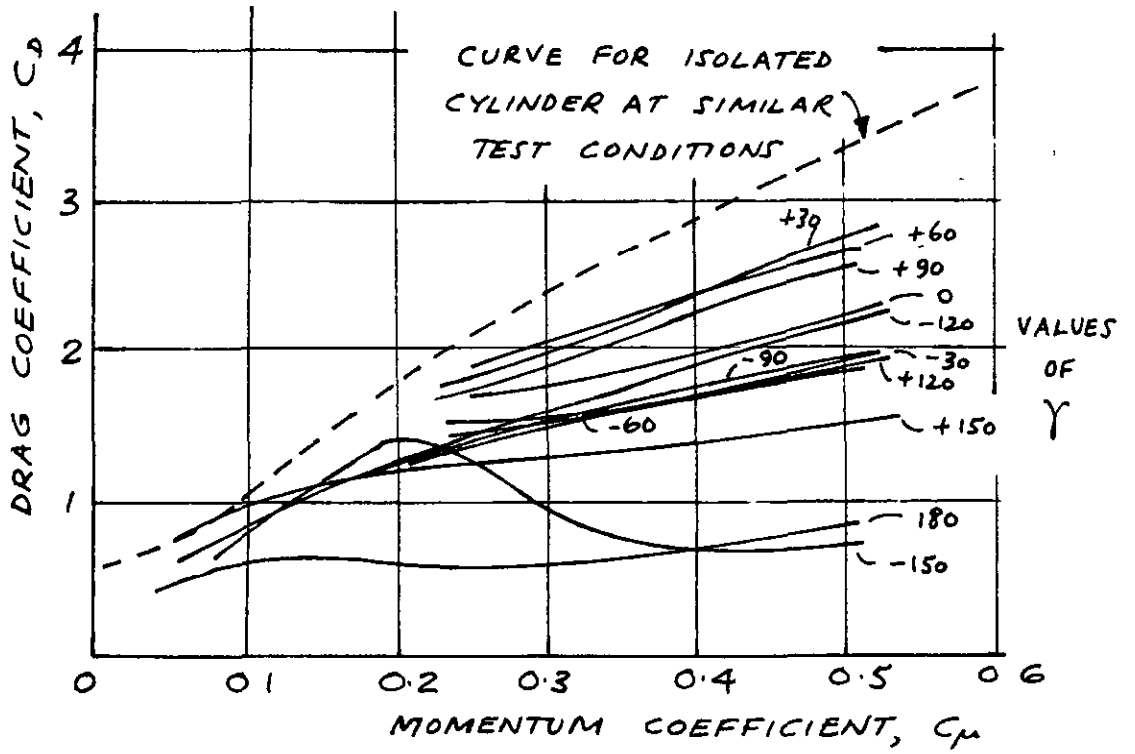

FIG. 31. LIFT AND DRAG COEFFICIENTS OF CYLINDERS WITH MUTUAL INTERFERENCE; OPPOSED BLOWING.

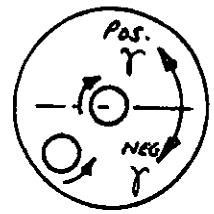

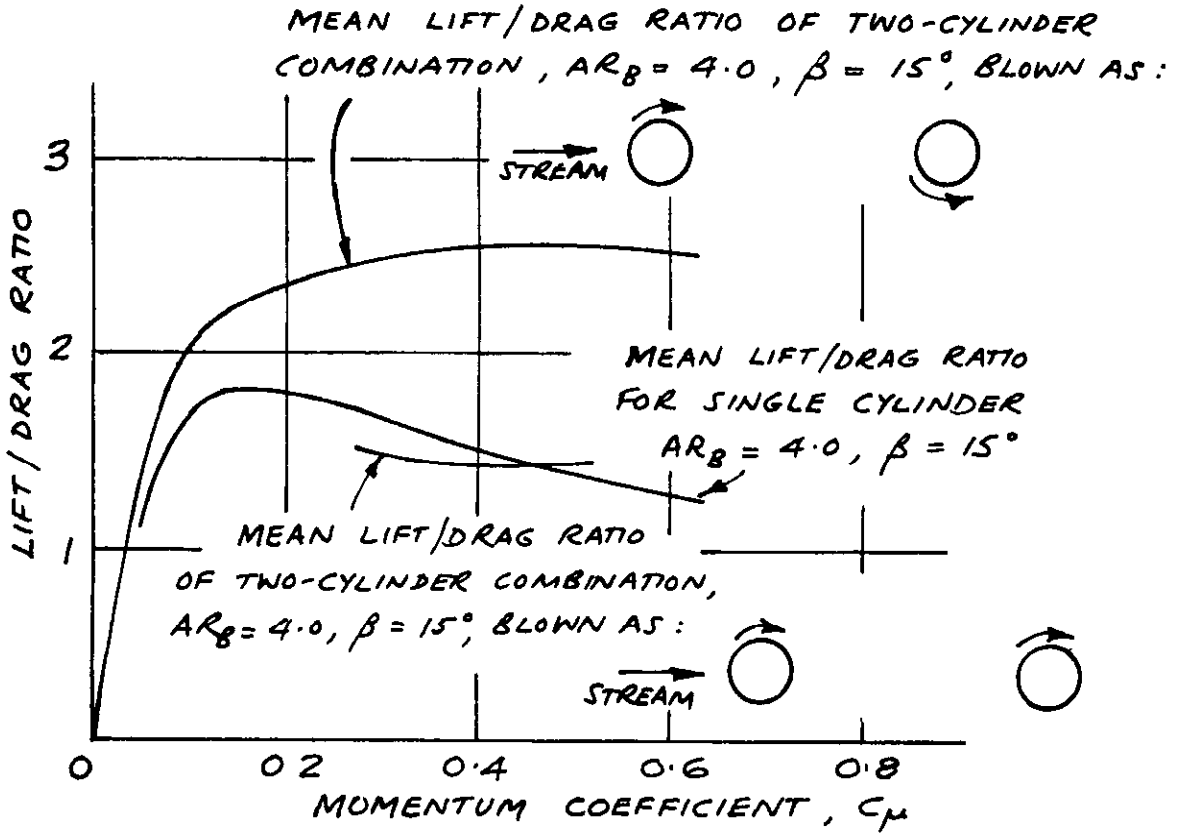

FIG. 32. (ABOVE AND RIGHT). EFFECT OF MUTUAL INTERFERENCE BETWEEN TWO CYLINDERS, DISPOSED AND BLOWN AS SHOWN, ON LIFT, DRAG AND L/D RATIO. SINGLE CYLINDER RESULTS SHOWN FOR COMPARISON. $AR_B = 4.0$, SLOT INCIDENCE $\beta = 15°$, REYNOLDS NO. $Re_D = 4.01 \times 10^5$.

FIG. 32

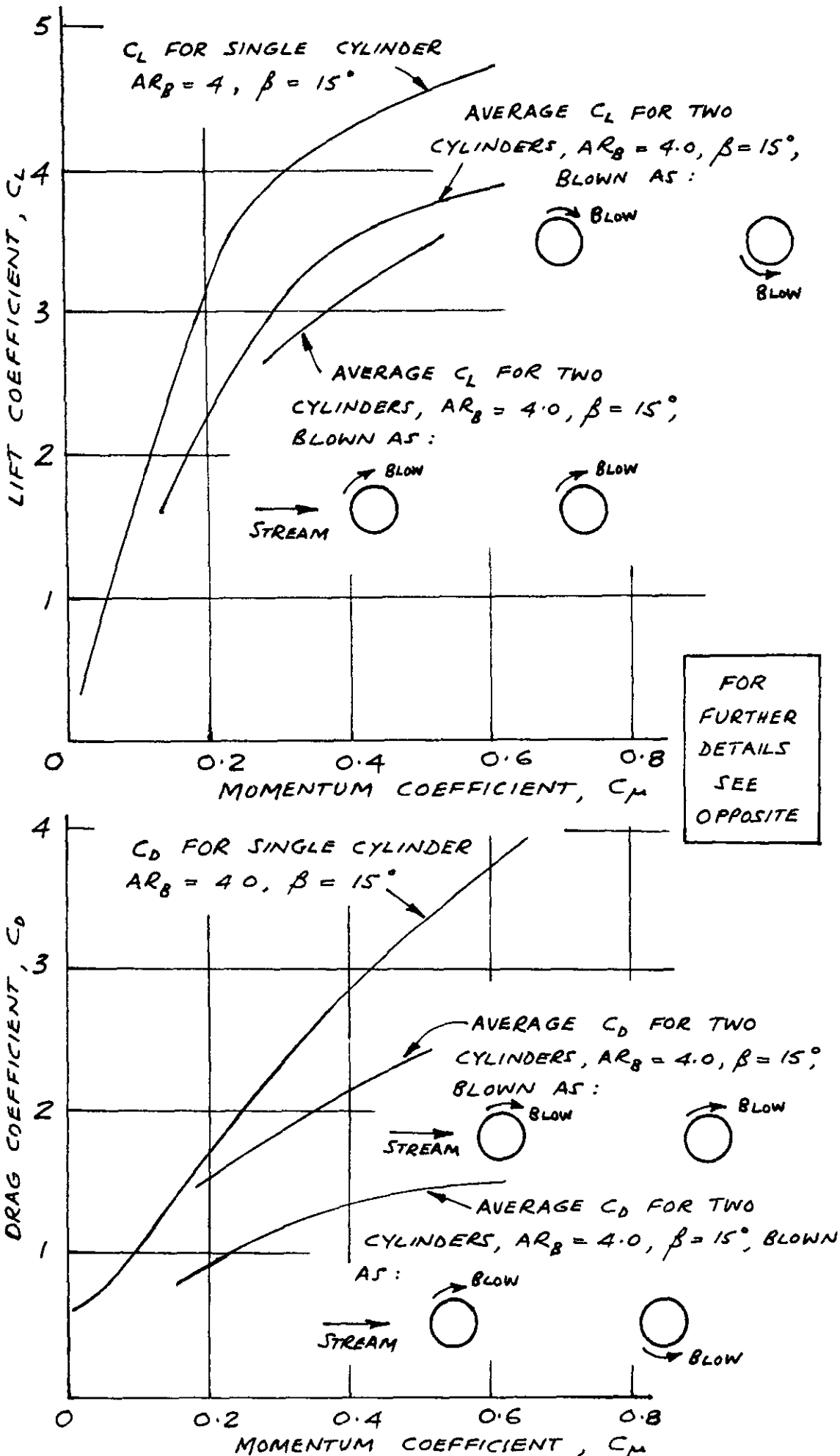
LIFT COEFFICIENT, C_L
5
4
3
2
1
0
0·2
0·4
0·6
0·8
MOMENTUM COEFFICIENT, C_μ
C_L FOR SINGLE CYLINDER
$AR_B = 4$, $\beta = 15°$
AVERAGE C_L FOR TWO CYLINDERS, $AR_B = 4.0$, $\beta = 15°$, BLOWN AS:
BLOW
BLOW
AVERAGE C_L FOR TWO CYLINDERS, $AR_B = 4.0$, $\beta = 15°$, BLOWN AS:
STREAM
BLOW
BLOW
FOR FURTHER DETAILS SEE OPPOSITE
DRAG COEFFICIENT, C_D
4
3
2
1
0
0·2
0·4
0·6
0·8
MOMENTUM COEFFICIENT, C_μ
C_D FOR SINGLE CYLINDER
$AR_B = 4.0$, $\beta = 15°$
AVERAGE C_D FOR TWO CYLINDERS, $AR_B = 4.0$, $\beta = 15°$, BLOWN AS:
STREAM
BLOW
BLOW
AVERAGE C_D FOR TWO CYLINDERS, $AR_B = 4.0$, $\beta = 15°$, BLOWN AS:
STREAM
BLOW
BLOW

FIG. 33

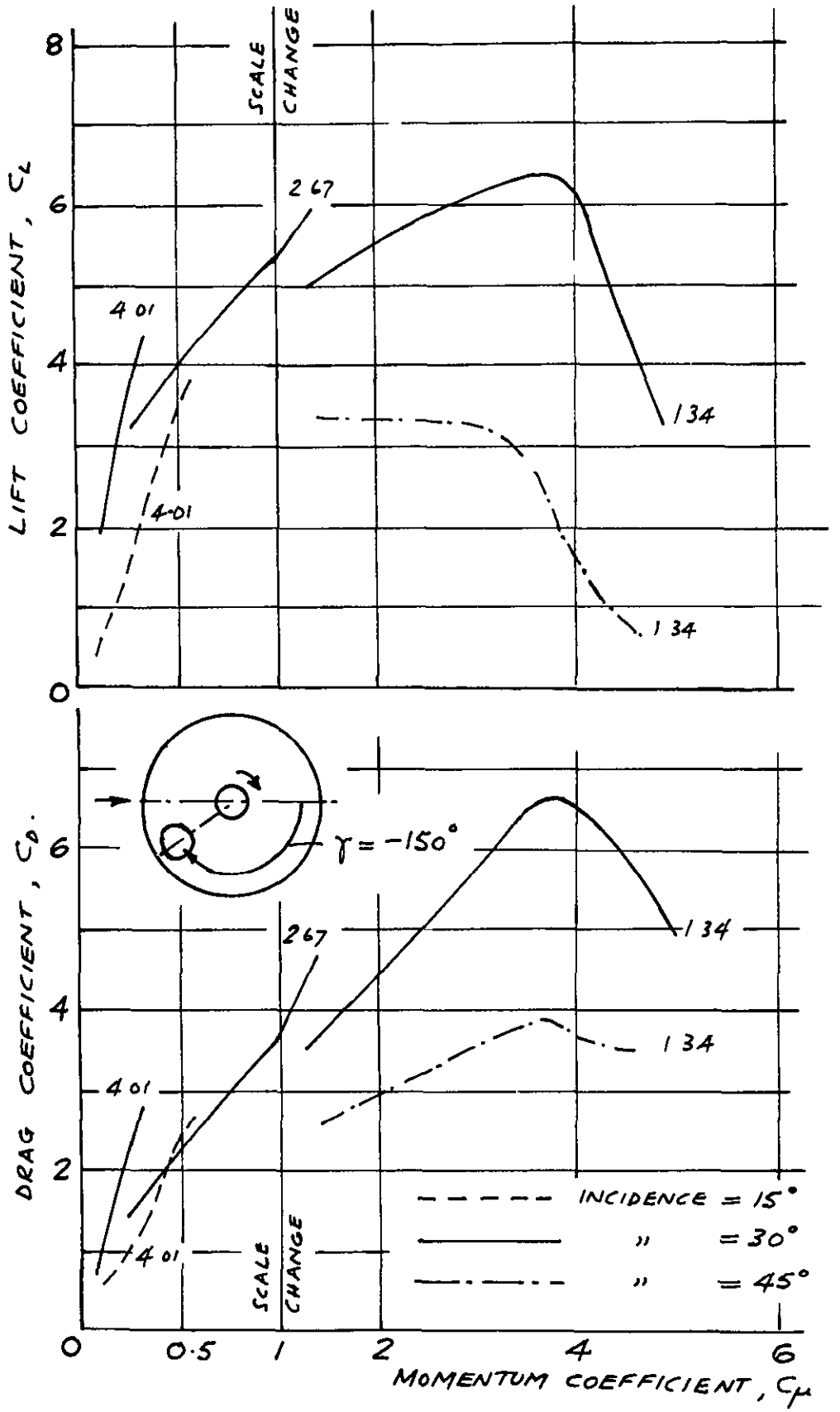

FIG. 33. COMPARISON OF RESULTS OBTAINED AT DIFFERENT INCIDENCES TWIN CYLINDER INTERFERENCE $\gamma = -150°$ VALUES ON CURVES ARE OF $Re_D \times 10^{-5}$.

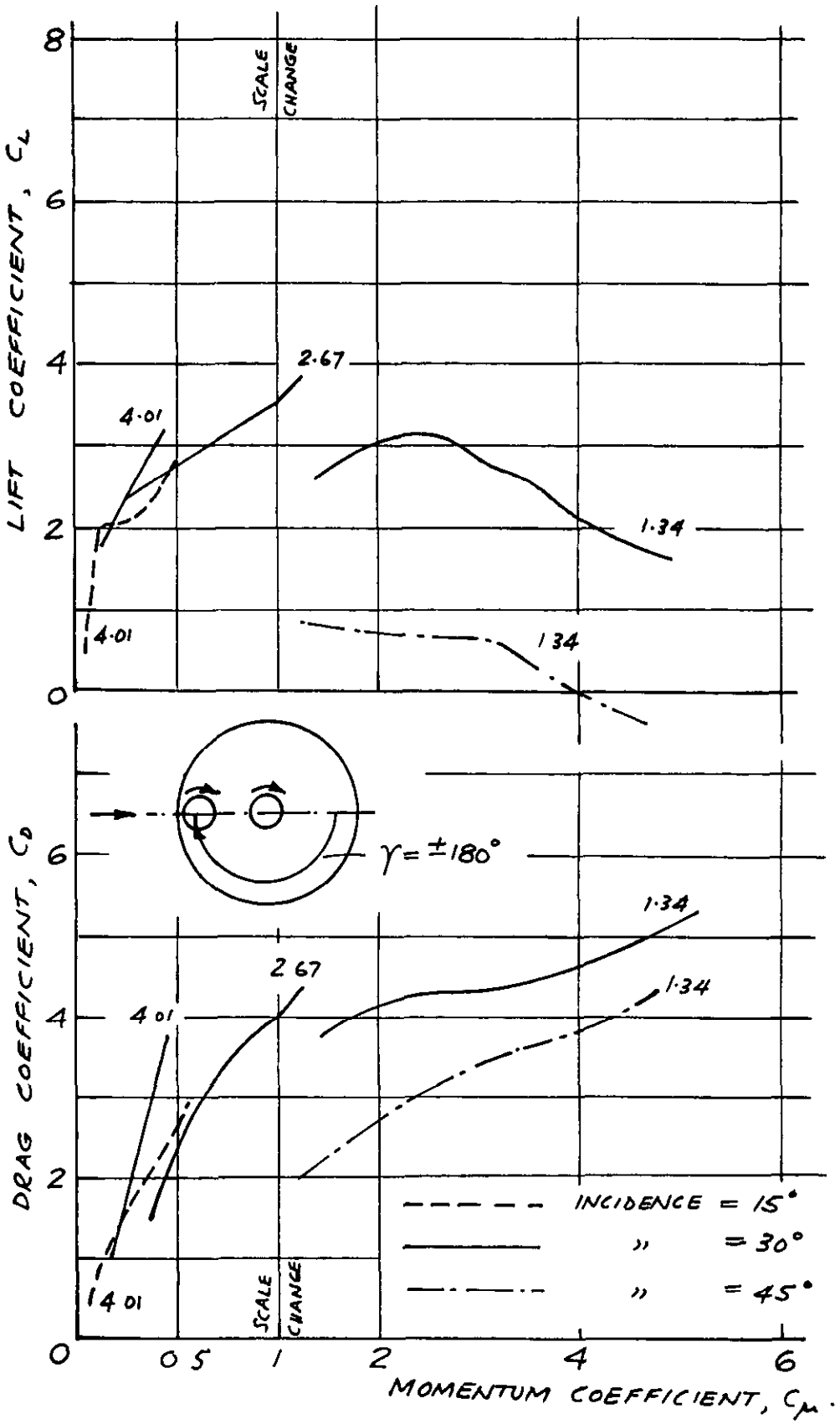

FIG 34. COMPARISON OF RESULTS OBTAINED AT DIFFERENT INCIDENCES TWIN CYLINDER INTERFERENCE $\gamma = 180°$. VALUES ON CURVES ARE OF $Re_D \times 10^{-5}$.

FIG. 35.

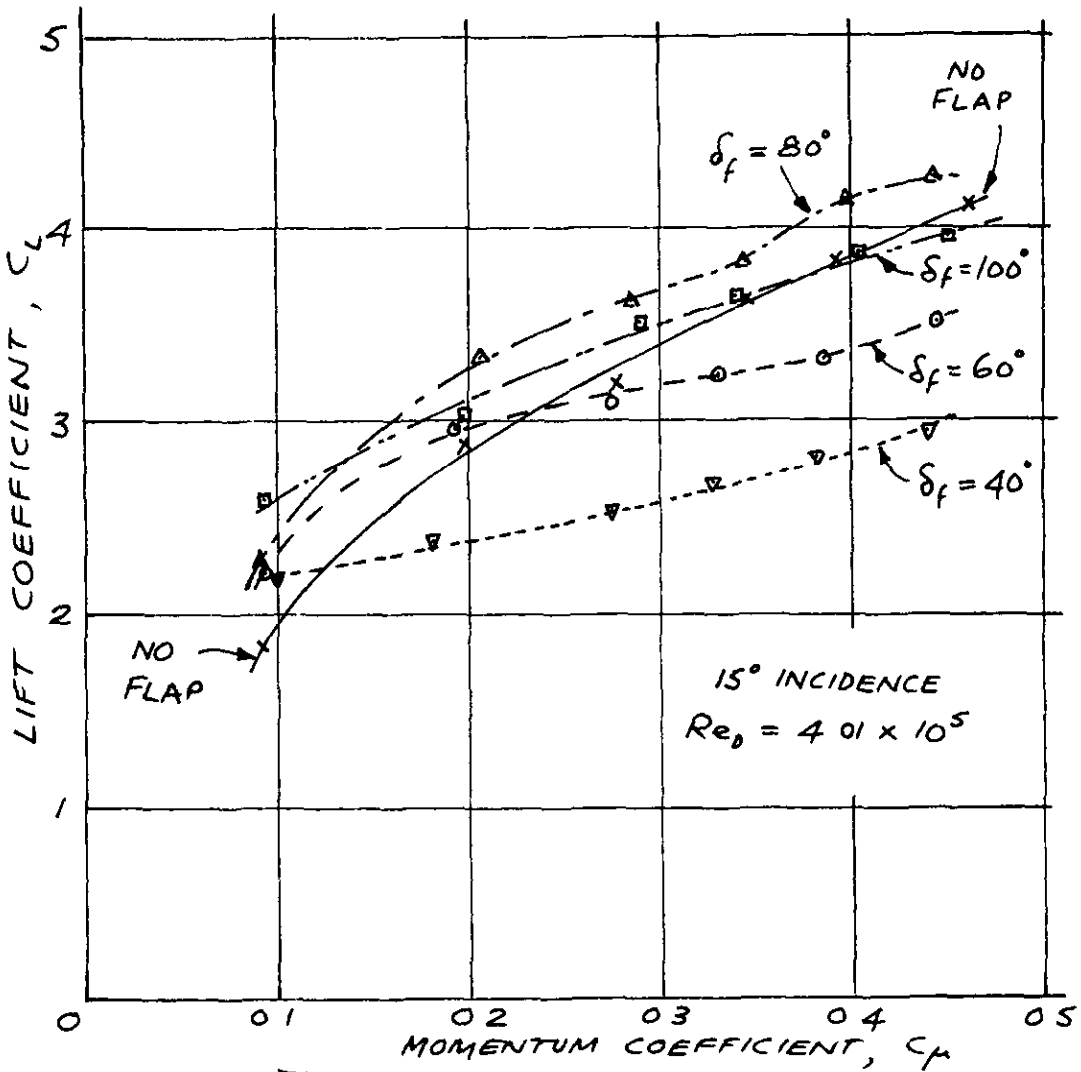

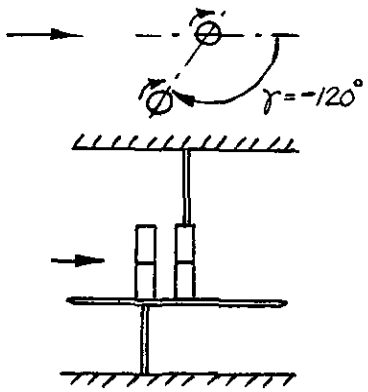

FIG 35 EFFECT OF USE OF A FLAP ON LIFT AND DRAG WITH MUTUAL INTERFERENCE BETWEEN TWO CYLINDERS BLOWING IN THE SAME DIRECTION $AR_B = 4$

$\gamma = -120°$

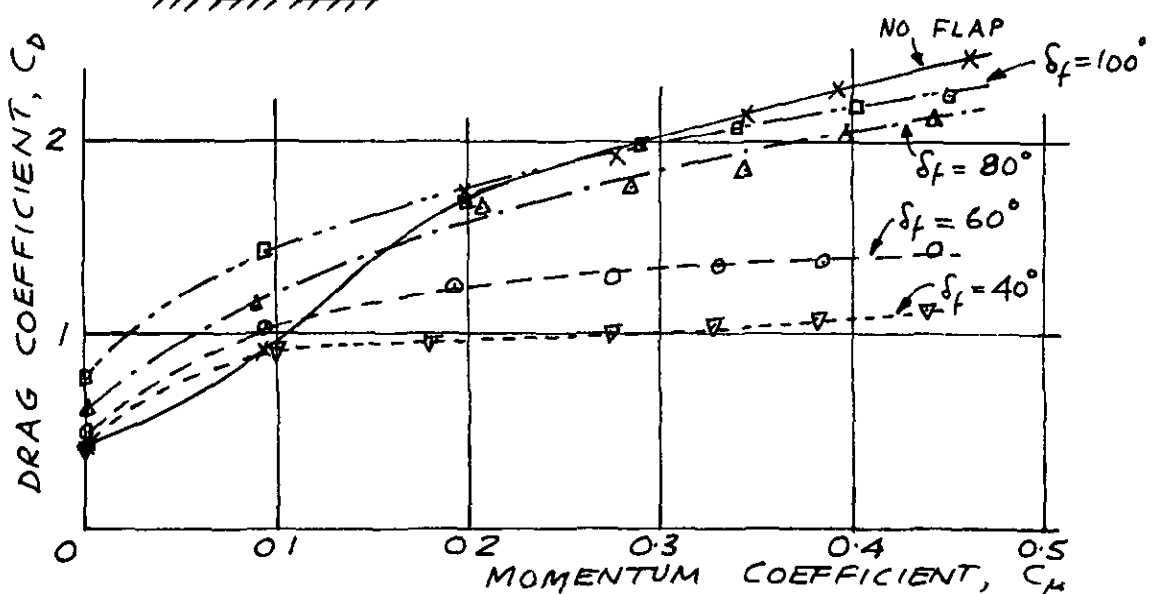

FIG. 36.

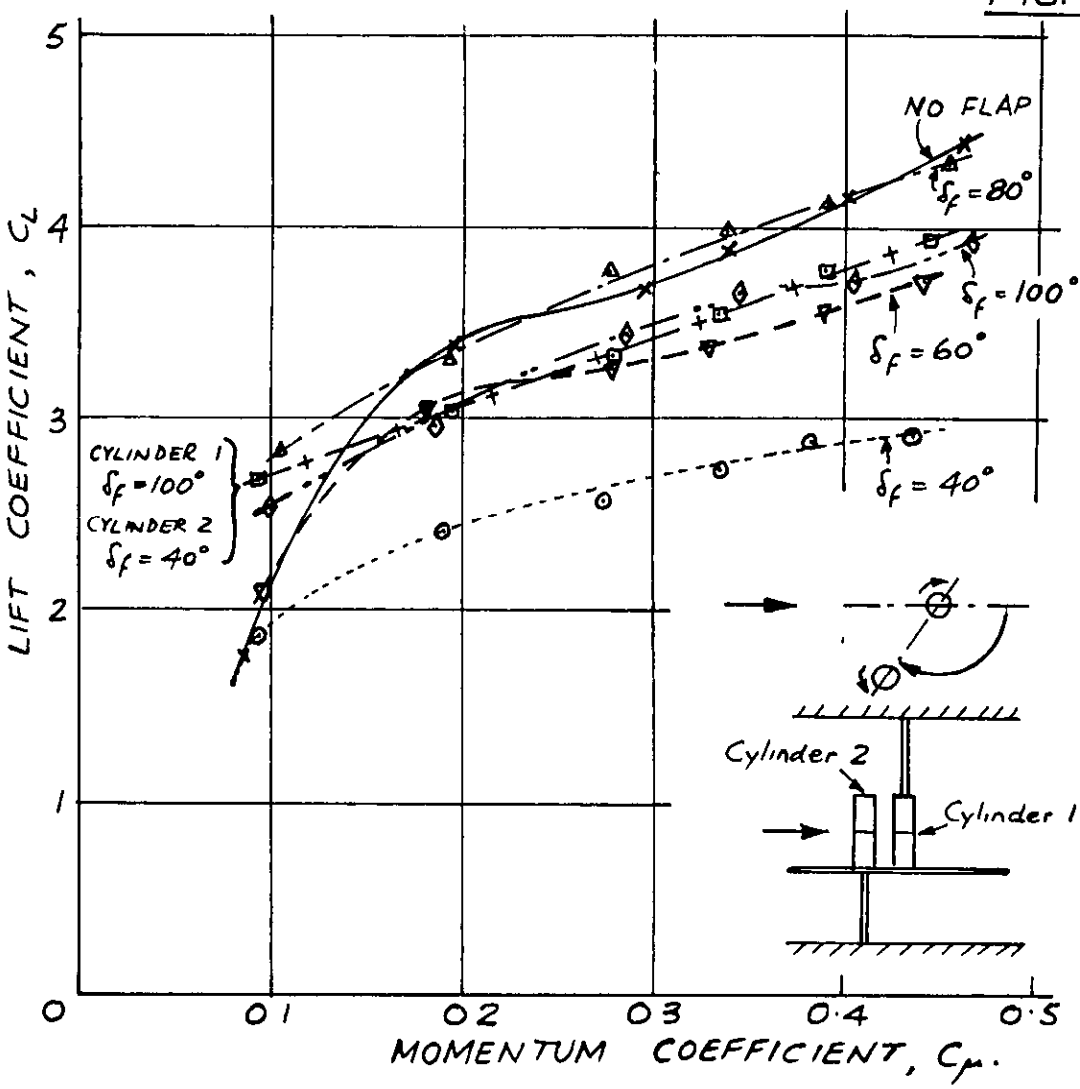

FIG 36 EFFECT OF USE OF A FLAP ON LIFT AND DRAG OF MUTUALLY-INTERFERING BLOWN CYLINDERS. CYLINDERS OPPOSITELY BLOWN. $AR_B = 4$. $\gamma = -120°$ 15° INCIDENCE $Re_D = 4{\cdot}01 \times 10^5$.

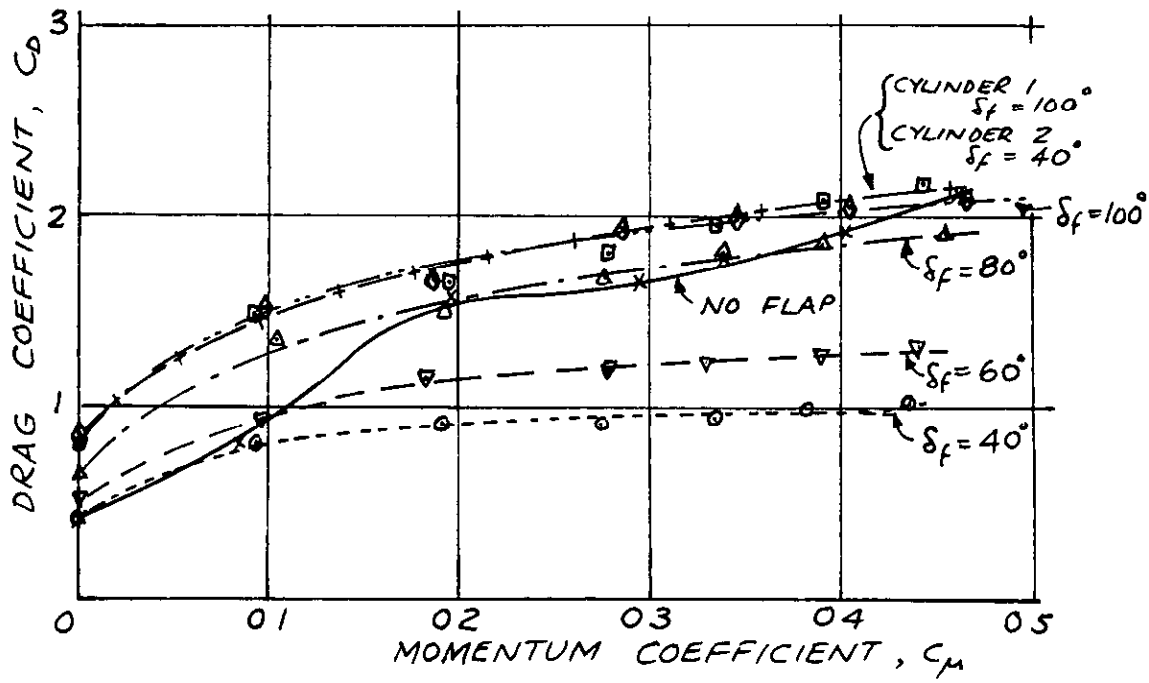

FIG 37

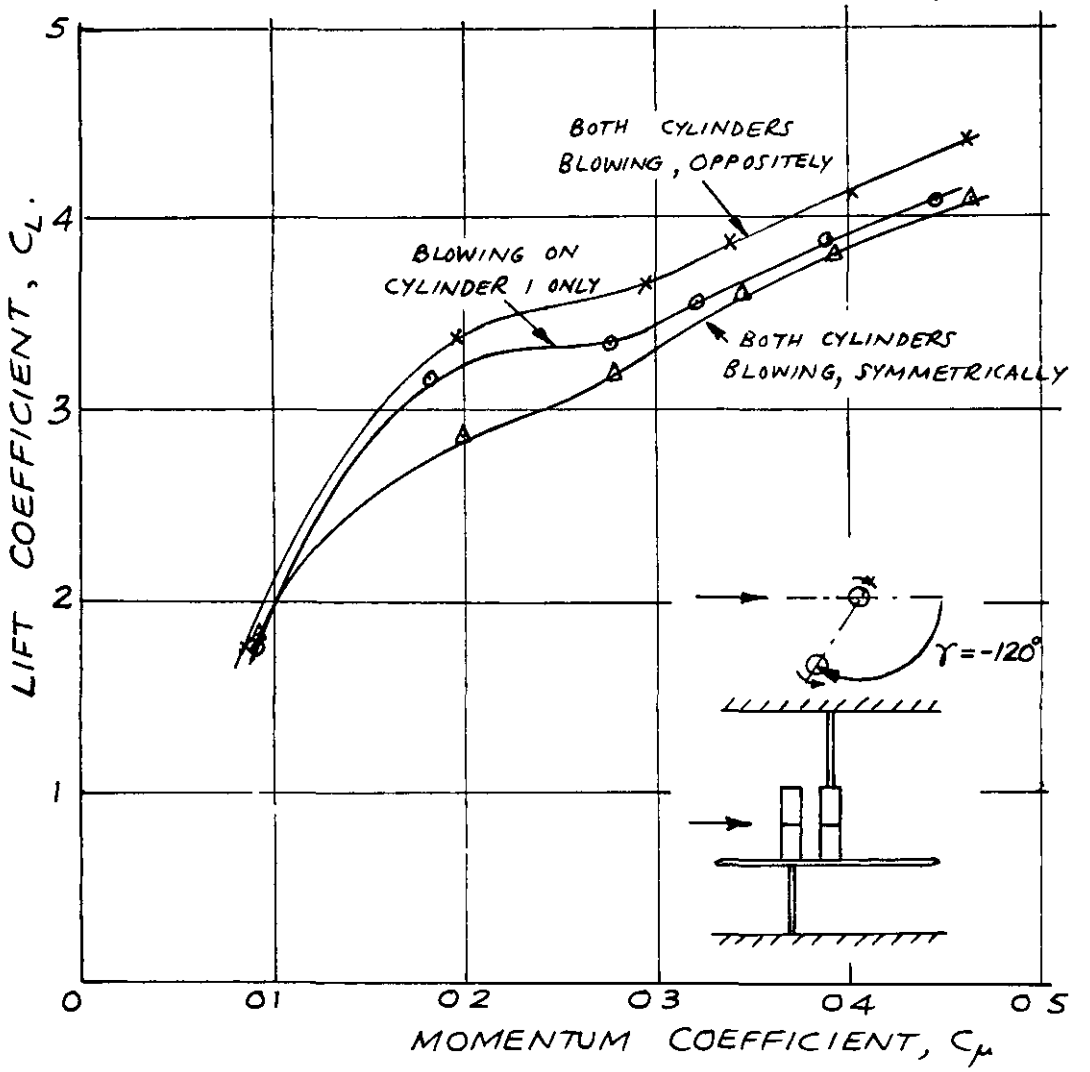

FIG 37. EFFECT OF DIRECTION OF BLOW ON PERFORMANCE OF MUTUALLY-INTERFERING BLOWN CYLINDERS $AR_B = 4.$ $\gamma = -120°$ 15° INCIDENCE. NO FLAP $Re_D = 4{\cdot}01 \times 10^5$

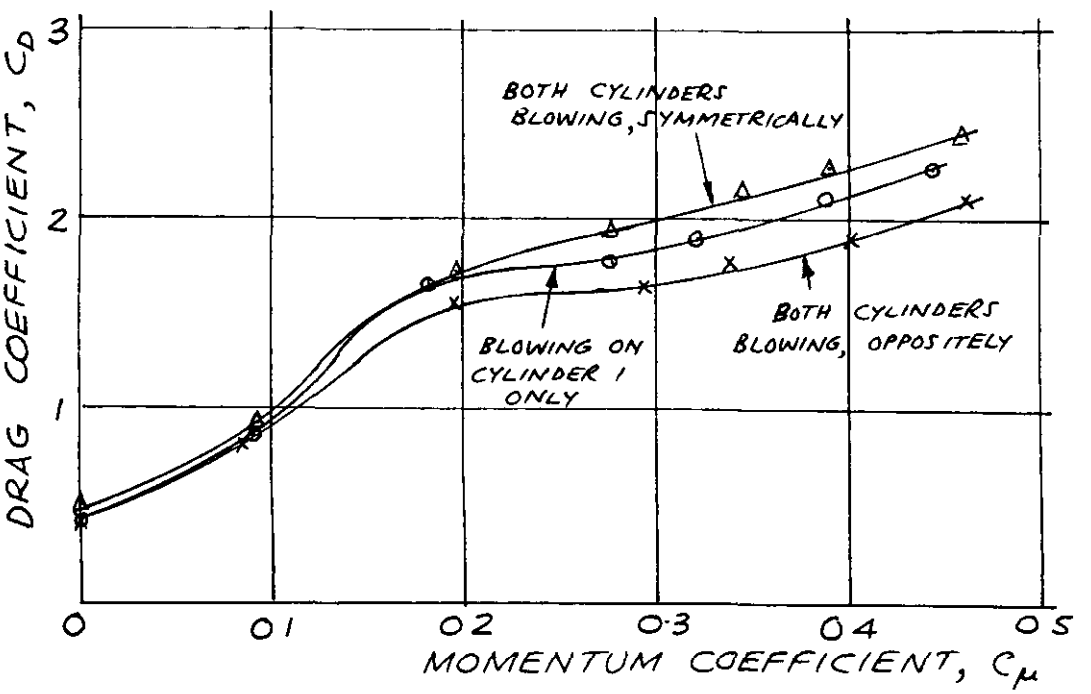

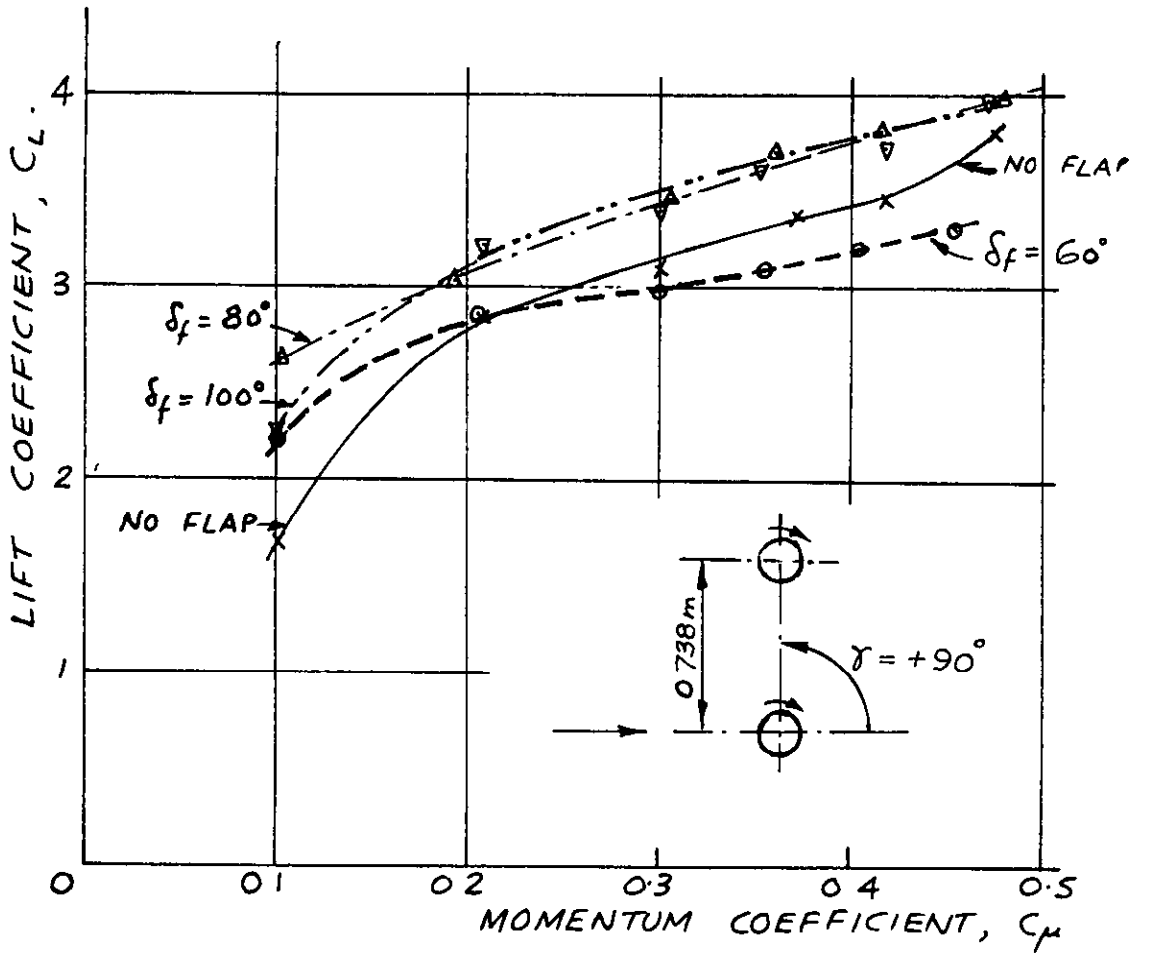

FIG. 38. EFFECT OF SEPARATION OF CYLINDERS ON PERFORMANCE OF MUTUALLY-INTERFERING BLOWN CYLINDERS. SEPARATION = 0·738m (29 IN.) $AR_B = 4$ $\gamma = 90°$. 15° INCIDENCE. $Re_D = 4\,01 \times 10^5$ SYMMETRICALLY BLOWN. (SEE ALSO OPPOSITE).

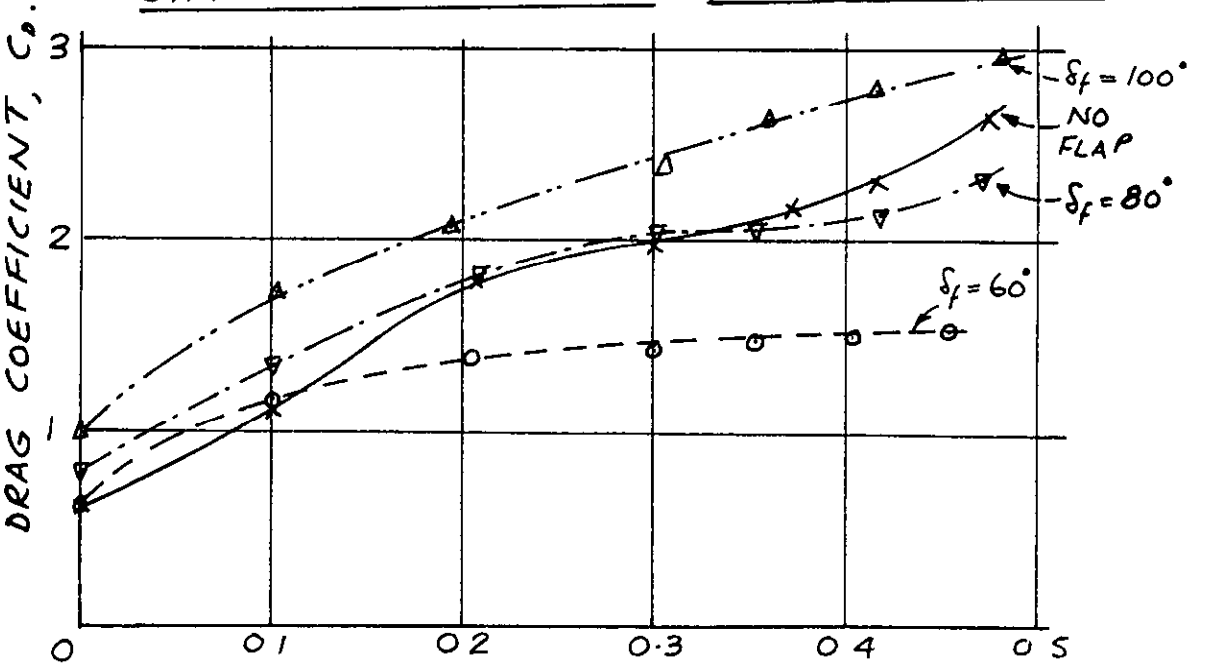

FIG. 39.

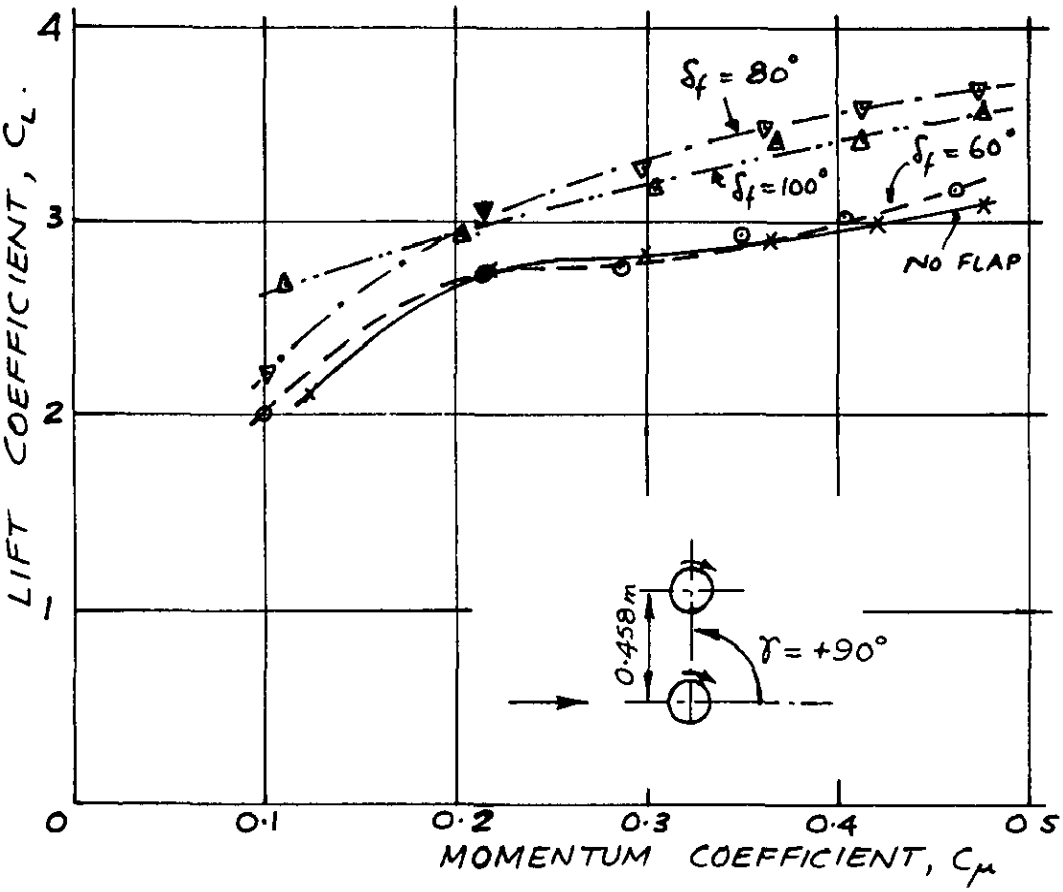

FIG. 39. EFFECT OF SEPARATION OF CYLINDERS ON PERFORMANCE OF MUTUALLY-INTERFERING BLOWN CYLINDERS SEPARATION = 0·458m (18 IN) $AR_B = 4$. $\gamma = 90°$ 15° INCIDENCE. $Re_D = 4{\cdot}01 \times 10^5$ SYMMETRICALLY BLOWN (SEE ALSO OPPOSITE)

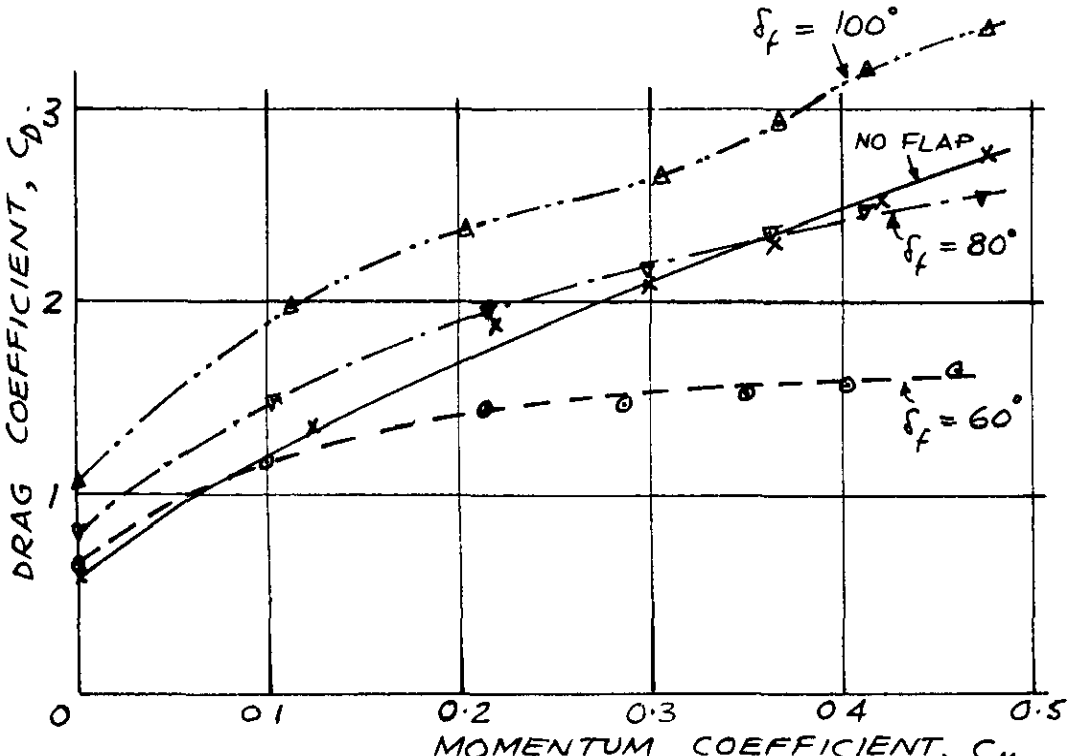

FIG 41.

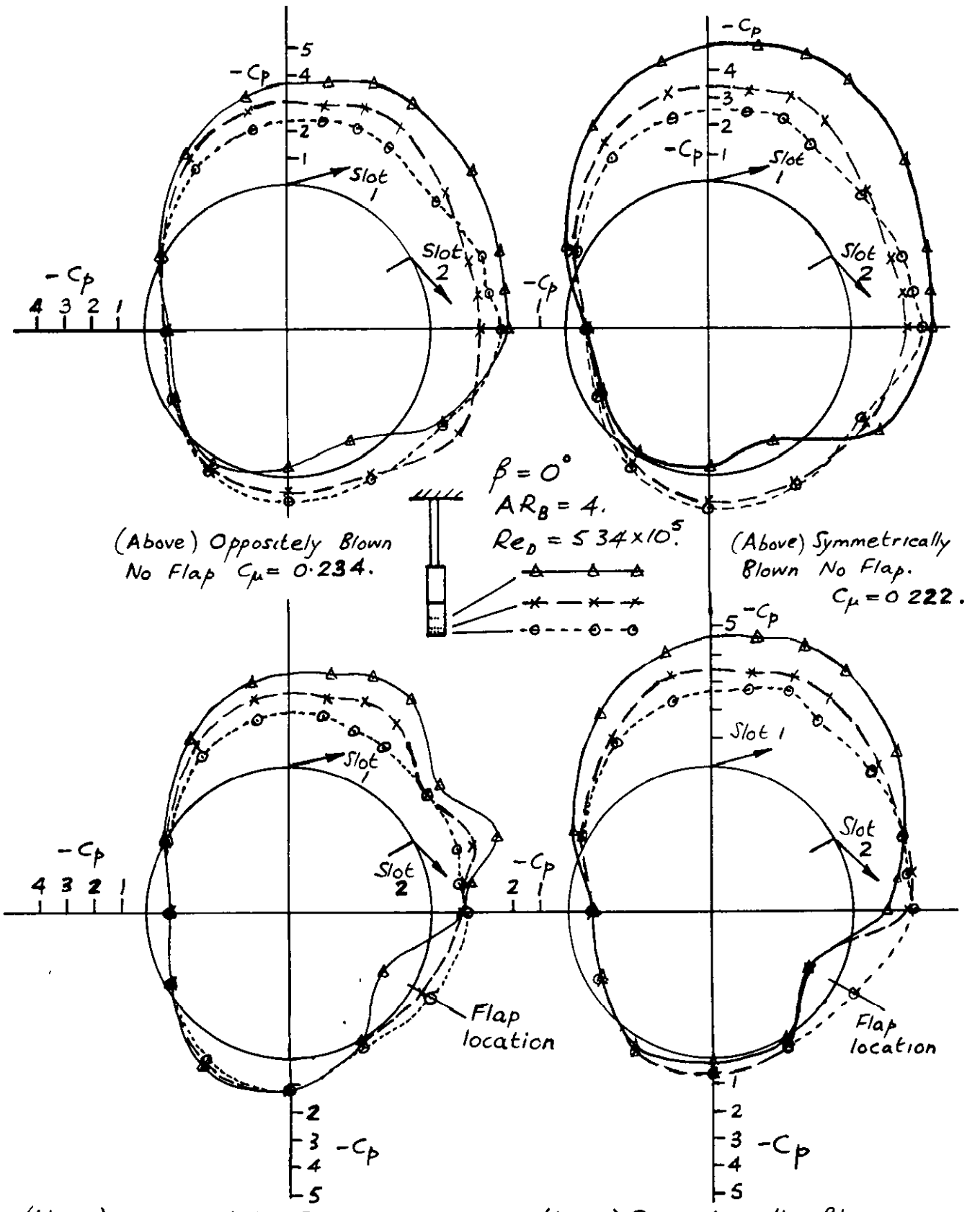

FIG 41. DISTRIBUTIONS OF STATIC PRESSURE ROUND BLOWN CYLINDER FOR FOUR DIFFERENT CONFIGURATIONS AT SIMILAR VALUES OF C_μ.

FIG 42

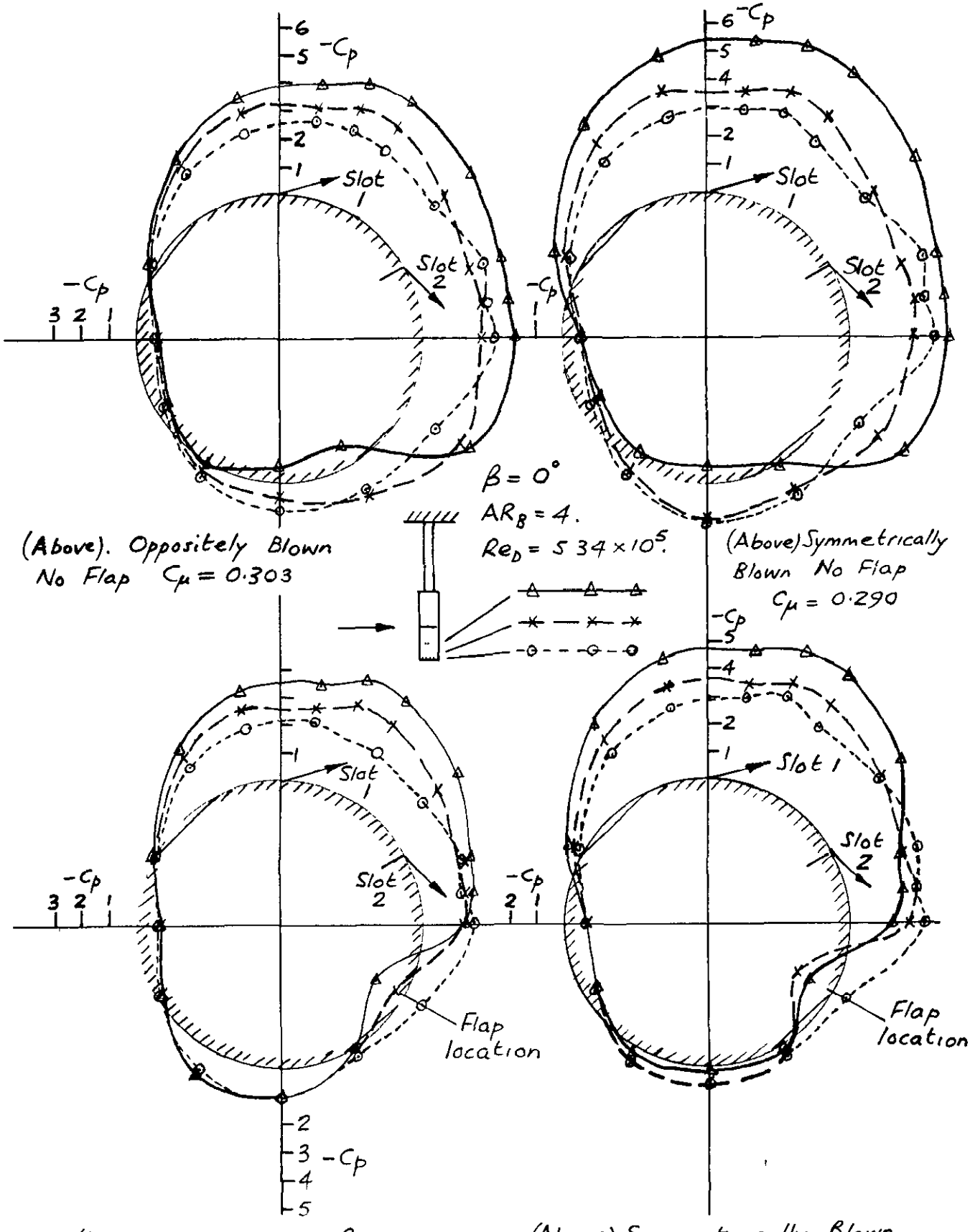

FIG 42. DISTRIBUTIONS OF STATIC PRESSURE ROUND BLOWN CYLINDER FOR FOUR DIFFERENT CONFIGURATIONS AT SIMILAR VALUES OF C_μ.

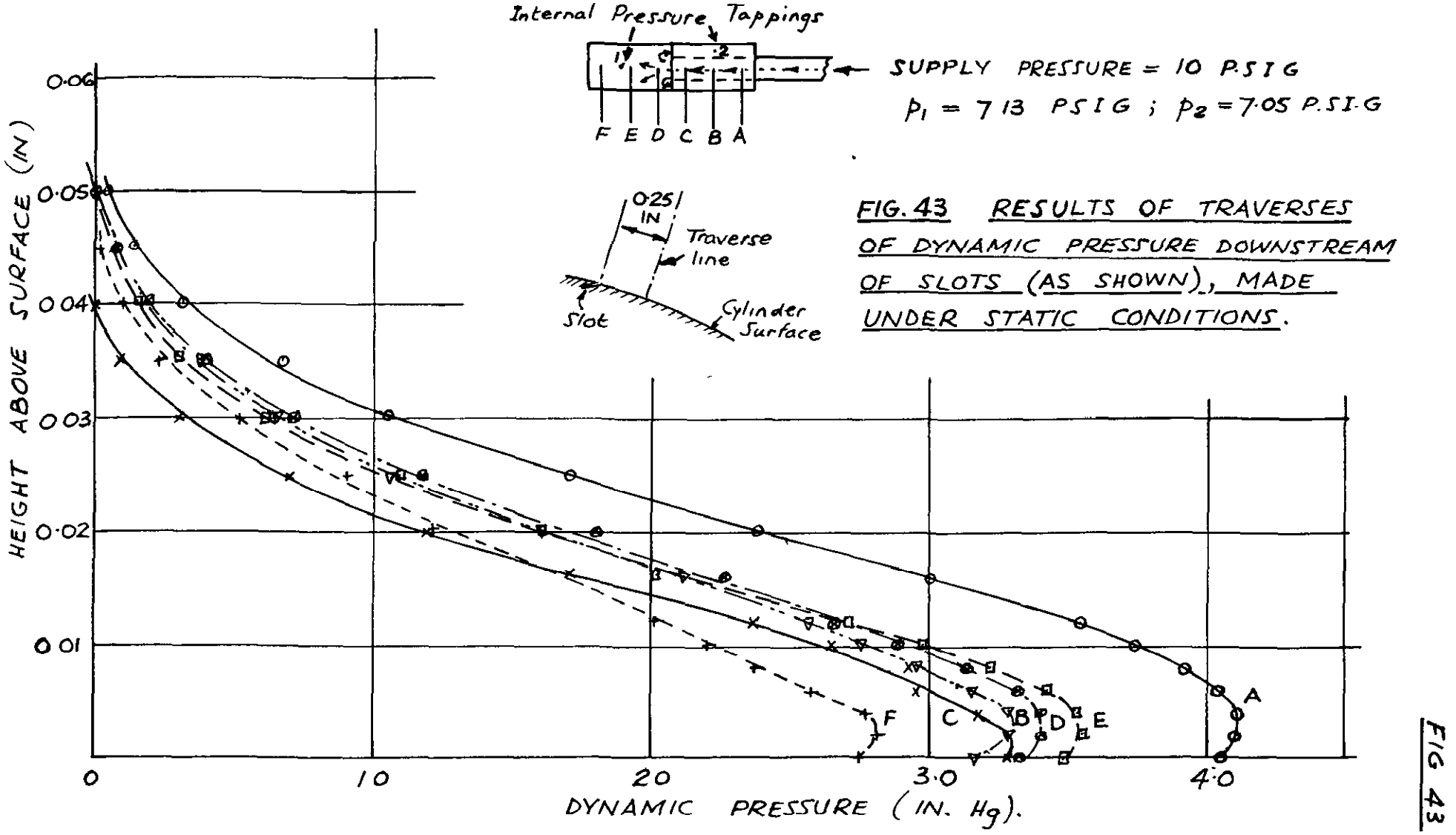

FIG. 43 RESULTS OF TRAVERSES OF DYNAMIC PRESSURE DOWNSTREAM OF SLOTS (AS SHOWN), MADE UNDER STATIC CONDITIONS.

FIG 43

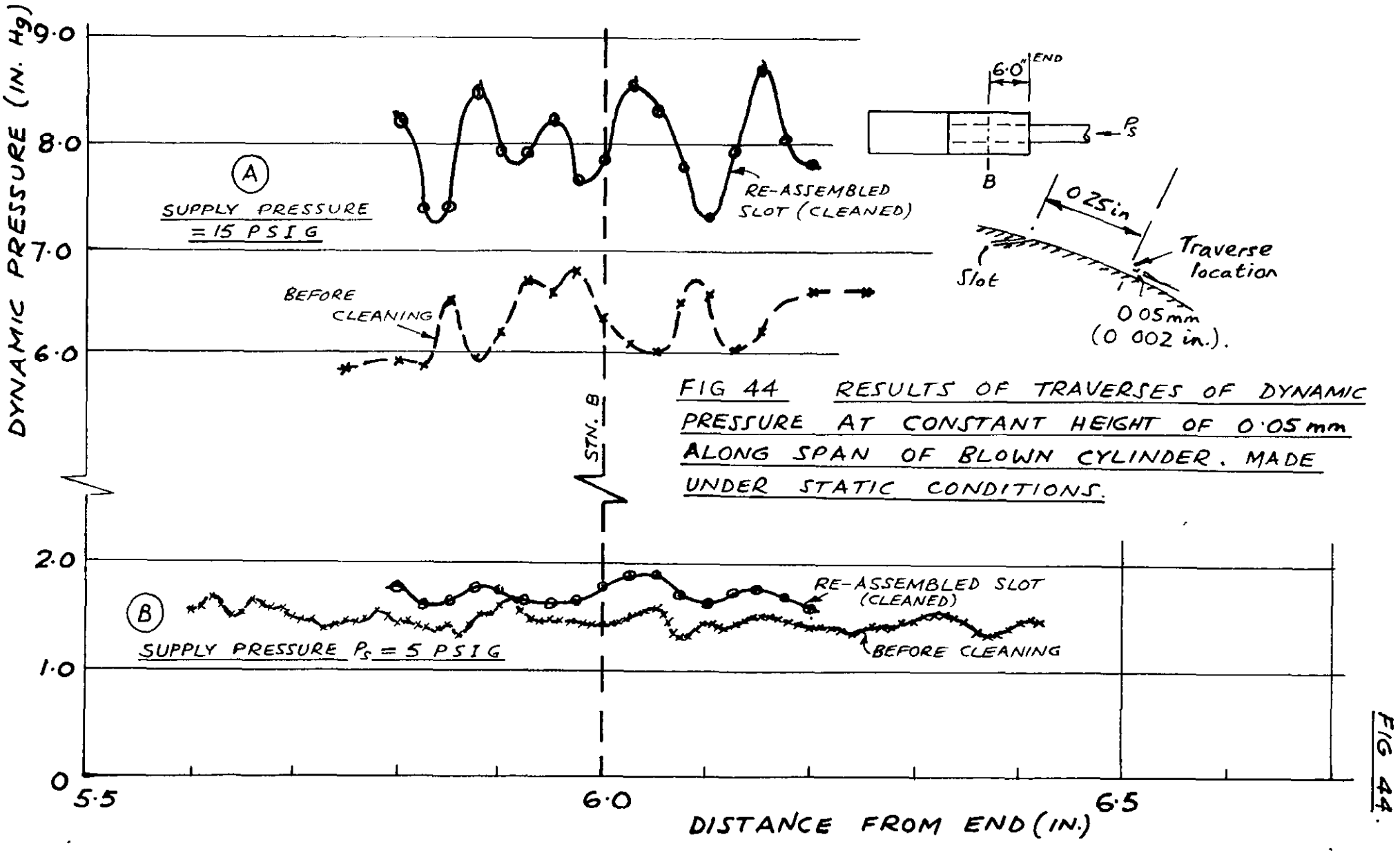

FIG 44 RESULTS OF TRAVERSES OF DYNAMIC PRESSURE AT CONSTANT HEIGHT OF 0·05 mm ALONG SPAN OF BLOWN CYLINDER. MADE UNDER STATIC CONDITIONS.

FIG 44.

FIG. 45. DYNAMIC PRESSURE PROFILES BEFORE AND AFTER THE SLOT WAS DISMANTLED AND CLEANED

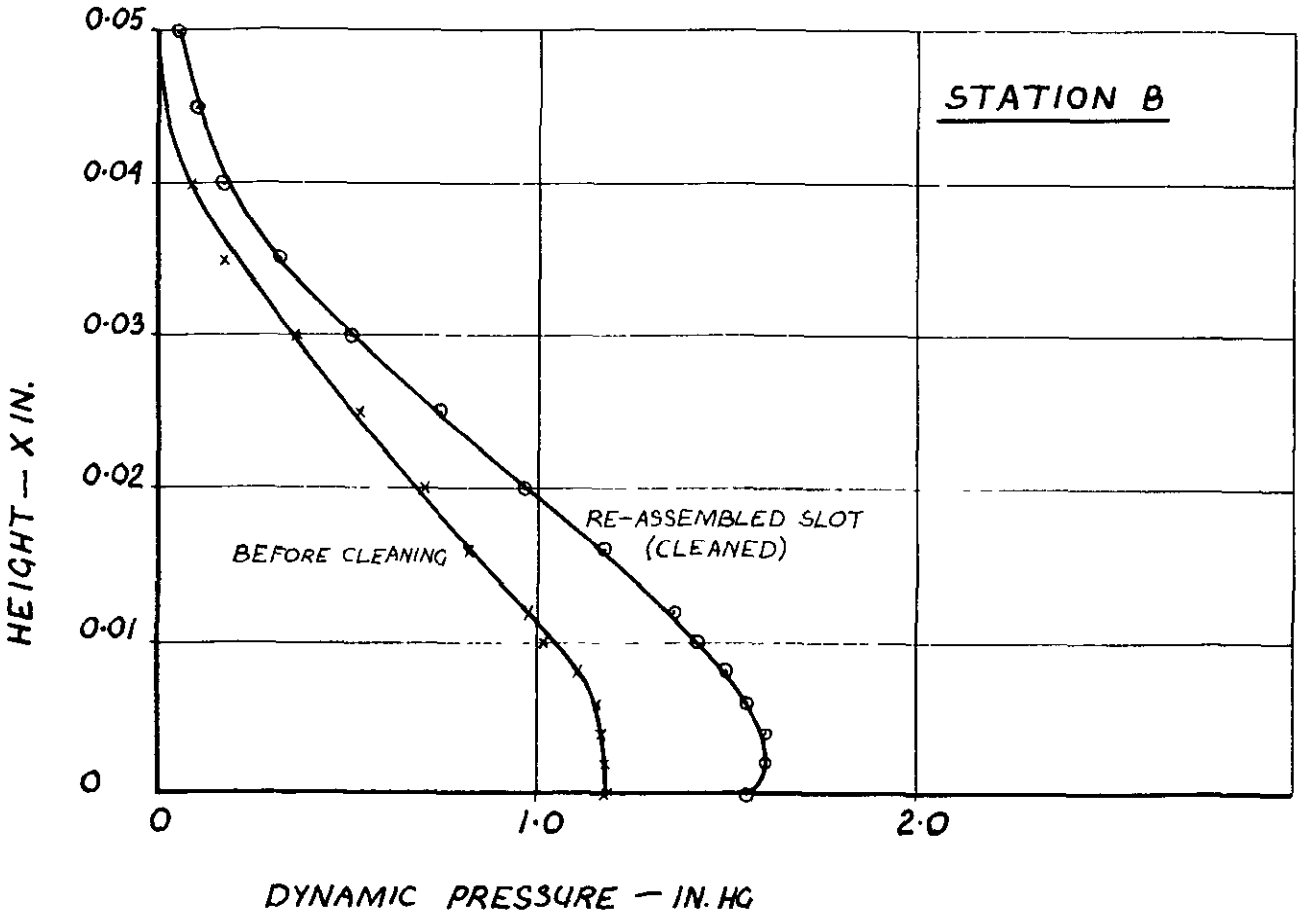

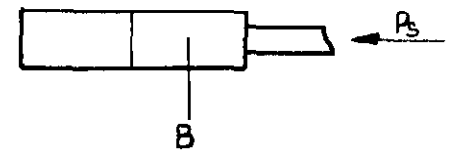

SUPPLY PRESSURE = 5 PSIG.

BUILD : 2 SECTIONS A.R = 4

FIG 45.

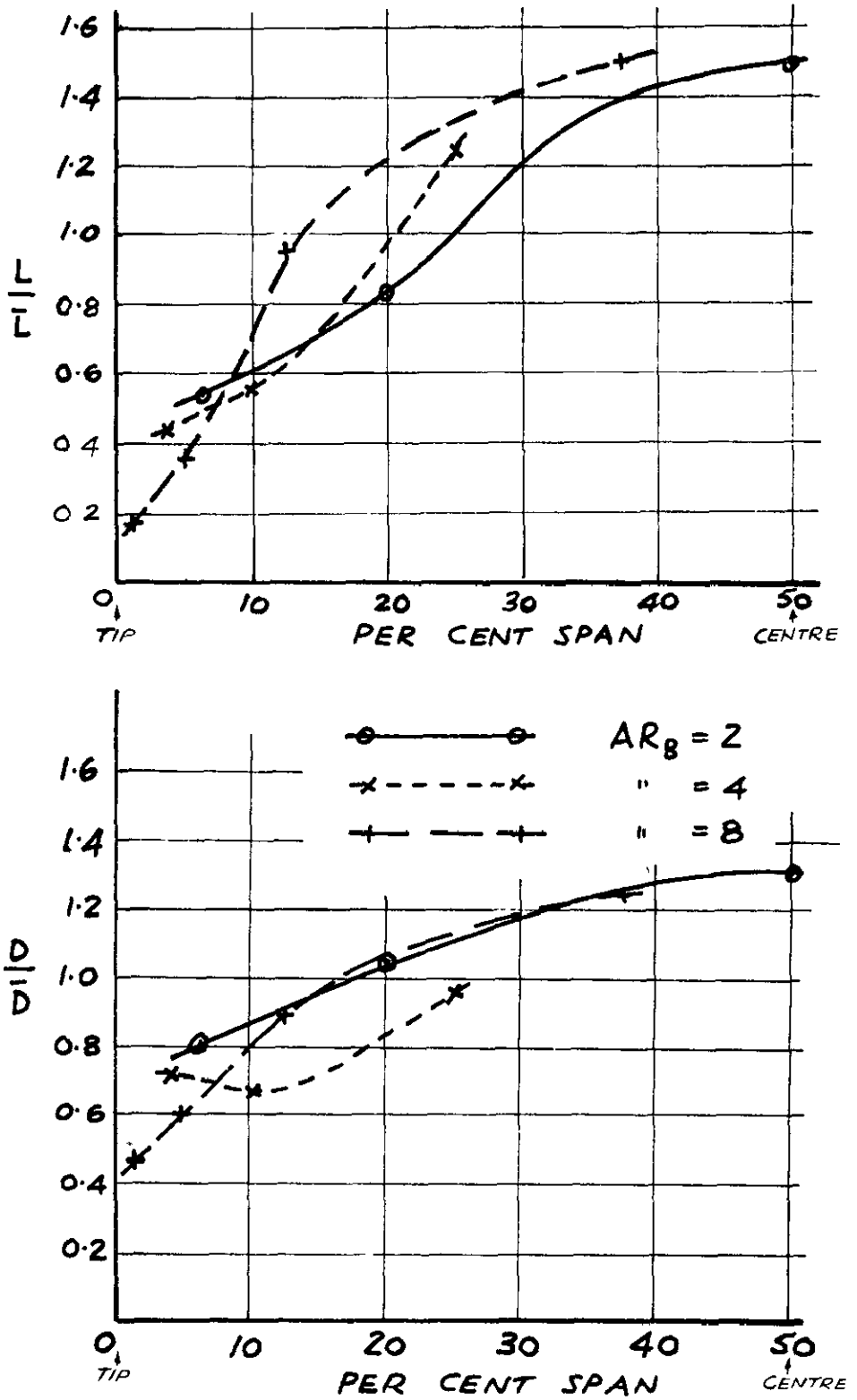

FIG. 46 LIFT AND DRAG LOADING DISTRIBUTIONS ALONG SPAN OF SYMMETRICALLY-BLOWN CYLINDERS FOR VARIOUS ASPECT RATIOS.
$C_\mu = 0.27$. $Re_D \approx 2 \times 10^5$. "BARRED" QUANTITIES INDICATE MEAN VALUES.

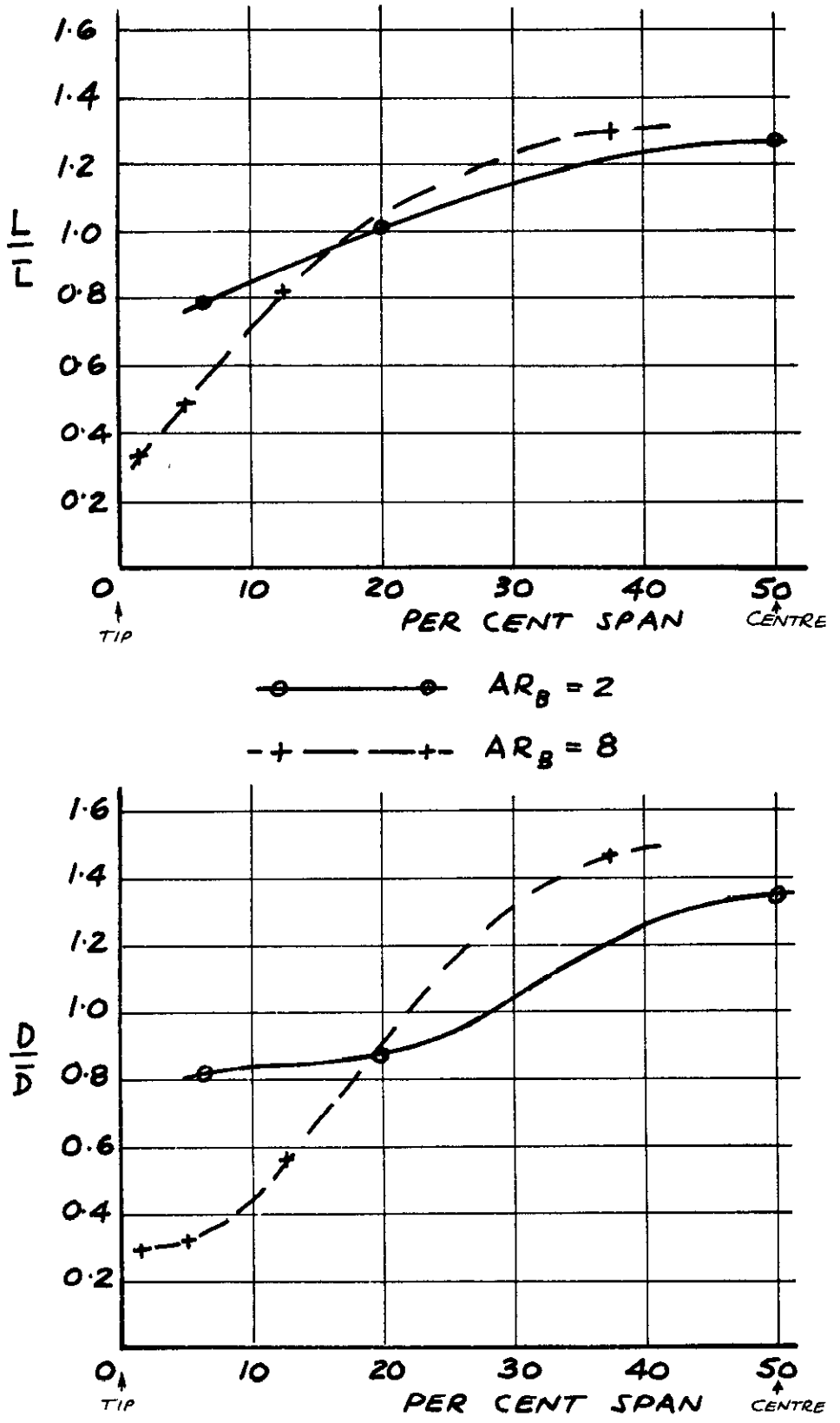

FIG. 47 LIFT AND DRAG LOADING DISTRIBUTIONS ALONG SPAN OF SYMMETRICALLY-BLOWN CYLINDERS FOR VARIOUS ASPECT RATIOS.
$C_\mu = 0.90$. $Re_D \approx 2 \times 10^5$. "BARRED" QUANTITIES INDICATE MEAN VALUES.

FIG. 48.

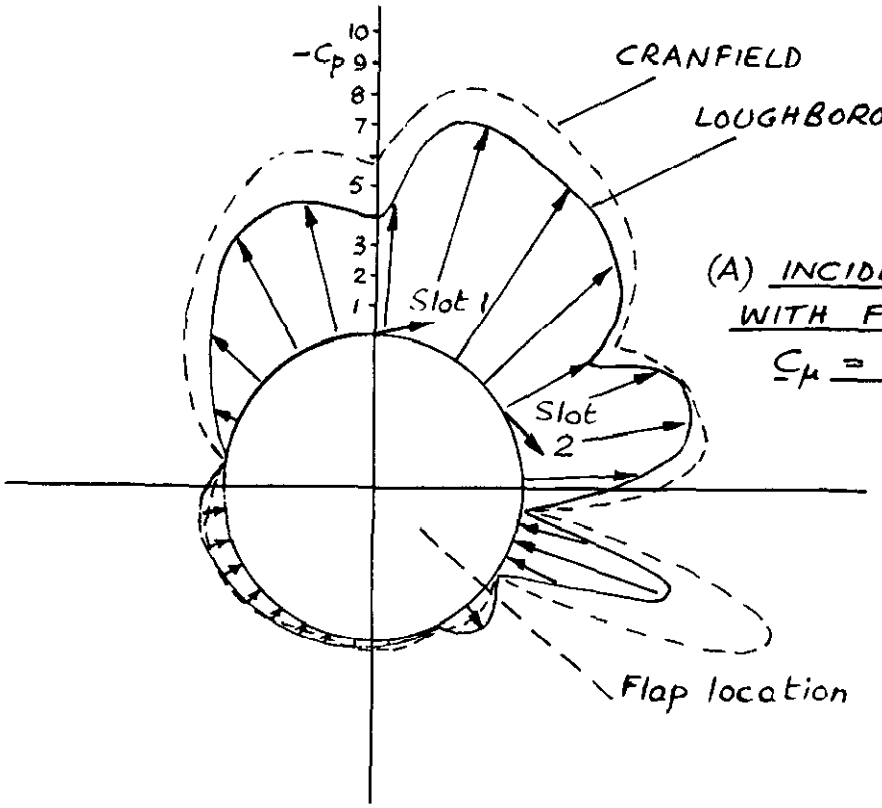

(A) INCIDENCE = 0°
WITH FLAP $S_f = 70°$
$C_\mu = 2.52$

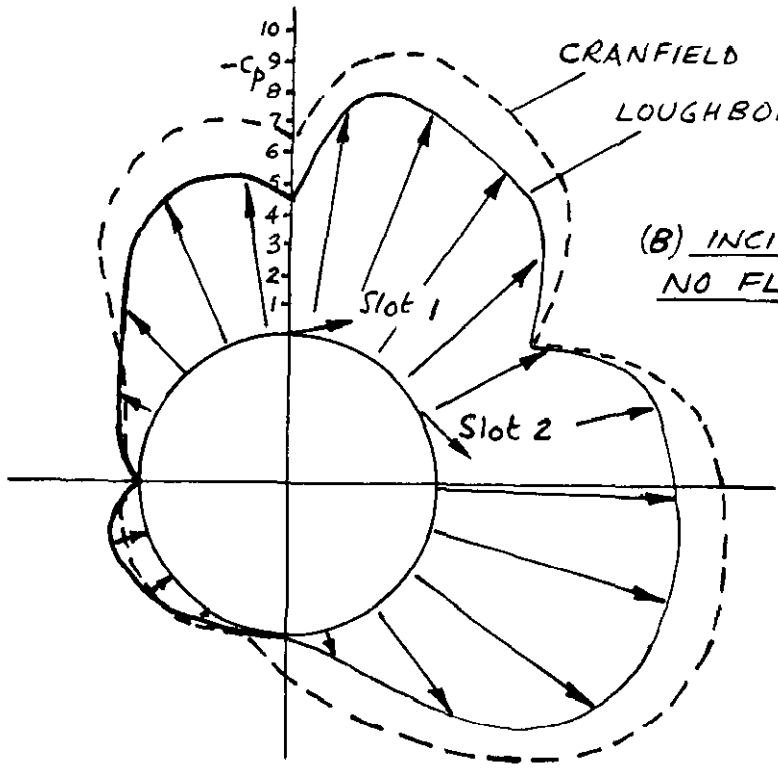

(B) INCIDENCE = 0°
NO FLAP. $C_\mu = 2.80$

FIG 48 COMPARISON OF RESULTS OF STATIC PRESSURE DISTRIBUTION TESTS AT CRANFIELD (CLOSED TUNNEL) AND LOUGHBOROUGH (OPEN-JET TUNNEL) WITH AND WITHOUT A FLAP FITTED, AT HIGH VALUES OF C_μ

$AR_B = 4$, $Re_D = 2 \times 10^5$ APPROX

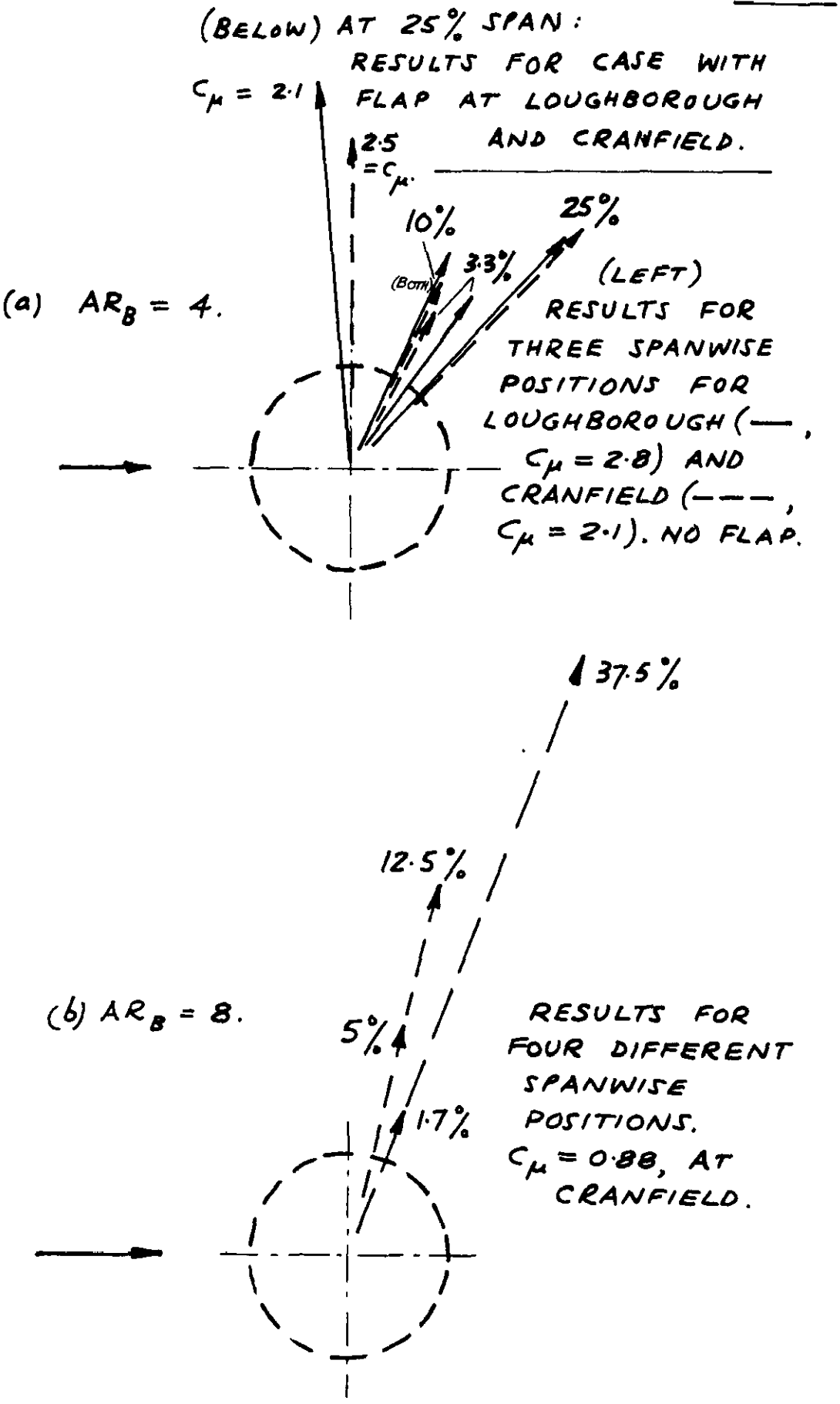

FIG. 49. VARIATION OF MAGNITUDE AND POSITION OF FORCE VECTORS IN TESTS AT LOUGHBOROUGH AND CRANFIELD. (FROM PRESSURE DISTRIBUTIONS).

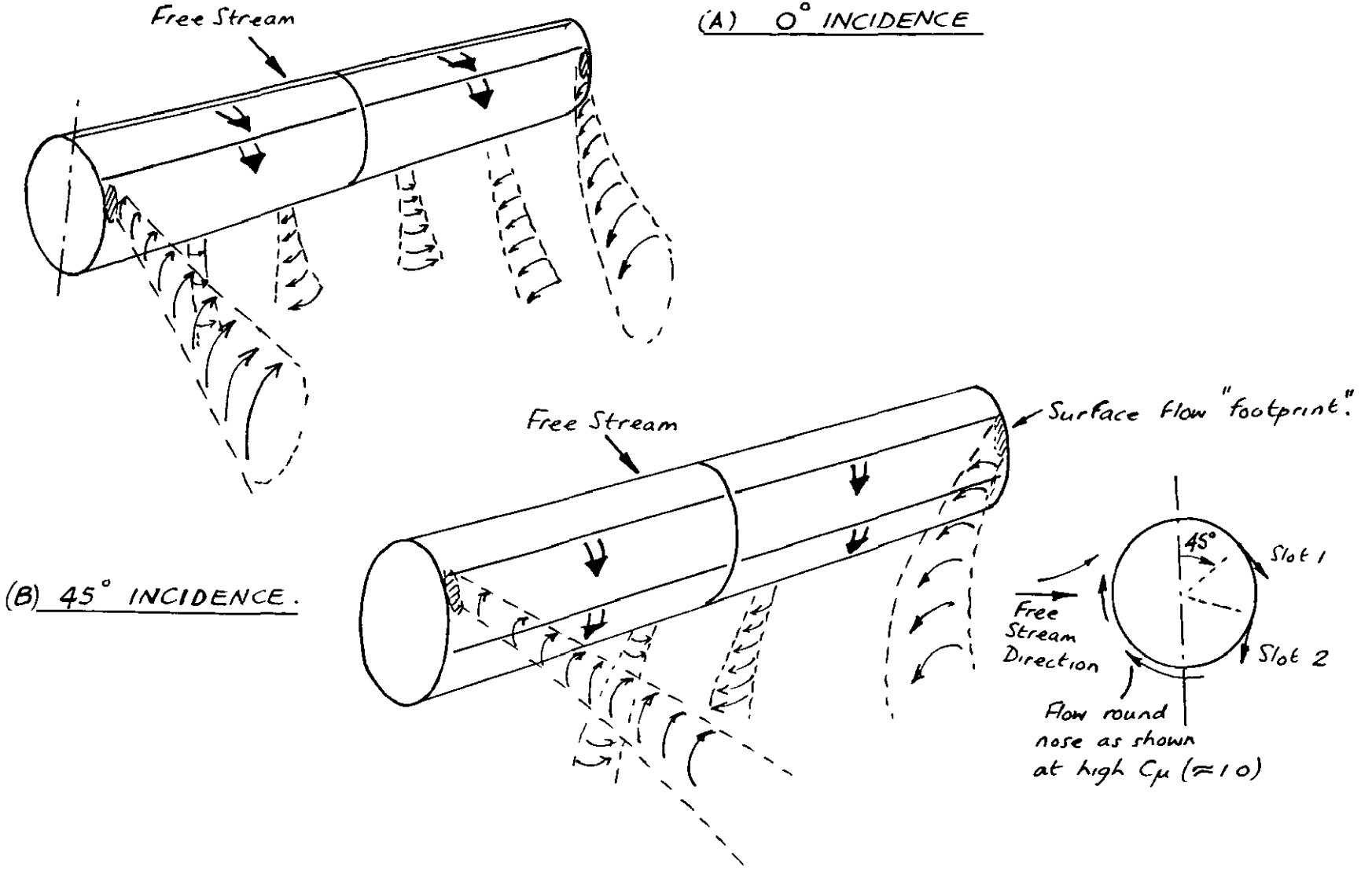

FIG 50 SKETCHES SHOWING RESULTS OF FLOW-VISUALIZATION TESTS ON AN $AR_B = 4$ MODEL SYMMETRICALLY BLOWN DERIVED FROM WOOL-TUFT, SURFACE-FLOW METHODS AND PADDLE-WHEEL VORTICITIMETER TESTS.

FIG 50.

(A) $AR_B = 4$ OPPOSED BLOWING

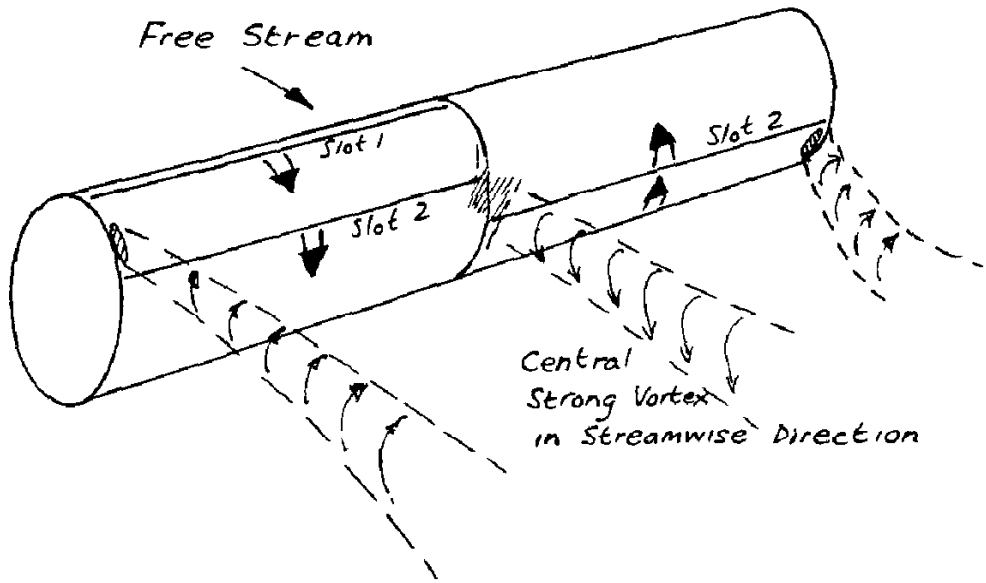

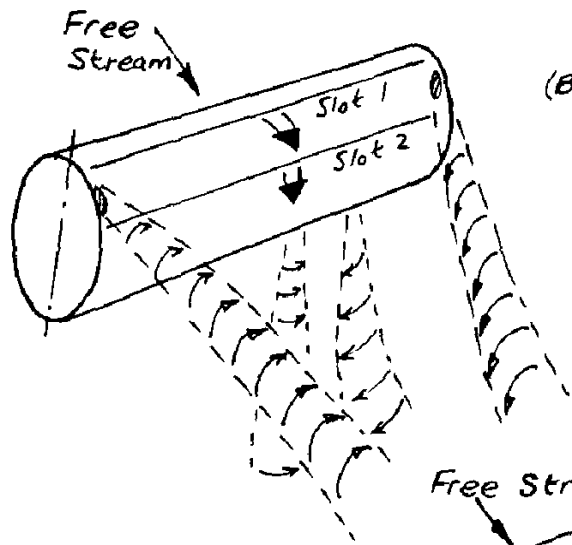

(B) $AR_B = 2$. LOW POSITIVE INCIDENCE. NO FLAP.

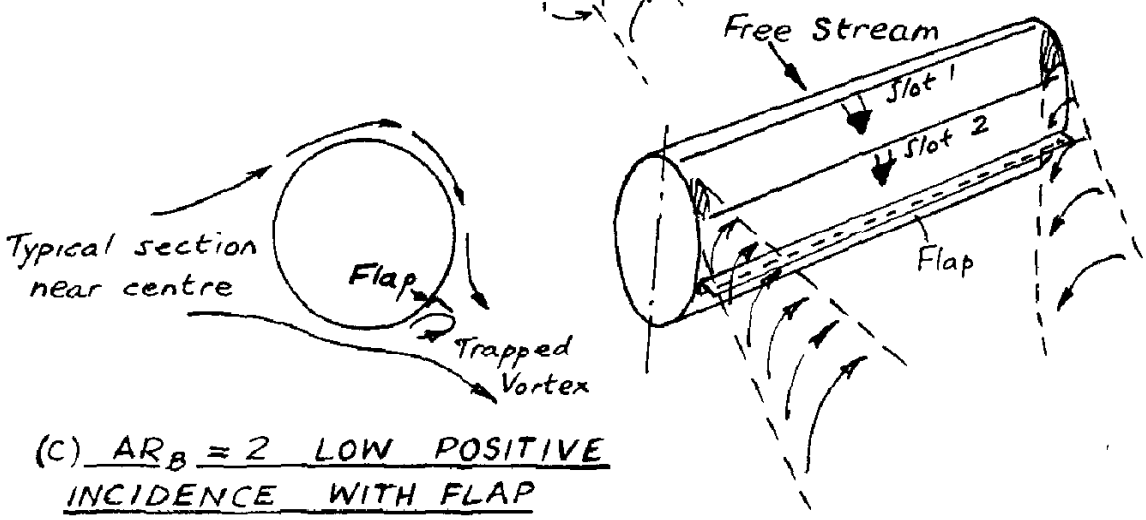

(C) $AR_B = 2$ LOW POSITIVE INCIDENCE WITH FLAP

FIG 51. SKETCHES SHOWING RESULTS OF FLOW-VISUALIZATION TESTS ON BLOWN CYLINDERS. DERIVED FROM WOOL-TUFT, SURFACE-FLOW METHODS AND PADDLE-WHEEL VORTICITIMETER TESTS

FIG 52

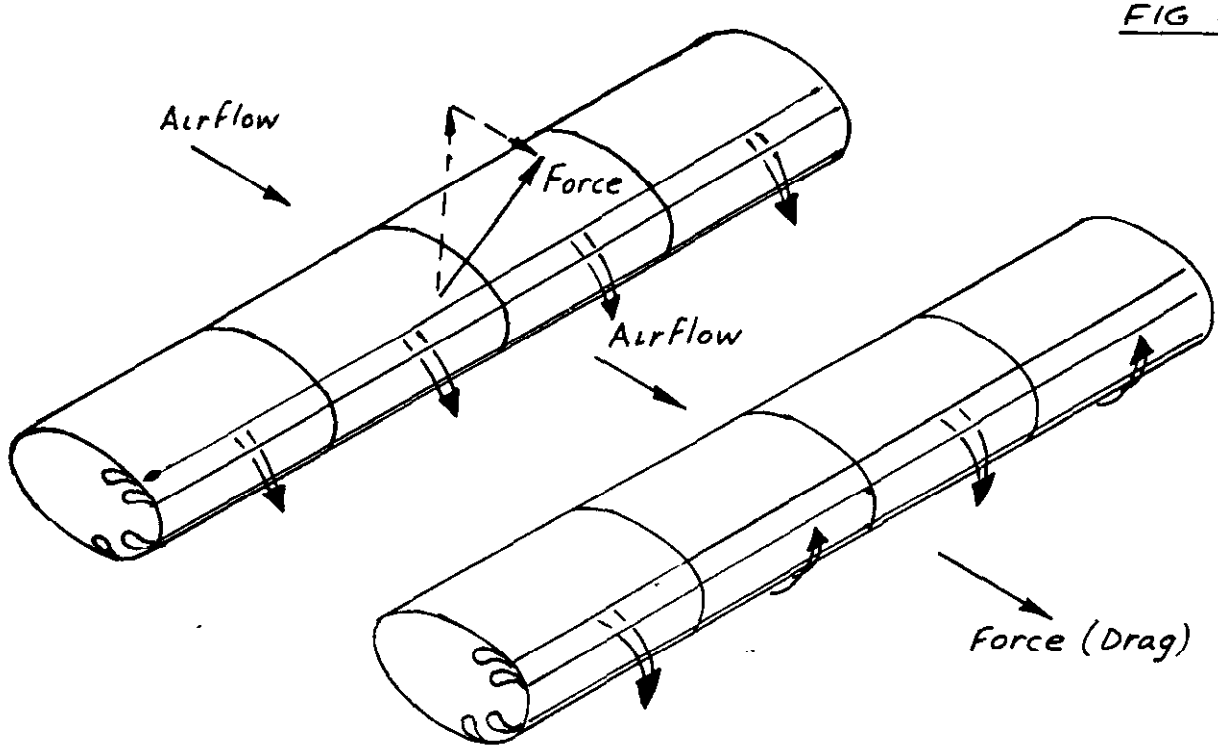

(a) ABOVE : ALTERNATIVE SINGLE-CYLINDER BLOWING ARRANGEMENTS GIVING LIFT + DRAG (SYMMETRICAL) OR DRAG (OPPOSED BLOWING).

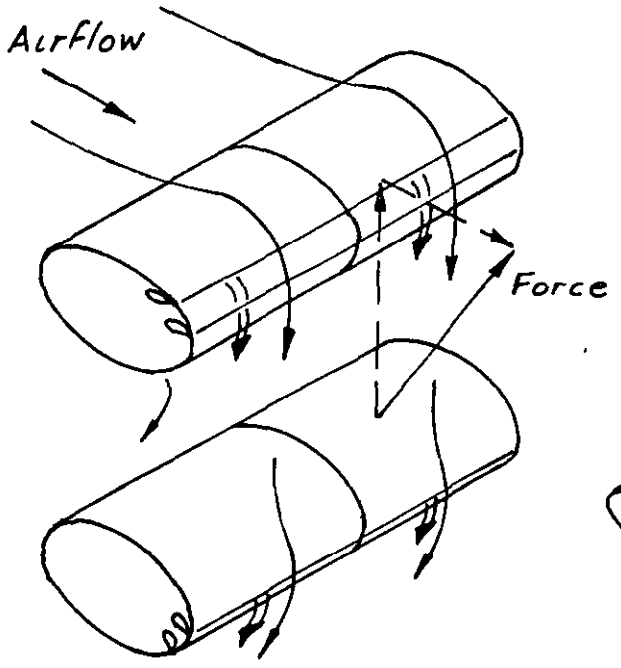

(b) TWIN CYLINDERS IN PROXIMITY

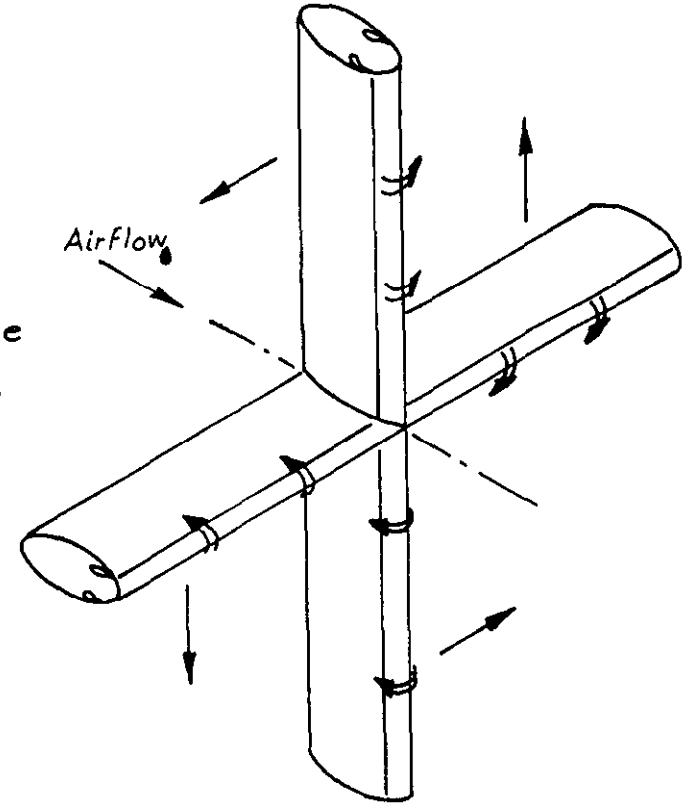

(c) CRUCIFORM ARRANGEMENT GIVING ROLL CONTROL

FIG 52. VARIOUS BLOWING ARRANGEMENTS WHICH COULD BE USED IN AIRCRAFT APPLICATIONS.

HER MAJESTY'S STATIONERY OFFICE

Government Bookshops

49 High Holborn, London WC1V 6HB
13a Castle Street, Edinburgh EH2 3AR
109 St Mary Street, Cardiff CF1 1JW
Brazennose Street, Manchester M60 8AS
50 Fairfax Street, Bristol BS1 3DE
258 Broad Street, Birmingham B1 2HE
80 Chichester Street, Belfast BT1 4JY

Government publications are also available through booksellers

C.P. No. 1232

SBN 11 470790 1